Multimodality Imaging of Diseases of the Thoracic Aorta in Adults: From the American Society of Echocardiography and the European Association of Cardiovascular Imaging
Endorsed by the Society of Cardiovascular Computed Tomography and Society for Cardiovascular Magnetic Resonance

Steven A. Goldstein, MD, Co-Chair, Arturo Evangelista, MD, FESC, Co-Chair, Suhny Abbara, MD, Andrew Arai, MD, Federico M. Asch, MD, FASE, Luigi P. Badano, MD, PhD, FESC, Michael A. Bolen, MD, Heidi M. Connolly, MD, Hug Cuéllar-Calàbria, MD, Martin Czerny, MD, Richard B. Devereux, MD, Raimund A. Erbel, MD, FASE, FESC, Rossella Fattori, MD, Eric M. Isselbacher, MD, Joseph M. Lindsay, MD, Marti McCulloch, MBA, RDCS, FASE, Hector I. Michelena, MD, FASE, Christoph A. Nienaber, MD, FESC, Jae K. Oh, MD, FASE, Mauro Pepi, MD, FESC, Allen J. Taylor, MD, Jonathan W. Weinsaft, MD, Jose Luis Zamorano, MD, FESC, FASE, Contributing Editors: Harry Dietz, MD, Kim Eagle, MD, John Elefteriades, MD, Guillaume Jondeau, MD, PhD, FESC, Hervé Rousseau, MD, PhD, and Marc Schepens, MD, *Washington, District of Columbia; Barcelona and Madrid, Spain; Dallas and Houston, Texas; Bethesda and Baltimore, Maryland; Padua, Pesaro, and Milan, Italy; Cleveland, Ohio; Rochester, Minnesota; Zurich, Switzerland; New York, New York; Essen and Rostock, Germany; Boston, Massachusetts; Ann Arbor, Michigan; New Haven, Connecticut; Paris and Toulouse, France; and Brugge, Belgium*

TABLE OF CONTENTS

From the Medstar Heart Institute at the Washington Hospital Center, Washington, District of Columbia (S.A.G., F.M.A., J.M.L., A.J.T.); Vall d'Hebron University Hospital, Barcelona, Spain (A.E., H.C.-C.); the University of Texas Southwestern Medical Center, Dallas, Texas (S.A.); the National Institutes of Health, Bethesda, Maryland (A.A.); the University of Padua, Padua, Italy (L.P.B.); Cleveland Clinic, Cleveland, Ohio (M.A.B.); Mayo Clinic, Rochester, Minnesota (H.M.C., H.I.M., J.K.O.); the University Hospital Zurich, Zurich, Switzerland (M.C.); Weill Cornell Medical College, New York, New York (R.B.D., J.W.W.); West-German Heart Center, University Duisburg-Essen, Essen, Germany (R.A.E.); San Salvatore Hospital, Pesaro, Italy (R.F.); Massachusetts General Hospital, Boston, Massachusetts (E.M.I.); the Methodist DeBakey Heart & Vascular Center, Houston, Texas; the University of Rostock, Rostock, Germany (C.A.N.); Centro Cardiologico Monzino, IRCCS, Milan, Italy (M.P.); University Hospital Ramón y Cajal, Madrid, Spain (J.L.Z.); Johns Hopkins University School of Medicine, Baltimore, Maryland (H.D.); the University of Michigan, Ann Arbor, Michigan (K.E.); Yale University School of Medicine, New Haven, Connecticut (J.E.); Hopital Bichat, Paris, France (G.J.); Hopital de Rangueil, Toulouse, France (H.R.); and AZ St Jan Brugge, Brugge, Belgium (M.S.).

> **Attention ASE Members:**
> The ASE has gone green! Visit www.aseuniversity.org to earn free continuing medical education credit through an online activity related to this article. Certificates are available for immediate access upon successful completion of the activity. Nonmembers will need to join the ASE to access this great member benefit!

Abbreviations

AAS = Acute aortic syndrome

AR = Aortic regurgitation

ASE = American Society of Echocardiography

BAI = Blunt aortic injury

BSA = Body surface area

CT = Computed tomography

CTA = Computed tomographic aortography

CXR = Chest x-ray

EACVI = European Association of Cardiovascular Imaging

EAU = Epiaortic ultrasound

GCA = Giant-cell (temporal) arteritis

ICM = Iodinated contrast media

IMH = Intramural hematoma

IRAD = International Registry of Acute Aortic Dissection

MDCT = Multidetector computed tomography

MIP = Maximum-intensity projection

MR = Magnetic resonance

MRI = Magnetic resonance imaging

PWV = Pulsewave velocity

STJ = Sinotubular junction

TA = Takayasu arteritis

TEE = Transesophageal echocardiography

TEVAR = Transthoracic endovascular aortic repair

3D = Three-dimensional

TTE = Transthoracic echocardiography

2D = Two-dimensional

ULP = Ulcerlike projection

PREAMBLE

Aortic pathologies are numerous, presenting manifestations are varied, and aortic diseases present to many clinical services, including primary physicians, emergency department physicians, cardiologists, cardiac surgeons, vascular surgeons, echocardiographers, radiologists, computed tomography (CT) and magnetic resonance (MR) imaging (MRI) imagers, and intensivists. Many aortic diseases manifest emergently and are potentially catastrophic unless suspected and detected promptly and accurately. Optimal management of these conditions depends on the reported findings from a handful of imaging modalities, including echocardiography, CT, MRI, and to a lesser extent invasive aortography.

In the past decade, there have been remarkable advances in noninvasive imaging of aortic diseases. This document is intended to provide a comprehensive review of the applications of these noninvasive imaging modalities to aortic disease. Emphasis is on the advantages and disadvantages of each modality when applied to each of the various aortic diseases. Presently, there is a lack of consensus on the relative role (comparative effectiveness) of these imaging modalities. An attempt has been made to determine first-line and second-line choices for some of these specific conditions. Importantly, we have emphasized the need for uniform terminology and measurement techniques. Whenever possible, these recommendations are evidence based, following a critical review of the literature. In some instances, the recommendations reflect a consensus of the expert writing group and include "vetting" by additional experts from the supporting imaging societies.

Because of the importance of prompt recognition to their successful treatment, this review emphasizes acute aortic syndromes (AAS), such as aortic dissection and its variants (e.g., intramural hematoma [IMH]), rupture of ascending aortic aneurysm, aortic trauma, and penetrating ulcer. Other entities, such as Takayasu aortitis (TA), giant-cell (temporal) arteritis (GCA), and mycotic aneurysm, are discussed briefly. Less common aortic diseases such as aortic tumors (because of their rarity) and congenital anomalies of the coronary arteries, aortic arch, and sinus of Valsalva aneurysms are not addressed. Several other topics are also beyond the scope of this review, including the important and emerging role of genetics in the evaluation and management of aortic diseases. Moreover, this document is not intended to replace or extend the recommendations of prior excellent guidelines in decision making and management for these conditions.[1]

To summarize, the focus of this document is the fundamental role of the major noninvasive imaging techniques. In addition to clinical acumen and suspicion, knowledge of these imaging modalities is crucial for the assessment and management of the often life-threatening diseases of the aorta.

I. ANATOMY AND PHYSIOLOGY OF THE AORTA

A. The Normal Aorta and Reference Values

The aorta is the largest and strongest artery in the body; its wall consists of three layers: the thin inner layer or intima, a thick middle layer or media, and a rather thin outer layer, or adventitia. The endothelium-lined aortic intima is a thin, delicate layer and is easily traumatized. The media is composed of smooth muscle cells and multiple layers of elastic laminae that provide not only tensile strength but also distensibility and elasticity, properties vital to the aorta's circulatory role. The adventitia contains mainly collagen as well as the vasa vasorum, which nourish the outer half of the aortic wall and a major part of the media.

The elastic properties of the aorta are important to its normal function. The elasticity of the wall allows the aorta to accept the pulsatile output of the left ventricle in systole and to modulate continued forward flow during diastole. With aging the medial elastic fibers undergo thinning and fragmentation. The ordinary concentric arrangement of the laminae is disturbed. These degenerative changes are accompanied by increases in collagen and ground substance. The loss of elasticity and compliance of the aortic wall contributes to the increase in pulse pressure commonly seen in the elderly and may be accompanied by progressive dilatation of the aorta.

A geometrically complex organ, the aorta begins at the bulb-shaped root (level 1 in Figure 1) and then courses through the chest and abdomen in a candy cane–shaped configuration, with a variable orientation to the long axis of the body, until it terminates in the iliac bifurcation. The aorta consists of five main anatomic segments: the aortic root, the tubular portion of the ascending aorta, the aortic arch, the descending thoracic aorta, and the abdominal aorta. The most proximal part of the ascending aorta, the aortic root (segment I in Figure 1), includes the aortic valve annulus, aortic valve cusps,
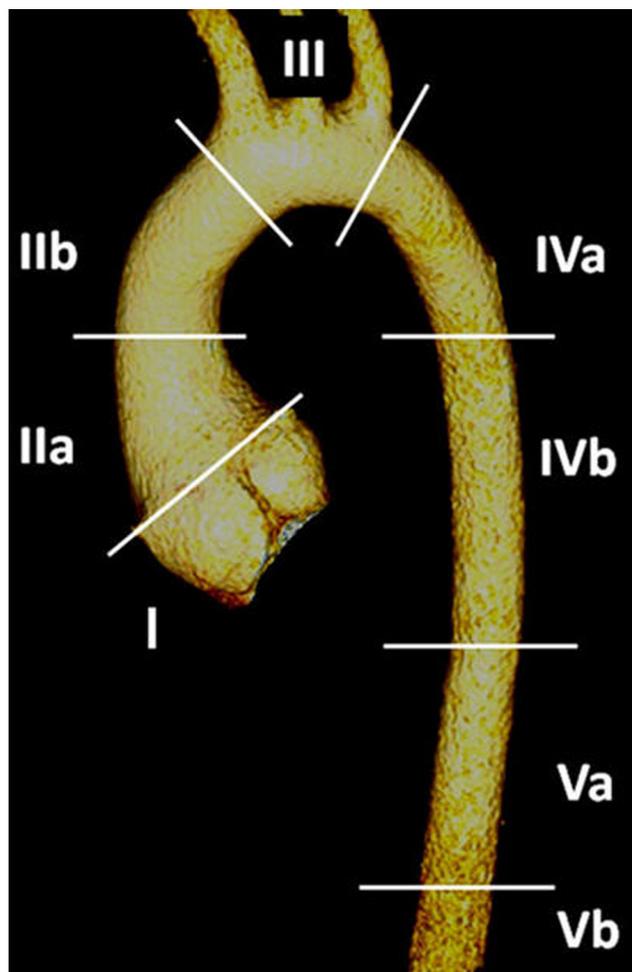
Figure 1 CT reconstruction of a normal aorta illustrating its segmentation as follows: segment I = aortic root; segment II = tubular ascending aorta (subdivided into IIa [STJ to the pulmonary artery level] and IIb [from the pulmonary artery level to the brachiocephalic artery]); segment III = aortic arch; segment IV = descending thoracic aorta (subdivided into IVa [from the left subclavian artery to the level of the pulmonary artery] and IVb [from the level of the pulmonary artery to the diaphragm]); and segment V = abdominal aorta (subdivided into Va [upper abdominal aorta from the diaphragm to the renal arteries] and Vb [from the renal arteries to the iliac bifurcation]).

Figure 2 Transthoracic echocardiogram in the parasternal long-axis view (zoomed on aortic root and ascending aorta) illustrating measurement of the aortic root diameter at sinus of Valsalva level at end-diastole using the leading edge–to–leading-edge method. asc Ao, Ascending aorta; LVOT, left ventricular outflow tract.

coronary ostia, and sinuses of Valsalva. Distally the root joins the tubular portion of the ascending aorta (segment II) at an easily recognized landmark termed the sinotubular junction (STJ). The tubular portion of the ascending aorta extends from the STJ to the origin of the brachiocephalic artery. This relatively long segment is subdivided into segment IIa, which extends from the STJ to the pulmonary artery level, and segment IIb, from the pulmonary artery level to the brachiocephalic artery. The aortic arch (segment III) extends from the brachiocephalic artery to the left subclavian artery. The descending thoracic aorta (segment IV) may be subdivided into the proximal part (segment IVa), which extends from the left subclavian artery to the level of the pulmonary artery, and the distal part (segment IVb), which extends from the level of the pulmonary artery to the diaphragm. The abdominal aorta (segment V) may be subdivided into the proximal part (segment Va), which extends from the diaphragm

to the ostia of the renal arteries, and the distal part (segment Vb), from the renal arteries to the iliac bifurcation.

1. Normal Aortic Dimensions. Because of the ease with which it can be visualized and its clinical relevance,[2,3] the aortic root is the segment for which the greatest amount of data are available. Several large studies have reported normal aortic root diameters in the parasternal long-axis view by two-dimensional (2D) transthoracic echocardiography (TTE).[4-10] Measurement of the aortic root diameter should be made perpendicular to the axis of the proximal aorta, recorded from several slightly differently oriented long-axis views. The standard measurement is taken as the largest diameter from the right coronary sinus of Valsalva to the posterior (usually noncoronary) sinus. Most studies report aortic root diameter measurements at end-diastole using the leading edge–to–leading edge technique (Figure 2).

In adults, aortic dimensions are strongly positively correlated with age[5-8,10,11] and body size.[4-6,8,10,11] They are larger in men than in women of the same age and body size.[6,12,13] Although in several reports, aortic diameters have been normalized to body surface area (BSA),[10,13,14] this approach has not been entirely satisfactory because it is systematically lower in smaller than in larger normal adults. Fortunately, among children, the regression line of aortic diameter and height (rather than BSA) has a near-zero intercept, so that normalization to height has proved to be a simple and accurate alternative in growing children.[15] Benchmark values from which the guidelines have been taken[1,16] come from the work of Roman et al.,[9] who reported normal root dimensions for three age groups (Figure 3).

The upper limit of normal aortic diameter has been defined as 2 SDs greater than the mean predicted diameter. The Z score (the number of SDs above or below the predicted mean normal diameter) is a useful way to quantify aortic dilatation. Among normal subjects, 95.4% have Z scores between −2 and 2. Therefore, an aortic diameter can be considered dilated when the Z score is ≥2. Using the Z score allows comparison of a given patient's aortic size at different time points, accounting for the effects of advancing age and increasing
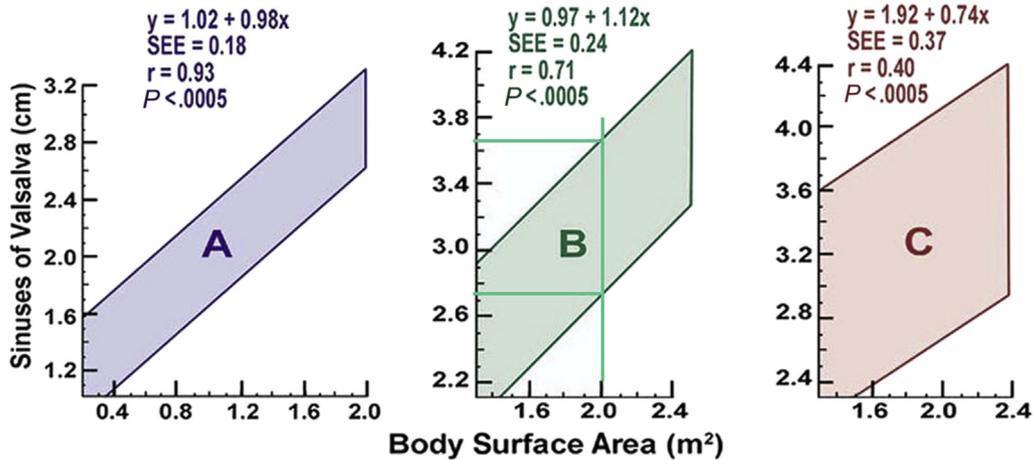
Figure 3 Aortic root diameter (*vertical axis*) in relation to BSA (*horizontal axis*) in apparently normal individuals aged 1 to 15 (*left panel, blue*), 20 to 39 (*center panel, green*), and ≥40 (*right panel, pink*) years. For example, an individual between the ages of 20 and 39 years (*center panel, green*) who has a BSA of 2.0 m² (*vertical green line*) has a normal root diameter range (2 SDs) between 2.75 and 3.65 cm, as indicated by the intersections of the *two horizontal green lines* with the *green-shaded* parallelogram.

Table 1 Normal aortic root diameter by age for men with BSA of 2.0 m²

	Age (y)					
	15–29	30–39	40–49	50–59	60–69	≥70
Mean normal (cm)	3.3	3.4	3.5	3.6	3.7	3.8
Upper limit of normal (cm) (95% CI)	3.7	3.8	3.9	4.0	4.1	4.2

Add 0.5 mm per 0.1 m² BSA above 2.0 m² or subtract 0.5 mm per 0.1 m² BSA below 2.0 m².[6]
CI, Confidence interval.

Table 2 Normal aortic root diameter by age for women with BSA of 1.7 m²

	Age (y)					
	15–29	30–39	40–49	50–59	60–69	≥70
Mean normal (cm)	2.9	3.0	3.2	3.2	3.3	3.4
Upper limit of normal (cm)	3.3	3.4	3.6	3.6	3.7	3.9

Add 0.5 mm per 0.1 m² BSA above 1.7 m² or subtract 0.5 mm per 0.1 m² BSA below 1.7 m².[6]

body size, thus distinguishing normal from pathologic growth. The *Z* score is therefore particularly useful for evaluating growing children.

It should be mentioned that aortic root dimensions may be increased by the hemodynamic effects of both endurance and strength exercise training in competitive athletes.[17-19] This aortic root enlargement appears to be greater at the sinuses of Valsalva than at the aortic annulus or STJ. However, it should be emphasized that the effects of exercise training on aortic diameters are relatively small and that marked enlargement should suggest a pathologic process.[17,18]

Recently, making use of a database consisting of a multiethnic population of 1,207 apparently normal adolescents and adults ≥15 years of age, investigators devised equations to predict mean normal aortic root diameter and its upper limit by age, body size (BSA or height), and gender[6] (Table 1 for men and Table 2 for women). These equations have been used graphically to depict the upper limits of the 95% confidence interval for normal aortic root diameter using surfaces to depict the interacting effects of age and body size (see Figure 4 for men and Figure 5 for women).

A noncontrast gated cardiac computed tomographic study,[20] including 4,039 adult patients, showed age, BSA, gender, and hypertension to be directly associated with thoracic aortic diameters perpendicular to the long axis of the aorta. These associations are concordant with those from echocardiographic studies. In another recent large study using similar methodology, the mean value of the diameters of the ascending aorta was 1.8 ± 0.2 cm/m² and of the descending thoracic aorta was 1.4 ± 0.2 cm/m², with the upper limits of normal being 2.1 and 1.8 cm/m², respectively.[21] However, more accurate normal values of thoracic aortic diameters may be obtained by anatomically correct double-oblique short-axis images using electrocardiographically gated multidetector CT or by MRI of axially oriented aortic segments. The upper limits of normal are 3.7 cm for the aortic root at the sinuses, 3.6 cm for the ascending aorta and 2.5 cm for the descending thoracic aorta by CT,[8] and 2.5 cm for the descending thoracic aorta and 2.0 cm for the upper abdominal aorta by MRI.[22] As with echocardiography, aortic root and ascending aortic diameters increase significantly with age and BSA on CT and MRI. Aortic root diameters increase 0.9 mm per decade in men and 0.7 mm per decade in women.[4]

The establishment of normative values and reference ranges, taking into account aging and gender, is of great importance for diagnosis, prognosis, serial monitoring, and determining the optimal timing for surgical intervention. Normal values and proximal aortic diameters have been reported using different imaging techniques, from the pioneer studies based on M-mode and 2D echocardiography[9,10] to more recent studies obtained using CT[7,8,20,23-25] and MRI.[5,26] Despite differences in image acquisition methods, temporal and spatial resolution, and signal-to-noise ratios, CT, MRI, TTE, and transesophageal echocardiography (TEE) have evolved as near equal standards for assessing aortic root size. Each of these modalities has

**Upper Limit of Aortic Root Diameter
For Age and BSA in Men ≥15 Years Old**
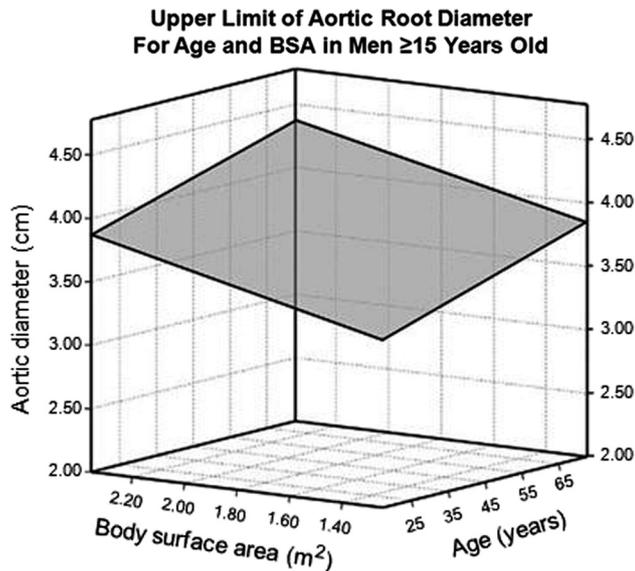
Figure 4 Surfaces representing aortic diameters at a 1.96 *Z* score (95% confidence interval) above the predicted mean for age and BSA in male subjects ≥15 years of age. (Adapted from Devereux *et al.*[6])

**Upper Limit of Aortic Root Diameter
For Age and BSA in Women ≥15 Years Old**
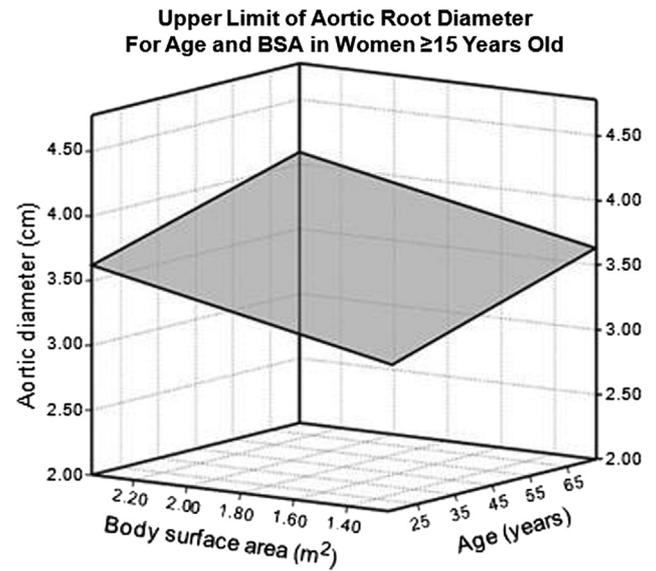
Figure 5 Surfaces representing aortic diameters 1.96 *Z* score (95% confidence interval) above the predicted mean value of aortic diameter for age and BSA in female subjects ≥15 years of age. (Adapted from Devereux *et al.*[6])

advantages and disadvantages, which have been discussed. It should be emphasized that normal aortic diameters vary systematically by age, gender, and body size, and reference values indexed to those parameters have been provided. Last, it is critically important to emphasize not only methodologic variance but also inter- and intraobserver variability. In several studies, variability of measurement of proximal aortic diameters ranges from 1.6 to 5 mm.[8,23,24,27,28] Given this degree of variability, apparent small changes in proximal aortic diameters on serial computed tomographic examinations may be within the range of measurement error. Accordingly, for all imaging techniques, we recommend that changes of ≤3 mm by electrocardiographically gated CT and ≤5 mm without electrocardiographic gating be viewed with caution and skepticism.

B. How to Measure the Aorta

Accurate and reproducible measurements of aortic dimensions are necessary for the detection and classification of aortic disease and for guiding therapeutic decisions. Modern imaging modalities enable one to make measurements far more accurately than did invasive contrast angiography, the only tool originally available.

Echocardiography, CT, and MRI each has particular strengths and limitations but can be adapted for the acquisition of views that allow measurement of the diameter or cross-sectional area of different segments of the aorta (Figure 1).

1. Interface, Definitions, and Timing of Aortic Measurements. The American Society of Echocardiography (ASE) proposed standards for measurement of the aortic root in 1978.[29] The ASE recommended measurement at end-diastole from the leading edge of the anterior root wall to the leading edge of the posterior aortic root wall. This technique was believed to minimize the impact of "blooming" of bright reflectors on this measurement. The ASE-recommended method was followed in many important

clinical and epidemiologic studies[10,13] that have reported normal limits for individuals of differing body size and age, and these normal limits have been incorporated into multiple guidelines for imaging in adults (Figures 4 and 5).[1,9,16] As a consequence, much of the available data on normal aortic root size as well as on the prevalence and prognostic significance of aortic dilatation in adults have emerged from echocardiography.[6,10,13]

Societal guidelines for measurement by CT or MRI are not currently available. Consequently, uniformity in measurement methods is lacking. Many research and clinical studies using these modalities have reported aortic measurements made from inner edge to inner edge on electrocardiographically gated or nongated images. The 2010 guidelines for the diagnosis and management of thoracic aortic disease took the opposite approach, recommending measurement of aortic diameter between external surfaces to avoid confounding by intraaortic thrombus or atheroma, as is commonly found in the abdominal but not in the ascending aorta.[1] Furthermore, there is no standardized "trigger time" (end-systole vs end-diastole) for image acquisition. Thus, the use of multiple imaging modalities such as CT, MRI, and 2D and three-dimensional (3D) echocardiography has led to nonuniformity in measurement techniques. Moreover, there is currently no standardized approach for reconciling aortic measurements across imaging modalities (echocardiography, CT, MRI, aortography) by trigger time (end-systole vs end-diastole) or by edge selection (leading edge, inner-inner, outer-outer). This writing committee had hoped to recommend a uniform and consistent measurement technique to minimize differences among these various imaging modalities. However, after much consideration, the group recommends that echocardiographic measurements continue to be made in the standard fashion from leading edge to leading edge, at end-diastole, and perpendicular to the long axis of the aorta. The advantages of end-diastolic measurements include greater reproducibility (because aortic pressure is most stable in late diastole) and the ease of identification of end-diastole by the onset of the QRS
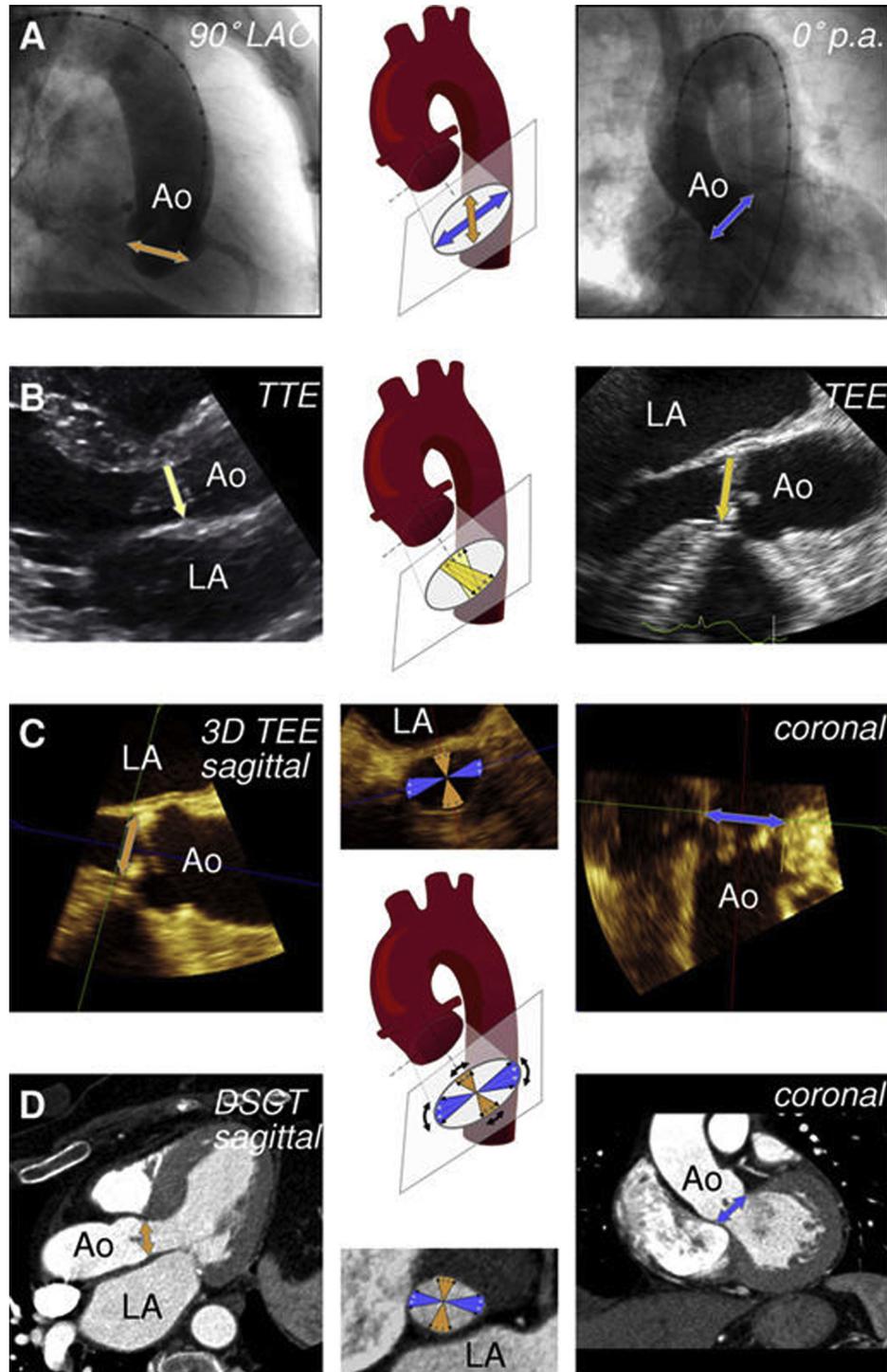
Figure 6 Models of the thoracic aorta showing the cut planes of the aortic annulus for each applied imaging modality. **(A)** Angiography in the 90° left anterior oblique (LAO) projection with an orange arrow indicating the sagittal annulus diameter (*left*) and in the 0° posteroanterior (p.a.) projection with a blue arrow indicating the coronal annulus diameter (*right*). **(B)** TTE (*left*) and 2D TEE (*right*) left ventricular outflow tract (LVOT) view of the aortic annulus. The cut planes slightly differ because parasternal and midesophageal acoustic are not quite comparable. Both the transthoracic and 2D transesophageal echocardiographic LVOT views resemble a sagittal view (*bright* and *dark yellow arrows*, respectively). The direction of the *arrows* in the aortic arch model and the echocardiographic images indicate the scanning direction. Individual adjustments in scan plane direction are shown in the model. **(C)** Three-dimensional transesophageal echocardiographic cropped images of a sagittal (*left*) and coronal (*right*) view with the corresponding diameters (*orange* and *blue arrows*). The sagittal and coronal cut planes are depicted in the aortic arch model and the anatomic short-axis view (*middle*). **(D)** Dual-source computed tomographic (DSCT) reconstructed images of a sagittal (*left*) and coronal (*right*) view with the corresponding diameters (*orange* and *blue arrows*). The sagittal and coronal cut planes are depicted in the aortic arch model and the anatomic short-axis view (*middle*). *AO*, Ascending aorta; *LA*, left atrium. (From Altiok *et al.*[418])
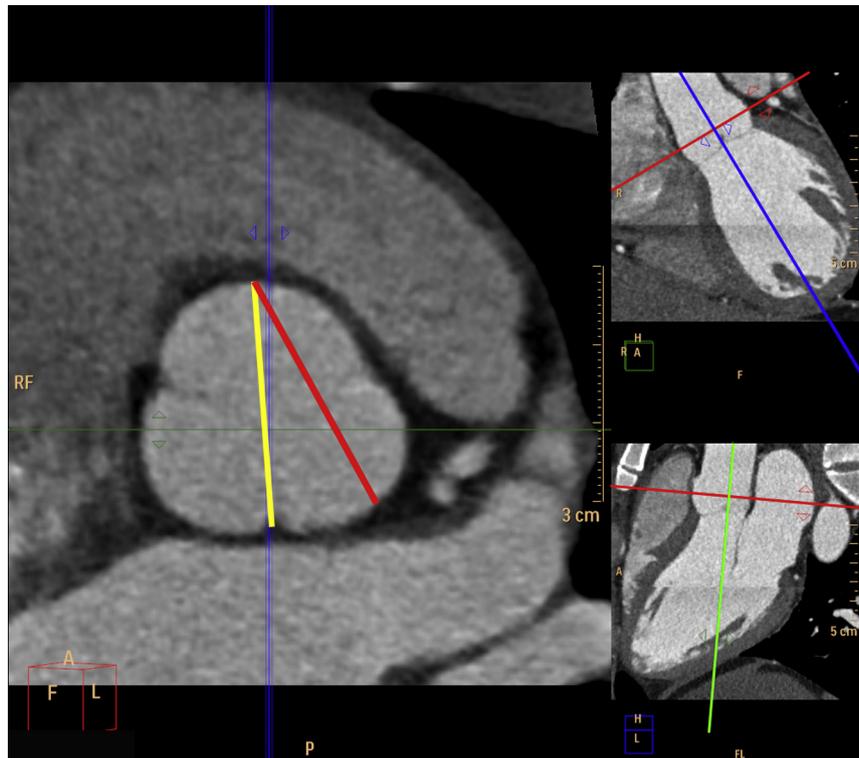
Figure 7 Aortic root measurements by CT. The aortic root diameter is commonly measured between the inner edges from one commissure to opposite sinus (*yellow line*) or from one sinus to another sinus (*red line*), as shown in the large image (*left*), which is a zoomed cross-sectional view of the aortic root at the sinus of Valsalva level using a double oblique image for orientation (shown in the *right panel*).

complex. Although other techniques use the inner edge–to–inner edge approach, there are currently insufficient data to warrant a change for echocardiography. Available data suggest that the echocardiographic leading edge–to–leading edge approach produces values comparable with those produced by the inner edge–to–inner edge approach on CT and MRI, is reproducible, and links to a large body of historical and prognostic data that have long guided clinical decision making.

For all modalities, it is desirable, whenever possible, to specify the locations of measurements, by referencing them to a given landmark. For example, with TEE, a measurement of the maximal diameter of the ascending aorta may be reported by its distance from the STJ. In the descending thoracic aorta, reference to the location of a measurement or abnormality is usually made by its distance from the incisors. Similar attempts should be made for measurements and findings with CT and MRI.

2. Geometry of Different Aortic Segments: Impact on Measurements.
Accurate and reproducible measurement of aortic diameter or cross-sectional area in a given segment requires three measurements of its diameter perpendicular to the long axis. In most cases, the largest correctly oriented measurement is reported.

a. Aortic Annulus.–Although the aortic annulus is approximately circular in children and young adults, it may become elliptical in older adults. Thus, 3D imaging by CT or echocardiography or 2D imaging in multiple planes (e.g., long-axis or sagittal and coronal planes) is required to measure a diameter that is accurate enough to be used when selecting patients for transcatheter aortic valve replacement (Figure 6).

b. Sinuses of Valsalva and STJ.–Aortic root diameter can be measured perpendicular to its long axis by 2D echocardiography or in analogous nontrue coronal and sagittal plane by MRI or CT. The variability in this measurement resulting from the orientation of the aortic root is overcome by choosing the largest diameter measured from the right coronary sinus of Valsalva to the posterior (usually noncoronary) sinus, parallel to the aortic annulus and perpendicular to the long axis of the proximal aorta in several slightly differently oriented long-axis views. Failure to search for the largest correctly oriented measurement can lead to underestimation of aortic root diameter. Aortic root diameter is commonly measured by CT or MRI between the inner edges from commissure to opposite sinus (Figure 7). Diameters measured using the sinus-to-sinus method are generally a mean of 2 mm larger than those measured by the sinus-to-commissure method[4,7] (Figure 8). However, using the sinus-to-sinus method has several advantages, including the ease of detecting cusp margins in computed tomographic or MRI transverse planes, close agreement with echocardiographic measurements, and greater feasibility in bicuspid valves. Thus, for aortic measurements by CT and MRI, it is recommended to average the three sinus-to-sinus measurements in end-diastole in the sinus-of-Valsalva plane. When the sinuses are unusually asymmetric, it may be preferable to report the three measurements individually.

c. Ascending Aorta and More Distal Segments.–The same basic principles apply to obtaining correct measurements of the other aortic segments. Conventional imaging by all modalities and techniques can be used to measure the diameter of aortic segments that are oriented along the long axis of the body. However, the necessity to avoid oblique imaging that can overestimate the aortic diameter applies to the
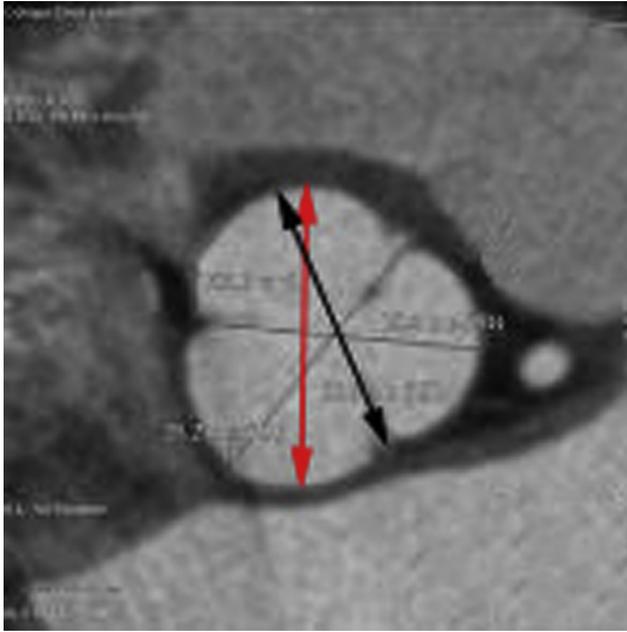
Figure 8 Computed tomographic scan image of aortic root illustrates that the mean difference of the aortic root diameter is about 2 mm larger measured by the anteroposterior diameter (*sinus-sinus*) shown by red arrow than by the sinus-commissure diameter (*black arrow*).

aortic arch and to portions of the descending thoracic and abdominal aorta that may take a tortuous course (Figure 9).

We emphasize that there is no standardized method for measuring the aorta across imaging modalities (echocardiography, CT, MRI, aortography). Although one of the major goals of this writing committee was to provide a uniform and universally accepted method to minimize differences among these various imaging modalities, no consensus could be reached. After much consideration, it is recommended that echocardiographic measurements continue to be made from leading edge to leading edge. Although other techniques use inner edge–to–inner edge or outer edge–to–outer edge approaches, there are currently insufficient data to warrant a change for echocardiography. Available data suggest that the echocardiographic leading edge–to–leading edge approach gives larger measurements compared with the inner edge–to–inner edge approach on CT (average difference, 2 mm), and the leading edge–to–leading edge method links to a large body of historical and, more important, prognostic data that influence decision making.[8] Out of concern that patient management might be adversely affected (i.e., intervention might be delayed, leading to a catastrophic complication such as rupture or dissection) by switching to a new protocol that would lead to a smaller measurement, it was decided to continue to recommend the leading edge–to–leading edge approach.

C. Aortic Physiology and Function

The aorta functions as both a conduit and a reservoir. Its elastic properties allow it to expand in systole and recoil during diastole. Thus, under normal conditions, a large proportion (up to 50%) of the left ventricular stroke volume is stored in the aorta (mainly in the ascending aorta) at end-systole, and the stored blood is then propelled forward during diastole into the peripheral circulation. This reservoir function is important for maintaining blood flow and arterial pressure throughout the cardiac cycle. The thoracic aorta is more distensible
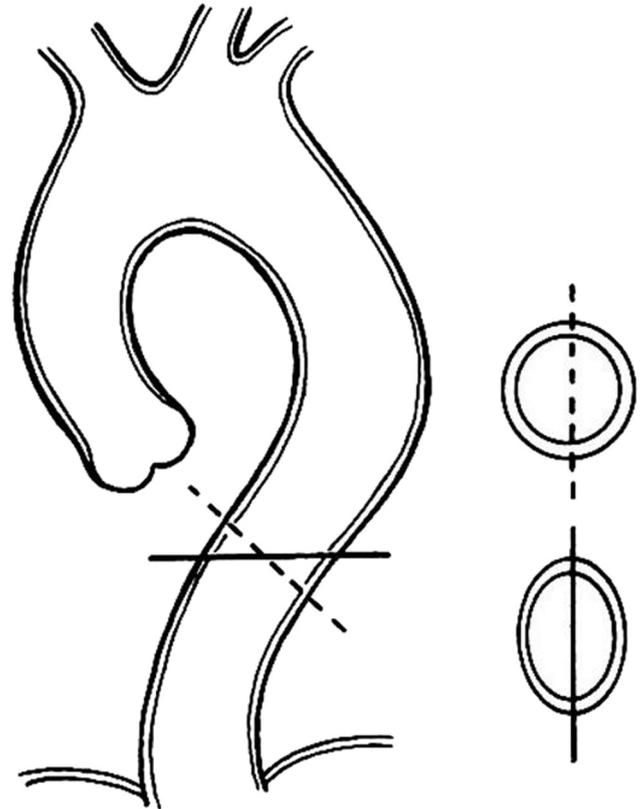
Figure 9 Diagram illustrating the potential pitfall of obtaining an oblique cut resulting in an "ellipsoid" cross-section that overestimates the true diameter. This is especially a problem when the descending aorta is tortuous.

than the abdominal aorta because its media contains more elastin. Aortic distensibility declines with age and as a result of premature degeneration in elastin and collagen associated with some disease states.[30] During left ventricular systole, this loss of aortic wall compliance results in increased systolic pressure and pulse pressure and, in turn, aortic dilatation and lengthening. The compliance of the aortic wall may be estimated by assessing change in aortic volume in relation to the simultaneous change in aortic pressure. This may be assessed locally by diameter or area change through the cardiac cycle in relation to pressure change (e.g., distensibility) or regionally by determination of the velocity of the pulse wave.

1. Local Indices of Aortic Function. Techniques that provide accurate definition of the aortic diameter or volume in systole and diastole can be used to evaluate the elastic properties of the aorta. The most commonly applied indices for clinical purposes are aortic distensibility and the stiffness index, which is less dependent on blood pressure. Aortic distensibility and the stiffness index can be determined from the changes in the aortic diameter from systole to diastole and from changes in the arterial pressure using the following formula:

$$\text{Distensibility}\left(10^{-3} \cdot \text{mm Hg}^{-1}\right) = \frac{\text{Area}_{\text{systole}} - \text{Area}_{\text{diastole}}}{\text{Area}_{\text{diastole}} \cdot \text{Pulse pressure}} \cdot 1,000.$$

For these calculations, the pulse pressure should be measured ideally at the same level of the aorta at which the aortic diameter is

Table 3 Plain CXR findings in aortic dissection

1. Mediastinal widening
2. Abnormalities in region of aortic knob
    1. Enlargement (expansion of aortic diameter)
    2. Presence of double density (due to enlargement of false lumen)
    3. Irregular contour
    4. Blurred aortic knob (indistinct aortic margin)
3. Displacement of intimal calcium
4. Discrepancy in diameters of ascending and descending aorta
5. Displacement of trachea, left main bronchus, or esophagus
6. Pleural effusion (more common on the left)
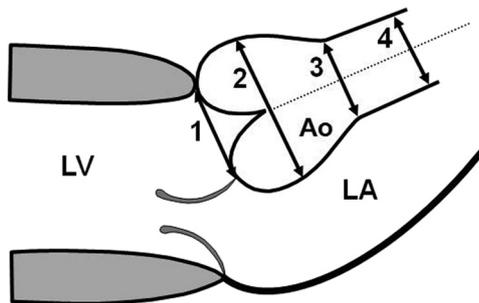
Figure 10 Sites for measurements of the aortic root and ascending aorta. This diagram illustrates the four sites at which measurements are recommended: 1 = aortic valve annulus (hinge point of aortic leaflets), 2 = aortic root at sinuses of Valsalva (maximal diameter, usually midpoint), 3 = STJ, 4 = proximal tubular portion of the ascending aorta. *Ao,* Aorta; *LA,* left atrium; *LV,* left ventricle.

Figure 11 Transthoracic echocardiographic suprasternal notch view of the distal ascending aorta (Asc Ao), aortic arch, supra-aortic vessels (*arrows*), and proximal descending thoracic aorta (Desc Ao).

measured. In clinical practice, however, brachial artery pressure can be used, even though the pulse pressure obtained from the brachial artery may be slightly higher than that obtained from the aorta because of the amplification phenomenon, which is more apparent in young individuals.[31]

2. Regional Indices of Aortic Stiffness: Pulsewave Velocity (PWV). PWV is defined as the longitudinal speed of the pulsewave in the aorta. PWV is inversely related to aortic elasticity. Hence, a stiffer aorta will conduct the pulsewave faster than a more compliant aorta. Central pressure, at the level of the ascending aorta, is produced as a combination of the antegrade wave from the left ventricle and the retrograde "reflective" waves from the periphery. In young individuals, because the aorta is more elastic, the pulsewave speed is low, so the retrograde flow arrives in the proximal aorta during diastole. As a result of aortic stiffening, the PWV increases, and the retrograde flow arrives in the proximal aorta earlier in systole, leading to a greater LV afterload and decreased diastolic pressure.

Reported normal values for invasively determined PWV measurements in middle-aged humans are 4.4 ± 0.4 m/sec in the aortic root, 5.3 ± 0.2 m/sec in the proximal descending thoracic aorta, 5.7 ± 0.4 m/sec in the distal thoracic descending aorta, 5.7 ± 0.4 m/sec in the suprarenal abdominal aorta, and 9.2 ± 0.5 m/sec in the infrarenal aorta.[32]

Carotid-femoral PWV is considered to be the gold-standard measure of arterial stiffness, especially because it is simple to obtain and because multiple epidemiologic studies have demonstrated its predictive value for cardiovascular events. However, the ability of a given individual's PWV value to predict aortic events has not been previously evaluated.[33] A recent expert consensus adjusted this threshold value to 10 m/sec by using the direct carotid-to-femoral distance.[34] The main limitation of PWV interpretation is that it is significantly influenced by arterial blood pressure. Multimodality imaging techniques provide a unique opportunity to assess aortic PWV by the formula:

$$\text{Aortic PWV(m/sec)} = \frac{\text{Distance}(mm)}{\text{Transit } time(msec)}.$$

Echocardiography can accurately estimate the transit time between aortic levels by the subtraction of the time between a fixed reference in the QRS complex and the beginning of the flow at the two levels studied. Distance can be grossly estimated externally with a tape.

MRI can measure the PWV using the transit time of the flow curves from a phase-contrast acquisition. Transit time can be calculated by the upslope approach, which has been described previously and correlates more with age and aortic stiffness indices than point-to-point approaches such as foot-to-foot and half-maximum methods.[35] Distance can accurately be measured at the centerline of the aorta between aortic levels studied.

A normal-size aorta may be functionally abnormal. Thus, determination of aortic function may help define the nature of the underlying disease and give prognostic information in some diseases. This was emphasized by Vriz *et al.*,[4] who stated that aortic stiffness should be taken into account when increases in aortic diameter are detected.

In summary, aortic biophysical properties can be easily and reliably assessed by imaging techniques, particularly Doppler echocardiography and phase-contrast MRI. This evaluation may provide

important pathophysiologic and prognostic information that may have clinical implications both in disease states and in the general population.

II. IMAGING TECHNIQUES

A. Chest X-Ray (CXR)

Most articles describing the use of imaging to evaluate patients with suspected AAS have focused on the role of CT, MRI, echocardiography, and aortography. Although routine CXR rarely provides a definitive diagnosis, it can provide several important diagnostic clues to aortic diseases that prompt further evaluation. Table 3 lists some of the common and uncommon plain CXR findings of aortic diseases.

Moreover, in cases of asymptomatic or chronic aortic diseases, CXRs may actually provide the first clue to aortic pathology. Importantly, CXR can identify other chest disorders that may contribute to a patient's illness (e.g., pneumonia, pneumothorax, rib fracture). Nevertheless, although CXR may be valuable, it is neither sensitive nor specific for AAS.[36-38] Moreover, normal results on CXR with respect to the aorta should never prevent or delay the further diagnostic evaluation of a patient with a suspected AAS.

In summary, although useful in drawing attention to the possibility of aortic disease, its low sensitivity, specificity, and interobserver agreement limit the role of the CXR.

B. TTE

The thoracic aorta should be routinely evaluated by TTE,[39-42] which provides good images of the aortic root, adequate images of the ascending aorta and aortic arch in most patients, adequate images of the descending thoracic aorta in some patients, and good images of the proximal abdominal aorta. New advances in imaging quality and harmonic imaging have significantly improved the assessment of the aorta by TTE.

The aortic root and proximal ascending aorta are best imaged in the left parasternal long-axis view. The left lung and sternum often limit imaging of the more distal portion of the ascending aorta from this transducer position. In some patients, especially those with aortic dilatation, the right parasternal long-axis view can provide supplemental information. The ascending aorta may also be visualized in the apical long-axis (apical three-chamber) and apical five-chamber views and (especially in children) in modified subcostal views.

There is usually no clear echocardiographic delineation between the sinus and tubular portion of the ascending aorta, but occasionally a fibrotic or sclerotic ridge, located at the STJ, is imaged. This ridge may be prominent and should not be confused with vegetation, abscess, mass, atherosclerotic plaque, dissection flap, or supra-aortic stenosis. The maximum diameter of the aorta is normally in the root (sinus portion), which is immediately distal to the aortic valve.

Echocardiographic measurements of the aortic root will vary in an individual patient at different levels (Figure 10).[3,43,44] The aortic diameter is smallest at the annulus and largest at the mid–sinuses of Valsalva. The tubular portion of the ascending aorta is typically about 10% smaller than the diameter at the sinus level.[45] The aortic arch is usually easily visualized from the suprasternal view. Portions of the ascending and descending aorta can be visualized simulta-
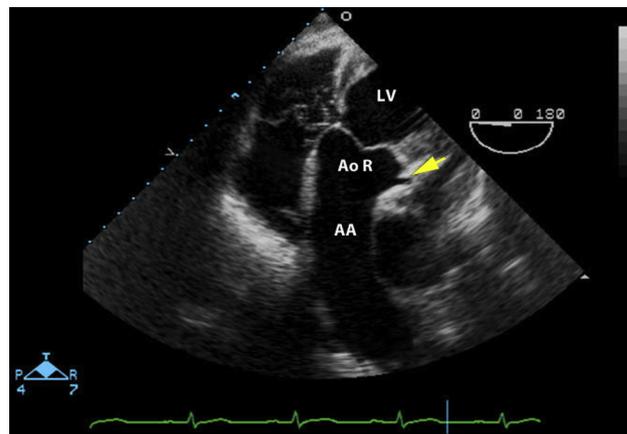
Figure 12 Transesophageal echocardiographic deep transgastric view, which illustrates the aortic root (Ao R), the entire ascending aorta (AA), and the proximal arch (not labeled). The left coronary artery is also imaged (*black arrow*).

neously. One or more of the three arch branches can usually be imaged: the left carotid and left subclavian arteries are identified in >90% of cases and the brachiocephalic (inniminate) artery in up to 90% (Figure 11). Just distal to the left subclavian artery is the level of the ligamentum arteriosum, which is a common site of atherosclerosis, and a shelf or indentation (a ductus diverticulum) is sometimes imaged in this region.

The descending thoracic aorta is often incompletely imaged by TTE. A cross-sectional view of the descending thoracic aorta may be seen in the parasternal long-axis view, as it passes posteriorly to the left atrium near the atrioventricular groove. It can also be seen in short axis in the apical four-chamber view. By rotating the transducer 90°, a long-axis view of the midportion of the descending thoracic aorta may be obtained. A portion of the descending thoracic aorta can also be imaged from a suprasternal view. In patients with left pleural effusion, scanning from the back may also provide satisfactory views of the descending thoracic aorta. However, the distal descending thoracic aorta frequently cannot be imaged clearly because of reduced resolution in the far field. Moreover, physical characteristics of some patients exceed the limit of ultrasound penetration.

The normal descending thoracic aorta is smaller than both the aortic root and ascending aorta. As it descends, its diameter progressively narrows from 2.5 to 2.0 cm. Larger dimensions are reported in patients with hypertension, aortic valve disease, and coronary atherosclerosis.[46] The aorta is consistently about 2 mm smaller in female than it is in male subjects.[47]

A substantial portion of the upper abdominal aorta can be easily imaged in subcostal views, to the left of the inferior vena cava. This should be routinely performed as a part of a 2D echocardiographic study.[16] Often the proximal celiac axis and the superior mesenteric artery can also be imaged. When present, aneurysmal dilatation, external compression, intra-aortic thrombi, protruding atheromas, and dissection flaps can be imaged, and flow patterns in the abdominal aorta can be assessed. The infrarenal abdominal aorta is best imaged as part of an abdominal ultrasound examination by use of a linear array probe.

In summary, to reliably evaluate patients with suspected aortic disease, the entire thoracic aorta must be imaged well. This is possible in some, but not all, patients on systematic TTE. TTE is particularly useful
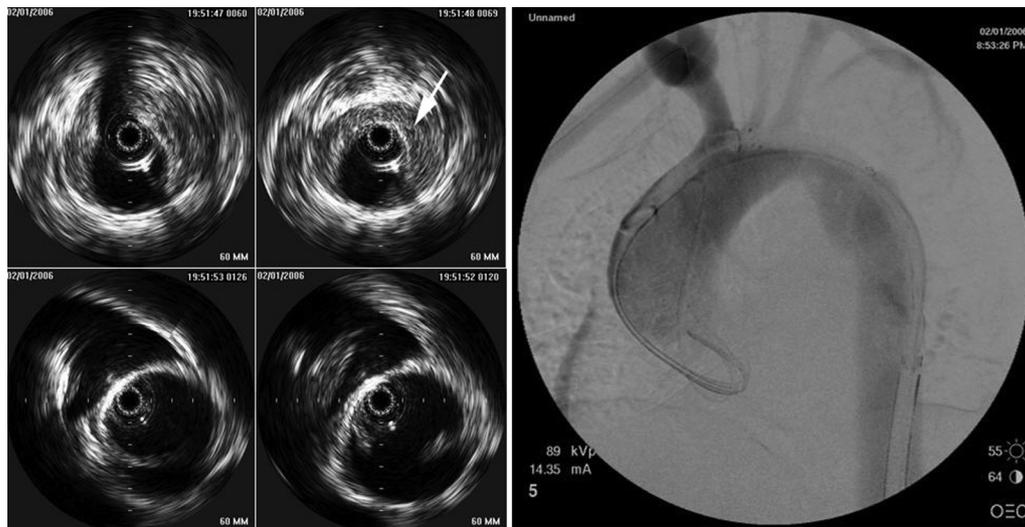
Figure 13 IVUS documentation of an IMH evolving to full dissection on (*left*) with corresponding contrast aortogram showing only luminal compression (*right*).
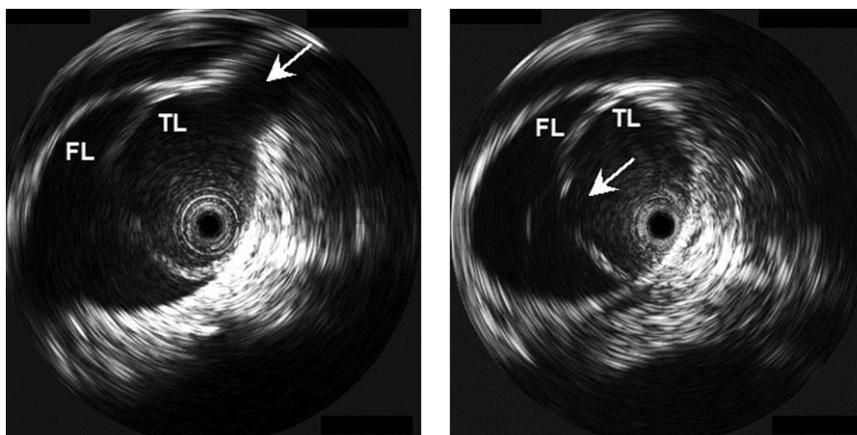
Figure 14 IVUS evaluation of an aortic dissection extending across the level of the left renal artery (*left frame, arrow*); the IVUS in the true lumen identifies the renal artery ostium and the reentry point (*right frame, arrow*) at the orifice level. *FL*, False lumen; *TL*, true lumen.

for evaluating the aortic root, and the ascending aorta and arch may also be adequately visualized in patients with good acoustic windows. TTE is less helpful for evaluating the descending thoracic aorta. However, TTE is an excellent screening tool for detecting aneurysms of the upper abdominal aorta.

C. TEE

TEE, introduced clinically in the late 1980s, has had a major impact on the evaluation of numerous diseases involving the aorta. TEE has two main advantages over TTE. First, superior image quality can be obtained from the use of higher frequency transducers than are possible with TTE. Second, because of the close proximity of the esophagus to the thoracic aorta, TEE provides high-quality imaging of nearly all of the ascending and descending thoracic aorta.[48-50] TEE incorporates all the functionality of TTE, including 3D imaging, which can reliably interrogate cardiovascular anatomy, function, hemodynamics, and blood flow. The current multiplane TEE transducer consists of a single array of crystals that can be rotated electronically or mechanically around the long axis of the ultrasound beam in an arc of 180°. With rotation of the transducer array, multiplane TEE produces a continuum of transverse and longitudinal image planes.

1. Imaging of the Aorta. As mentioned, the anatomic proximity of the thoracic aorta and the esophagus allows superb visualization of the aorta using TEE. The multiplane transesophageal echocardiographic examination of the aorta is conducted as follows[51]: with the tip of the transesophageal echocardiographic probe in the esophagus, the ascending aorta is best visualized from a 100° to 140° view: the image is analogous to the transthoracic echocardiographic parasternal long-axis view (but "flipped" upside down if the transesophageal echocardiographic probe "bang" is at the top). This view can be optimized by carefully rotating the transducer between 100° and 140°. Short-axis views of the aortic root and ascending aorta can be obtained from the 45° to 60° angle, usually with an anteflexed probe. From the midesophagus at 0°, the probe needs to be rotated posteriorly to obtain short-axis images of the descending thoracic aorta.

Figure 15 Volume-rendered image from an electrocardiographically gated thoracic computed tomographic aortogram in the presurgical study of a patient with ascending aortic aneurysm. Note the excellent quality of both the aortic and coronary vessels, with calcified atheromatous plaques of the coronary arteries.

While keeping the thoracic aorta in view, the probe can be withdrawn to image upper thoracic levels of the descending aorta or advanced to sequentially image the lower thoracic and upper abdominal aorta. With the transducer array at 90°, a longitudinal view of the aorta can be obtained.

By advancing the probe into the stomach, the proximal portion of the abdominal aorta and the celiac trunk can be seen. The mid and distal abdominal aorta are usually not seen because of difficulty maintaining good contact with the mucosa of the stomach. To obtain images of the arch, the transesophageal echocardiographic probe needs to be facing posteriorly and withdrawn from the midesophagus. With the transducer array at 90°, a short-axis view of the transverse arch can be obtained. It is usually possible to visualize the takeoff of the left subclavian artery, but the left common carotid and brachiocephalic arteries can be difficult or impossible to image and usually require careful clockwise rotation of the probe. A portion of the distal ascending aorta and proximal aortic arch may not be visible because of interposition of the trachea. This "blind spot" can be partially resolved with longitudinal views. An additional view, the deep transgastric view, can sometimes image the entire ascending aorta and often the proximal arch (Figure 12).

D. Three-Dimensional Echocardiography

Real-time 3D TEE, a relatively new technology, appears to offer some advantages over 2D TEE in a growing number of clinical applications.[52-56] However, as of this writing, there is limited information regarding the clinical application of this novel technology to the thoracic aorta.[57]

Moreover, 3D TEE has some limitations. Like 2D TEE, it often fails to adequately visualize the distal ascending aorta and the aortic arch and its branches, because of interposition of the trachea. In addition, spatial imaging of the thoracic aorta is limited because of the 90° image sector, which is too narrow to include long segments of the thoracic aorta and therefore limits topographic orientation. In summary, recent advances in 3D TEE provide an opportunity to reconsider the role of TEE for diagnosing and monitoring patients with aortic diseases. Future experience will be required to verify its benefits and establish its value relative to CT and MRI.

E. Intravascular Ultrasound (IVUS)

IVUS is performed by introducing a miniature, high-frequency (10–30 MHz) ultrasound transducer mounted on the tip of a disposable catheter, through a large arterial (usually femoral) sheath, and advanced over conventional guidewires using fluoroscopic guidance. Less commonly, the IVUS imaging catheter can be inserted into the femoral vein, navigated into the inferior vena cava, and aimed at the adjacent aorta. IVUS produces an axial view that is a 360° real-time image. Consecutive axial images can be obtained during a "pullback" of the ultrasound catheter. This procedure can be safely performed in a few minutes.[58]

Because of its intraluminal position, IVUS permits visualization of the aortic wall from the inside. This intraluminal perspective can provide information that supplements the other imaging modalities.[59-62] Using the pullback technique, luminal diameter, cross-sectional area, and wall thickness can be measured. In addition to providing measurements, IVUS also provides qualitative information on nearly all aortic pathologies, including aortic aneurysms, aortic dissections, atherosclerosis, penetrating ulcers, and traumatic lesions (Figures 13 and 14). Unlike TEE, IVUS can also determine the dissection characteristics in the abdominal aorta.

1. Limitations. The normal aorta appears on IVUS as a circular cross-sectional image with an intact wall and a clear lumen. The ultrasound catheter and the guidewire are seen within the lumen. In some instances, it can be difficult to obtain complete cross-sectional images of the aorta within a single frame of the image display at the arch and locations where the aorta is significantly dilated, because of difficulty maintaining the ultrasound catheter in a central and coaxial orientation and because of the limited penetration with high-frequency transducers. This limitation can be partially overcome by periodic reorientation of the ultrasound catheters. There are also concerns with IVUS measurements. Off-center measurements or those taken in tortuous portions of the aorta (tangential measurements on a curve) do not reflect a true centerline diameter, may provide an oblique slice, and are less accurate than centerline computed tomographic measurements.[63] Another major limitation of IVUS is that it lacks Doppler capabilities (color Doppler can detect flow into small arteries, false luminal flow, and endoleaks). Last, the high cost of the disposable transducers and invasive nature of the technique limit IVUS for most clinical applications other than guidance of endovascular procedures.

F. CT

Multidetector computed tomographic scanners (≥64 detector rows) are the currently preferred technology for aortic imaging. Computed tomographic aortography (CTA) remains one of the most frequently
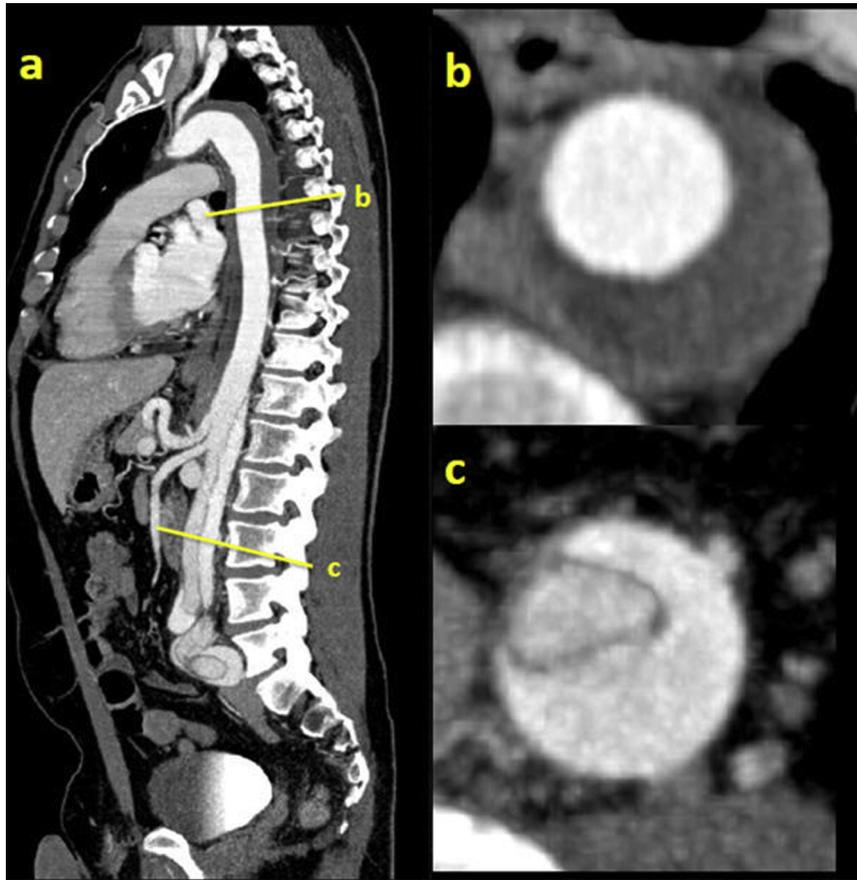
Figure 16 Sagittal multiplanar reformatted **(A)** and double oblique images **(B, C)** from a computed tomographic aortogram in a patient with AAS. The anatomic locations of the planes of **(B)** and **(C)** are marked on **(A)**. Note the transition from a type B acute IMH involving the descending thoracic aorta to a type B aortic dissection involving the abdominal aorta.

used imaging techniques for diagnosis and follow-up of aortic conditions in acute as well as chronic presentations. This popularity reflects its widespread availability, accuracy, and applicability, even for critically ill patients or those with relative contraindications to MRI such as permanent pacemakers and defibrillators. Multidetector CT (MDCT) provides extensive z-axis coverage (in the long axis of the body), with high spatial resolution images acquired at modest radiation exposure within a scan time lasting a few seconds.[1,64] Furthermore, CTA allows simultaneous imaging of vascular structures, including the vessel wall and of solid viscera.[65] The minimization of operator variability and the capacity of delayed reprocessing of source images make it an ideal technique for comparative follow-up studies.[1,64]

The latest innovations in clinical practice include electrocardiographically gated[66] aortic computed tomographic studies leading to high-quality, precise imaging of the ascending aorta, as well as simultaneous evaluation of the coronary arteries[67] (Figure 15). Electrocardiographically gated CTA adds valuable information in the study of aortic pathology involving the aortic root and valve,[68] in congenital heart disease,[69] for simultaneous aortocoronary evaluation,[66] for planning of endovascular therapy,[68,70] for imaging of the postsurgical ascending aorta,[71] and to show dynamic changes of true luminal compression in aortic dissection.[72]

The main drawbacks of CT are the use of ionizing radiation and iodinated contrast media (ICM).[73] Using optimal acquisition methods, large reductions in ionizing radiation dose can be achieved. These include the use of tube current modulation, prospective electrocardiographically

triggered acquisitions, or tube voltage reductions to 80 to 100 kV. Radiation dose becomes most relevant in younger men and premenopausal women. Contrast-associated nephropathy[74] may be avoided or significantly decreased by proper patient hydration and use of the minimum volume of low- or iso-osmolar ICM.[75] The rate of adverse reactions to low-osmolar ICM in CT is approximately 0.15%, with most cases self-resolving and mild.[76] Among patients with renal insufficiency, the rates of contrast-associated nephropathy are low. Pooled data from recently published prospective studies have shown an overall rate of contrast-associated nephropathy of 5% after intravenous injection of ICM in 1,075 patients with renal insufficiency, with no serious adverse outcomes (dialysis or death).[74]

The current generation of computed tomographic scanners is able to significantly decrease the effective radiation dose and the total volume of ICM required for aortic imaging.[77] Additionally, CT for follow-up of aortic expansion may be performed without ICM, relying on noncontrast images only.

1. Methodology. *a. CTA.*—The combination of wide multidetector arrays with short gantry rotation times in ≥64-detector computed tomographic scanners results in standard acquisition times of 3 to 4 sec for the thoracic aorta and <10 sec for the thoracoabdominal aorta and the iliofemoral arteries.

The minimal technical characteristics of state-of-the-art CTA are a slice thickness of ≤1 mm and homogeneous contrast enhancement in the aortic lumen. Complete examination of the aorta from the
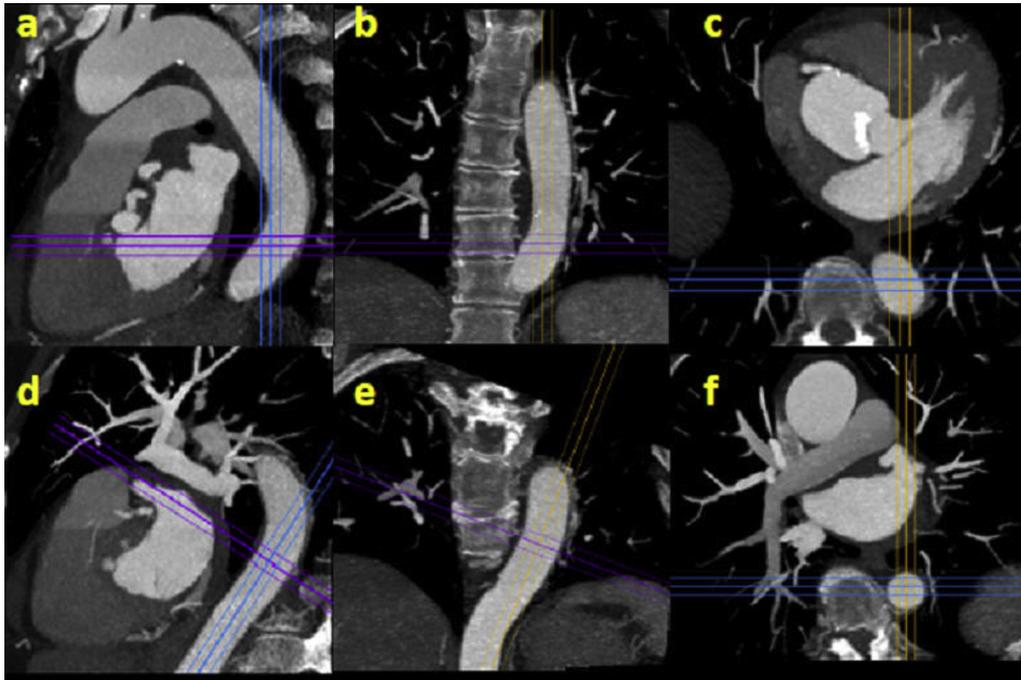
Figure 17 The methodology of double oblique aortic images. Multiplanar reformatted images **(A–F)** in different planes obtained from a computed tomographic aortogram **(C)** corresponds to the axial source image and shows an elliptical descending aorta. The sagittal **(A)** and coronal **(B)** correlates show the reference planes of **(C)** as well as the tortuosity of the aortic segment, which results in a distorted shape. The plane is corrected in both the sagittal **(D)** and coronal **(E)** images to achieve perpendicularity to the aortic flow, resulting in a corrected true transversal image of the aortic lumen, which is circular in this case.

supra-aortic vessels to the femoral arteries is needed for evaluation before transthoracic endovascular aortic repair (TEVAR), but as a general rule the scan length (anatomic scan range) on CTA should be individually tailored to avoid unnecessary exposure to ionizing radiation.[1]

i. Noncontrast CT before Aortography In the acute setting of a suspected AAS, it is important to initiate the protocol by a noncontrast thoracic computed tomographic scan to rule out IMH. This scan identifies concentrated hemoglobin in recently extravasated blood within the aortic wall that shows a characteristically high computed tomographic density (40–70 Hounsfield units),[78] facilitates the characterization of the hematoma,[79] can identify vascular calcifications, and provides a baseline examination for postcontrast evaluation.

ii. Electrocardiographically Gated CTA Motion artifacts involving the thoracic aorta are evident in most (92%) standard nongated computed tomographic angiograms. Because of the limited temporal resolution of CT, imaging artifacts arising from the peduncular motion of the heart, the circular distension of the pulsewave, aortic distensibility, and the hemodynamic state may appear as a "double aortic wall" on standard nongated CTA.[8,23,24,80,81] This finding may also lead to a false-positive diagnosis of a dissection flap[64,67,80] and impair accurate measurement of the aortic root and ascending aorta.[67,82]

Prospective or retrospective synchronization of data acquisition with the electrocardiographic tracing eliminates these artifacts, thereby improving the accuracy of diagnosis and reproducibility of aortic size measurements.[67] Low-dose prospective electrocardiographically gated CT protocols have the advantage of decreased radiation exposure compared with the standard technique.[83]

iii. Thoracoabdominal CT after Aortography A late thoracoabdominal scan (~50 msec after bolus injection) improves the detection
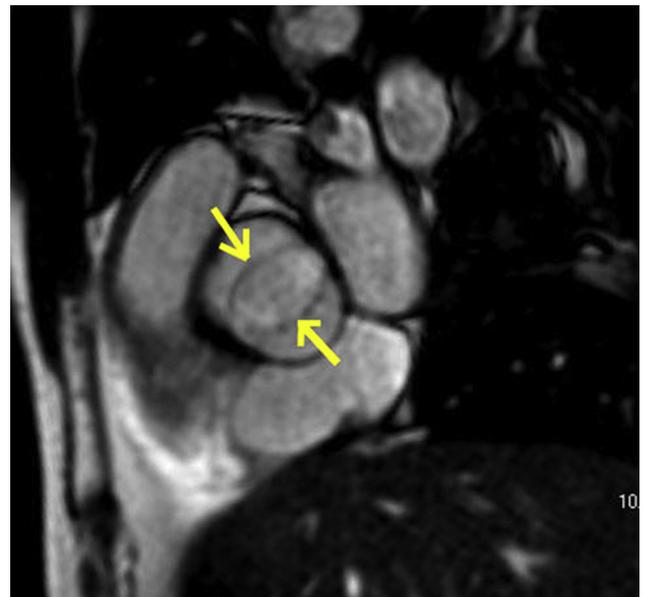
Figure 18 Image from a 44-year-old man with BAV. Single end-systolic image from cine steady-state free precession (SSFP) sequence depicts a bicuspid valve (*yellow arrows*) with normal leaflet thickness and unrestricted opening.

of visceral malperfusion in the acute setting of aortic dissection,[65] detects slow endograft leaks,[84] distinguishes slow flow from thrombus in the false lumen,[85] and allows alternative abdominal diagnoses in the absence of acute aortic pathology.
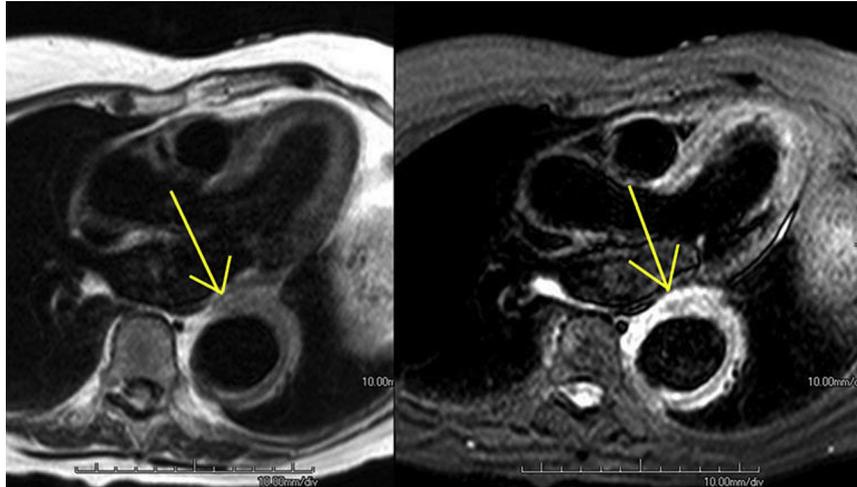
Figure 19 Images from a 54-year-old woman with an elevated sedimentation rate and dilatation of the descending aorta. Wall thickening is well depicted in dark (*black*) blood images (*left, yellow arrow*). Short tau inversion recovery (STIR) images (*right*) demonstrate bright signal in the aortic wall (*yellow arrow*), a result consistent with edema. Surgical repair was performed in this patient, and histology was consistent with GCA.
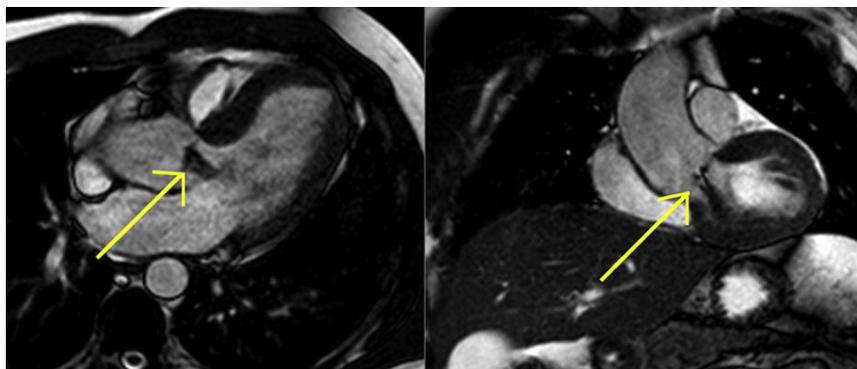
Figure 20 Images from a 60-year-old man with moderately severe aortic insufficiency. Three-chamber (*left*) and coronal oblique (*right*) cine steady-state free precession (SSFP) images depict dark signal (*yellow arrows*) caused by intravoxel dephasing associated with the posteriorly directed jet of insufficiency.

iv. Exposure to Ionizing Radiation Radiation minimization protocols include limiting scan range, prospectively electrocardiographically triggered acquisitions,[66] and using low tube voltage (80–100 kV) for low–body weight patients (<85 kg) without risking loss of diagnostic quality.[77] Application of iterative reconstruction algorithms provide the opportunity for even larger reductions in scan acquisition parameters. Despite progress in radiation reduction, the use of alternative methods such as MRI and echocardiography remains a consideration for serial studies.[1]

v. Measurements In contrast with other aortic imaging techniques, CTA depicts the aortic wall, thereby permitting measurement of both the inner-inner (luminal) and outer-outer (total) aortic diameters. Imaging artifacts from the highly contrasted lumen frequently impair the visualization of a thin and healthy wall in the ascending aorta.[24]

Multiplanar reconstruction of the axial source data can create aortic images in a plane perpendicular to the aortic lumen direction (double-oblique or true short-axis images of the aorta; see Figures 16 and 17). This method corrects shape distortions introduced by aortic tortuosity.[8,86,87] In cases of noncircular aortic shape, both major and minor diameters should be measured. The manual procedure of double-oblique images is time consuming and may add observer variability.[88] Automated aortic segmentation software is available at many institutions but, like most automated software, has limitations and requires manual adjustment.

The measurement technique must be highly reproducible to correctly assess follow-up studies. Accurate assessment of aortic morphologic changes can be achieved by side-by-side comparison of source axial images from two or more serial computed tomographic aortographic examinations with anatomic landmark synchronization and a slice thickness ≤1 mm. Electrocardiographically gated or triggered imaging is an additional refinement that further reduces variability, with a maximum interobserver variability of ±1.2 mm in the ascending aorta.[89] Measures in the axial plane are valid only for aortic segments with a circular shape and craniocaudal axis, like the midascending and the descending aorta.[1] Distortion in the axial image introduced by aortic tortuosity may be minimized by measuring the lesser diameter.[90] Interobserver variability is always higher than intraobserver variability,[91,92] suggesting that follow-up of aortic disease in a specific patient should be performed by a single experienced observer.[88,89]

In summary, CTA is one of the most used techniques in the assessment of aortic diseases. Advantages of CTA over other imaging
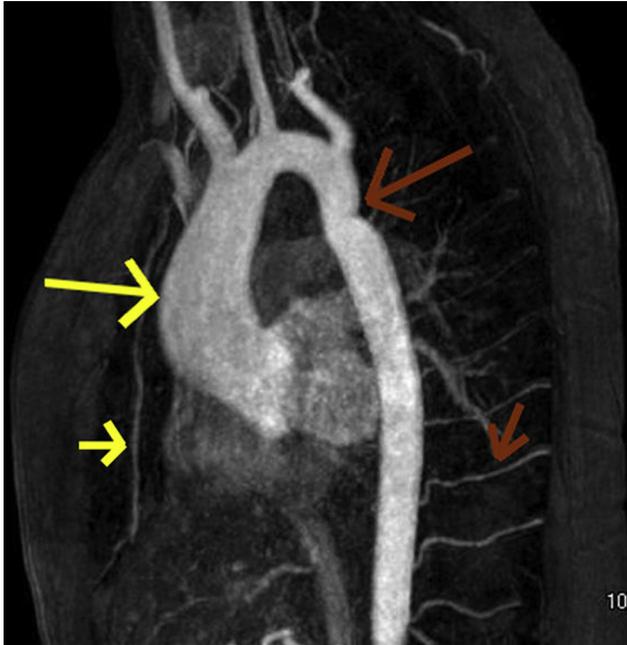
Figure 21 MIP image obtained from MRA in a 60-year-old man with a dilated ascending aorta (*large yellow arrow*). There was suspicion of coarctation of the descending aorta raised by surface echocardiographic imaging; however, MRA revealed a mild kink in the isthmus without significant stenosis (*large red arrow*) and normal-sized intercostal (*small red arrow*) and internal mammary (*small yellow arrow*) arteries, results consistent with pseudocoarctation.

modalities include the short time required for image acquisition and processing, the ability to obtain a complete 3D data set of the entire aorta, and its availability. Moreover, MDCT permits a correct evaluation of the coronary arteries and aortic branch disease. Its main drawbacks are the radiation exposure and need for contrast administration.

G. MRI

MRI is a versatile tool for assessing the aorta and aorta-related pathologies. This imaging modality can be used to define the location and extent of aneurysms, aortic wall ulceration, and dissections and to demonstrate areas of wall thickening related to aortitis or IMH. MRI can also be used for preoperative and postoperative evaluation of the aorta and adjacent structures. Additionally, MRI can provide functional data, including quantification of forward and reverse aortic flow, assessment of aortic wall stiffness and compliance, and aortic leaflet morphology and motion (Figure 18). All of this information is obtainable without the burden of ionizing radiation and, in some instances, without the need for intravenous contrast.

MR images are based on the signal collected from hydrogen nuclei,[93] which align and process along the axis of the magnetic field when a patient enters the scanner. This precession can be altered by applying magnetic field pulses in a controlled fashion to create "pulse sequences." After these pulse sequences are applied, the signal from the hydrogen nuclei is measured and then processed to produce MR images. The versatility of MRI can be attributed to the multiple types of pulse sequences that can be used to define structure, characterize tissue, and quantify function.

1. Black-Blood Sequences. Black-blood MRI sequences, acquired with spin-echo techniques, and often including inversion recovery pulses, are useful for defining morphology across a spectrum of aortic conditions without the need for intravascular contrast medium.[94-97] With these sequences, the use of multiple radiofrequency pulses nulls the signal from moving blood, causing the dark blood appearance; mobile protons in stable or slowly moving structures (e.g., aortic wall) provide the signal in the image. Aortic wall morphology can be defined and tissue characterized with T1- and T2-weighted sequences and their variants, including T2-weighted dark-blood techniques and T2 turbo spin-echo and short-tau inversion recovery sequences (Figure 19).[98-100] Each of these imaging protocols has relative strengths and limitations; for example, T2-weighted MRI is sensitive to areas of increased water content, as is often noted in pathologic conditions, but is limited by relatively low signal-to-noise ratio. MRI of the thoracic aorta can be obtained with high spatial resolution, with in-plane resolution typically in the range of 1.5×1.5 mm and submillimeter acquisition achievable with more specialized MRI sequences.[101,102]

2. Cine MRI Sequences. Bright-blood imaging with approaches such as steady-state free precession and gradient-echo techniques is useful for obtaining high–temporal resolution cine images of flow in the aorta. In these images, the blood pool is bright compared with the adjacent aortic wall, which is typically intermediate in signal. Cine imaging can demonstrate flow within aortic lumens (true or false), and areas of low signal caused by intravoxel dephasing can be seen with complex flow patterns associated with valvular stenosis or regurgitation (Figure 20).[103]

3. Flow Mapping. Velocity-encoded phase-contrast imaging can be used to quantify aortic flow. The phase-contrast technique is based on the fact that protons undergo a change in phase that is proportional to velocity when they pass through a magnetic field gradient consisting of equal pulses that are of opposite polarity and slightly offset in time. Blood flow can be quantified by integrating these measured velocities within the aortic lumen throughout the cardiac cycle with values that have shown strong agreement with phantom models and other measurement approaches.[104] Phase-contrast imaging of the aorta can be used to assess forward flow and stenotic and regurgitant valves[105,106] and can aid in assessment of congenital heart disease.[107] Phase-contrast imaging is typically acquired in a single in-plane or through-plane direction, with some applications allowing flow encoding in multiple directions.[108,109]

4. Contrast-Enhanced MR Angiography (MRA). Contrast-enhanced MRA can provide a 3D data set of the aorta and branch vessels, allowing complex anatomy and postoperative changes to be depicted through postprocessing techniques such as maximum-intensity projection and multiplanar reformatting (Figure 21). In patients with contraindications to contrast or in cases of difficult intravenous access, a 3D angiogram of the aorta can still be obtained with unenhanced segmented steady-state free precession angiography.[110] When precise dimensions of the aortic root and proximal ascending aorta are needed, electrocardiographically gated techniques can be used.[101,110] Improved scanning speed allows time-resolved MRA.[111] Although contrast timing for contrast-enhanced MRA can be a challenge, particularly in the concurrent assessment of the aorta and pulmonary arteries or veins, the use of newer blood-pool contrast agents can circumvent the limitations of traditional interstitial gadolinium contrast agents and in conjunction with
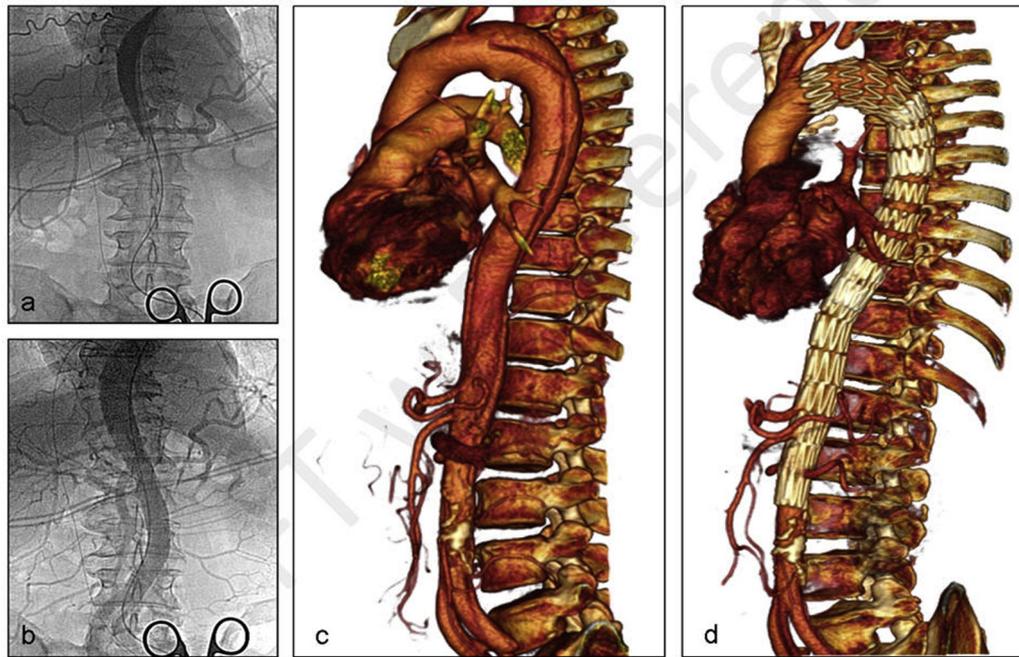
Figure 22 Contrast aortogram (*left*) before **(A)** and after **(B)** endovascular repair showing relief of malperfusion syndrome. Three-dimensional CTA (*right*) shows corresponding computed tomographic angiographic reconstructions before **(C)** and after **(D)** repair.
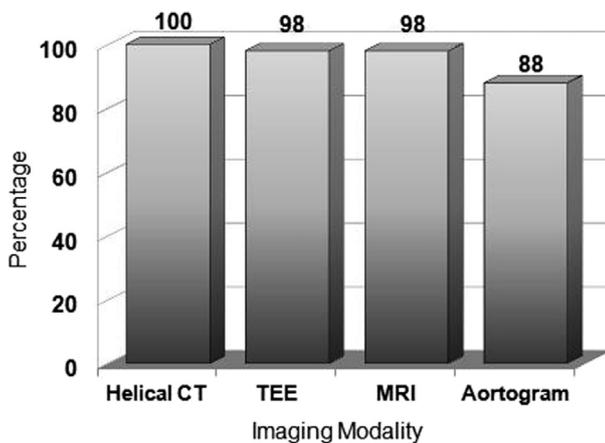
Figure 23 Sensitivity of imaging modalities in evaluating suspected aortic dissection in a meta-analysis of 1,139 patients. © Massachusetts General Hospital Thoracic Aortic Center; reproduced with permission.
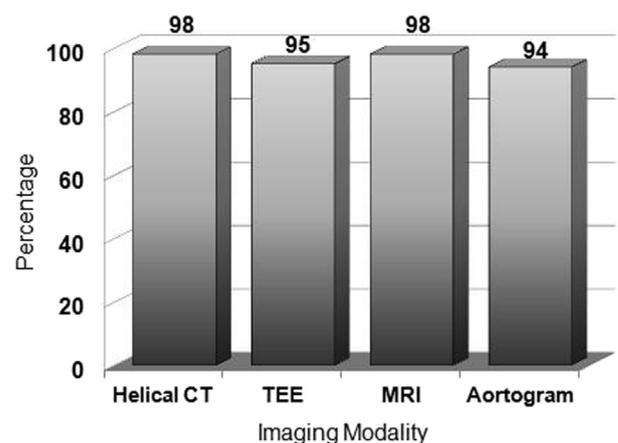
Figure 24 Specificity of imaging modalities in evaluating suspected aortic dissection in a meta-analysis of 1,139 patients. © Massachusetts General Hospital Thoracic Aortic Center; reproduced with permission.

electrocardiographic and respiratory gating has been shown to increase vessel sharpness and reduce artifacts.[112]

MRI may also be used as a tool to investigate aortic physiology. Quantification of stiffness, an important predictor of cardiovascular outcome, can be obtained with pulsewave measurements from high–temporal resolution cine imaging.[113] MRI can provide insight into the elastic properties of the aorta, quantify the resultant blood flow,[114] and estimate aortic wall shear stress.[115]

5. Artifacts. Similar to echocardiographic imaging, MRI artifacts occur. Consequently, consistently recognizing artifacts can prevent misinterpretation. The reader is referred to two excellent reviews for a detailed discussion of these.[116,117]

H. Invasive Aortography

Once considered the reference standard for the diagnosis of acute aortic diseases, invasive catheter-based aortography has largely been replaced by less invasive techniques, including CT, MRI, and TEE.[42,118-124] These noninvasive imaging modalities provide higher sensitivity and specificity for detecting AAS and enable the assessment of aortic wall pathologies that are not seen on lumenograms (as obtained by contrast aortography). In addition, CT, MRI, and TEE also provide greater sensitivity in detecting supporting findings such as pericardial or pleural hemorrhage or effusion. Moreover, aortography is time consuming and incurs a risk for contrast-induced nephropathy. Thus, invasive aortography
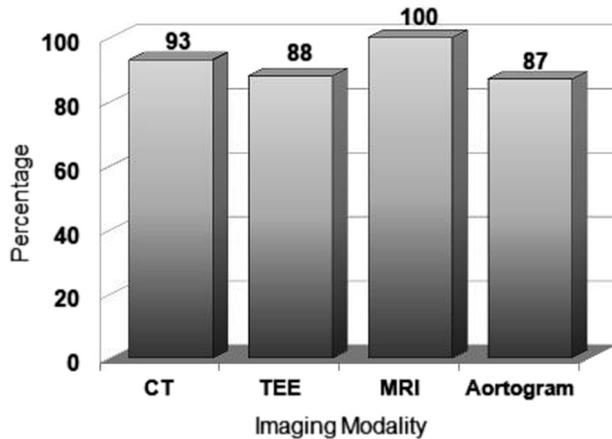
Figure 25 "Real-world" sensitivity of imaging modalities in evaluating suspected aortic dissection in a sample of 618 patients in the IRAD. © Massachusetts General Hospital Thoracic Aortic Center; reproduced with permission.

Table 4 Comparison of five imaging modalities for diagnostic features of AAS

Diagnostic performance	CTA	TTE	TEE	MRA	Angiography
Sensitivity	+++	++	+++	+++	++
Specificity	+++	++	+++	+++	+++
Ability to detect IMH	+++	+	++	+++	−
Site of intimal tear	+++	−	++	+++	++
Presence of AR	−	+++	+++	++	+++
Coronary artery involvement	+	−	++	+	+++
Presence of pericardial effusion	++	+++	+++	++	−
Branch vessel involvement	++	−	+	++	+++

CTA, Computed tomographic angiography; +++, very positive; ++, positive; +, fair; −, no.
Adapted from Cigarroa et al.[182] and Isselbacher.[243]

no longer has a role as a primary diagnostic modality for AAS.[42,120-122,124]

Although invasive aortography has been replaced for diagnostic purposes, it continues to be useful to guide endovascular procedures and to screen for endoleakage. Intraprocedural contrast aortography is often essential to identify aortic side branches and provide important landmarks during the endovascular procedure. Figure 22 reveals the resolution of distal dynamic aortic obstruction after a stent graft was placed in a type B dissection. IVUS is an alternative imaging technique during endovascular procedures.[59,60,62,125,126]

I. Comparison of Imaging Techniques

With advances in imaging technology, there are now multiple modalities well suited to imaging the thoracic aorta, including CTA, MRA, echocardiography, and aortography.[1,127] No single modality is preferred for all patients or all clinical situations. Instead, the choice of imaging modality should be individualized on the basis of a patient's clinical condition, the relevant diagnostic questions to be answered, and local institutional factors such as expertise and availability. A few pertinent comments follow.

When assessing broadly for the presence of thoracic aortic aneurysms (TAAs), or to size such aneurysms, CTA or MRA is preferred,

Table 5 Practical assessment of five imaging modalities in the evaluation of suspected AAS

Advantages of modality	CTA	TTE	TEE	MRA	Angiography
Readily available	+++	+++	++	+	+
Quickly performed	+++	+++	++	+	+
Performed at bedside	−	+++	+++	−	−
Noninvasive	+++	+++	+	+++	−
No iodinated contrast	−	+++	+++	+++	−
No ionizing radiation	−	+++	+++	+++	−
Cost	++	+	++	++	+++

CTA, Computed tomographic angiography; +++, very positive; ++, positive; +, fair; −, no.
Adapted from Cigarroa et al.[182] and Isselbacher.[419]

Table 6 Benign conditions or findings that can mimic AAS on the basis of imaging studies

Aortitis
Atheromatous plaque
Prior surgery of aorta
Pericardial recess
Remnant of a nonpatent PDA
Artifacts on CT (streak and motion)
Reverberation artifacts in ascending aorta on TEE
Innominate vein
Periaortic fat and hemiazygos sheath may mimic IMH

PDA, Patent ductus arteriosus.

as all segments of the thoracic aorta are well visualized. As well, the aorta and its branches can be displayed in multiple planar views, which permits more accurate diameter measurements than axial imaging. In addition, both modalities can provide a reconstructed, surface-shaded 3D display of the aorta, which is helpful in demonstrating the anatomic relations of the aorta and its branch vessels. In contrast, TEE is not generally preferred for routine aortic imaging, because it is semiinvasive, is relatively unpleasant for the patient, does not provide full visualization of the arch vessels, and does not permit easy identification of landmarks when comparing serial examinations to assess aortic changes over time.

When the region of clinical interest is specifically the aortic root, such as in screening for or following Marfan syndrome, TTE may be preferred, because the aortic root is generally well visualized and easily measured, whereas on conventional nongated CTA, the aortic root may be poorly visualized because of its angulation and significant motion artifact produced by the beating heart. On the other hand, echocardiography is less consistently able to image the distal ascending aorta, aortic arch, and descending thoracic aorta. To image these segments, CTA and MRA are preferred. Another consideration in selecting an imaging modality is the previous modality used. When following a patient with an enlarging aortic aneurysm, it is best to use the same imaging modality for future imaging, so that a comparison of one study with the next is comparing apples to apples rather than apples to oranges.

For imaging of suspected AAS, the primary consideration should be the accuracy of the imaging modality, given the serious
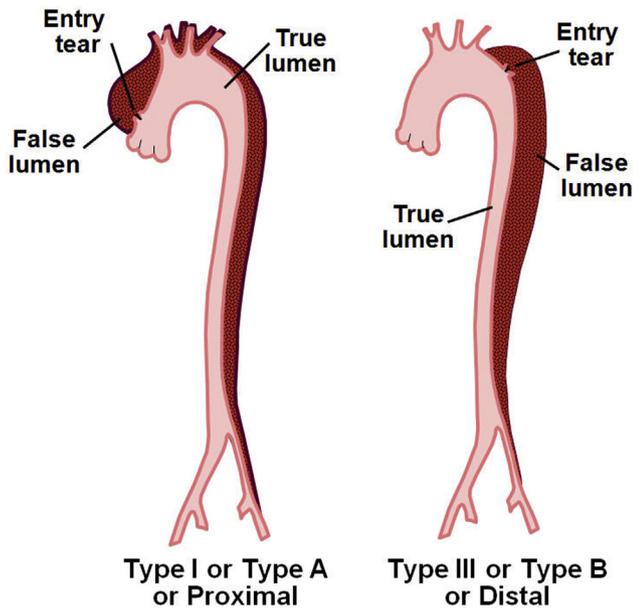
Figure 26 Diagram illustrating the two commonly used classification systems for aortic dissection. In the older of the two, the DeBakey system, type I dissection originates in the ascending aorta and propagates distally to includes at least the arch and typically the descending aorta. Type II dissection, not shown (the least common type) originates in and is confined to the ascending aorta. Type III dissection originates in the descending thoracic aorta (usually just distal to the left subclavian artery) and propagates distally, usually to below the diaphragm. The Stanford system, in a simpler scheme, divides dissections into two categories: those that involve the ascending aorta, regardless of the site of origin, are classified as type A, and those beginning beyond the arch vessels are classified as type B. The majority of dissections, whether type A or type B, propagate beyond the diaphragm to the iliac arteries.

consequences of false-positive and particularly of false-negative results. There have been a number of studies carried out over the past two decades comparing CTA, MRA, TEE, and aortography for the diagnosis of aortic dissection, and a recent meta-analysis by Shiga et al.[122] showed that CTA, MRA, and TEE are all outstanding, with sensitivities of 98% to 100%, as shown in Figure 23. On the other hand, aortography has a sensitivity of only 88%, perhaps reflecting the fact that IMH often goes undetected with this technique. In the same meta-analysis, the specificity of the four imaging modalities was roughly equivalent at 94% to 98%, as shown in Figure 24. Therefore CTA, MRA, and TEE are all reasonable first-line imaging studies to choose for this purpose.

It is important to note, however, that the research studies that evaluate the accuracy of imaging modalities are usually performed at centers of excellence and interpreted by designated experts in aortic imaging, and it is therefore reasonable to suspect that accuracy may be lower when the same imaging modalities perform in the "real-world" setting. Indeed, a report from the International Registry of Acute Aortic Dissection (IRAD) examined this very question, and the results are shown in Figure 25.[120] The real-world sensitivity of both CTA and TEE is lower than in the above meta-analysis, probably reflecting a lesser degree of expertise among the readers. Interestingly, the real-world sensitivity of MRA remained at 100%, which may reflect the fact that MR angiograms tend to be read by specialists (e.g., vascular radiologists) rather than general radiologists

(e.g., emergency department radiologists). The diagnostic and practical features of each of the five common imaging modalities are summarized in Tables 4 and 5.

III. ACUTE AORTIC SYNDROMES

A. Introduction

The term AAS[128] refers to the spectrum of aortic pathologies, including classic aortic dissection, IMH, penetrating aortic ulcer (PAU), and aortic aneurysm rupture (contained or not contained). Although the pathophysiology of these heterogeneous conditions differs, they are grouped because they share common features: (1) similar clinical presentation ("aortic pain"), (2) impaired integrity of the aortic wall, and (3) potential danger of aortic rupture requiring emergency attention.[128-133] Moreover, some of these conditions may represent stages in the evolution of the same process. We have elected not to include, as some authors do, aortitis and traumatic aortic rupture, because they have totally distinct clinical and pathophysiologic profiles.[128] Clinical databases, such as the IRAD, have contributed tremendously to our knowledge of these acute aortic pathologies.[134]

Because of the life-threatening nature of these conditions, prompt and accurate diagnosis is paramount. Misdiagnosis of these conditions, usually because of confusion with myocardial ischemia, can lead to untimely deaths. Table 6 lists some less urgent conditions that can potentially mimic AAS.

The noninvasive imaging techniques that play a fundamental role in the diagnosis and management of patients with AAS include CTA, TTE, TEE and MRI. Some patients may require more than one noninvasive imaging study and, in rare instances, invasive aortography may be necessary. Imaging is used to confirm or exclude the diagnosis, determine the site(s) of involvement, delineate extension, and detect complications to plan the most appropriate management approach.

B. Aortic Dissection

1. Classification of Aortic Dissection. Accurate classification of aortic dissection is important because significant differences in clinical presentation, prognosis, and management depend on the location and extent of the dissection. Figure 26 illustrates the two commonly used classifications: the DeBakey system (types I, II, and III)[124,125] and the Stanford system (types A and B).[126] Dissections involving the aortic arch without involving the ascending aorta are classified as type B in the Stanford system. The majority of dissections, whether type A or type B, propagate beyond the diaphragm to the iliac arteries.

The appropriate management of aortic dissections depends not only on the location of the dissection but also on the time that has elapsed between onset of the process and the patient's presentation. Although the adjectives *acute*, *subacute*, and *chronic* are often applied, there is no standard definition for these time periods.[135-138] There is a 24-hour "hyperacute" period during which dissections involving the ascending aorta carry a risk for rupture approaching 1% per hour. Studies have shown that 75% of aortic dissection–related deaths occur in the initial 2 weeks. At the opposite extreme are "old dissections" encountered incidentally during aortic imaging or surgery. These are clearly "chronic." Hirst *et al.*, Levinson *et al.*, and DeBakey considered an aortic dissection to be "acute" when the onset of
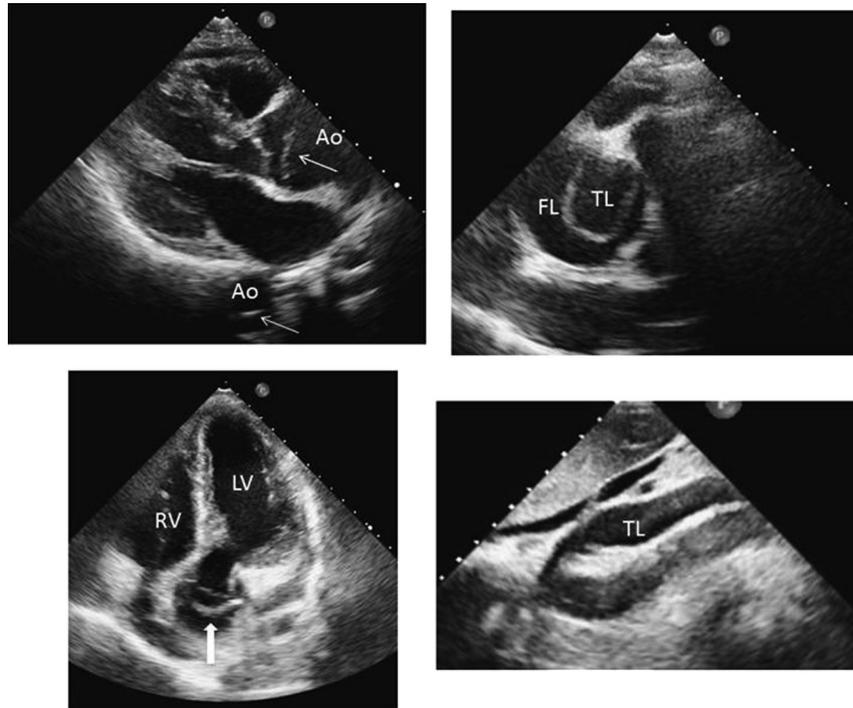
Figure 27 Acute aortic dissection evaluated by TTE. (*Top left*) Parasternal long-axis view showing a flap in the proximal ascending aorta (Ao) (*arrow*) and a flap in the thoracic descending aorta (*arrow*). (*Top right*) Parasternal short-axis view of the proximal ascending aorta showing the presence of a typical true lumen (TL) and false lumen (FL) divided by a flap. (*Bottom left*) Five-chamber apical view showing the presence of a flap in the proximal ascending aorta (*arrow*). (*Bottom right*) Subcostal view of the descending abdominal aorta with a clear flap inside the aortic lumen. *LV*, Left ventricle; *RV*, right ventricle.
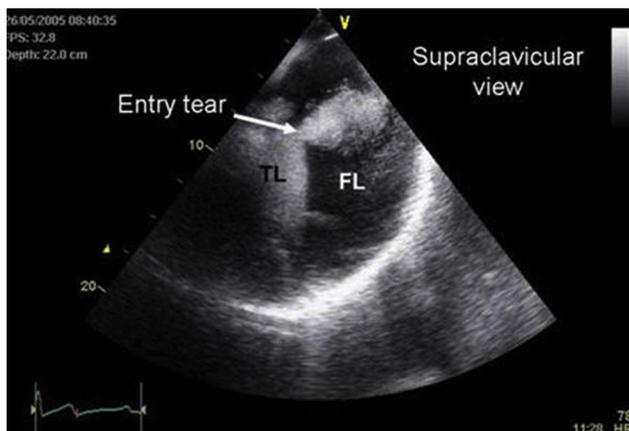
Figure 28 Proximal descending thoracic aorta visualized from supraclavicular view. Use of contrast echo illustrates entry tear (*arrow*) by showing contrast emanating from true lumen (TL) to false lumen (FL).
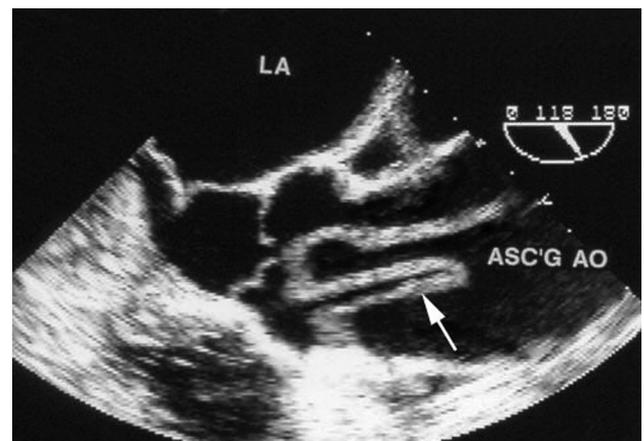
Figure 29 Transesophageal echocardiographic longitudinal view of the aortic root and ascending aorta (ASC'G AO) illustrating a folded, convoluted dissection flap (*arrow*) that had marked oscillation in real-time. *LA*, Left atrium.

symptoms was <2 weeks in duration at the time of diagnosis.[139-143] The subsequent 2-month period was designated "subacute," and beyond the second month, an aortic dissection was termed "chronic". We endorse this classification, as it has some basis in pathologic observations. The extremely high initial death rate declines after 2 weeks. Moreover, friable aortic tissue extends beyond 2 weeks. By 6 to 8 weeks, the outer aortic wall has largely "healed," in that it has developed scar, a reasonable marker for the beginning of the chronic stage.[144] It must be acknowledged that any time-based division of "acute" from "subacute" and "subacute" from "chronic" is arbitrary.

Nevertheless, such distinctions are necessary for analyzing outcomes. Moreover, some imaging features of acute and chronic dissections are different. In chronic dissection, the dissection flap tends to be thicker, more echodense, and relatively immobile (as distinct from the oscillating flaps seen in acute dissection).

2. Echocardiography (TTE and TEE). The sensitivity of 2D TTE by fundamental imaging was previously reported to be only 70% to 80% for the detection of type A dissection. However, because of new transducers with improved resolution, harmonic imaging, and

Table 7 Role of echocardiography in detecting evidence of aortic dissection and echocardiographic definitions of main findings

Diagnostic goals	Definition by echocardiography
Identify presence of a dissection flap	Flap dividing two lumens
Define extension of aortic dissection	Extension of the flap and true/false lumens in the aortic root(ascending/arch/ descending abdominal aorta)
Identify true lumen	Systolic expansion, diastolic collapse, systolic jet directed away from the lumen, absence of spontaneous contrast, forward systolic flow)
Identify false lumen	Diastolic diameter increase, spontaneous contrast and or thrombus formation, reverse/delayed or absent flow
Identify presence of false luminal thrombosis	Mass separated from the intimal flap and aortic wall inside the false lumen
Localize entry tear	Disruption of the flap continuity with fluttering or ruptured intimal borders; color Doppler shows flow through the tear
Assess presence, severity and mechanisms of AR	Anatomic definition of the valve (bicuspid, degenerated, normal with/without prolapse of one cusp); dilation of different segments of the aorta; flap invagination into the valve; severity by classic echocardiographic criteria
Assess coronary artery involvement	Flap invaginated into the coronary ostium; flap obstructing the ostium; absence of coronary flow; new regional wall motion abnormalities
Assess side-branch involvement	Flap invaginated into the aortic branches
Detect pericardial and/or pleural effusion	Echo-free space in the pericardium/pleura
Detect signs of cardiac tamponade	Classic echocardiographic and Doppler signs of tamponade
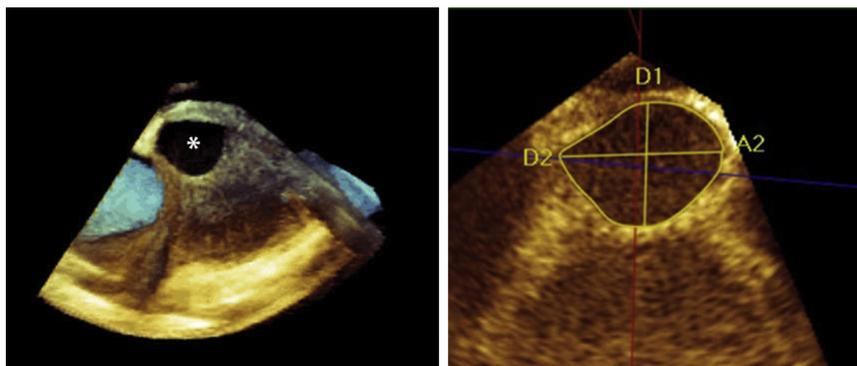
Figure 30 Three-dimensional TEE showing the entry tear of a type B aortic dissection located in the proximal descending aorta. (*Left*) Live 3D image showing a large entry tear (*asterisk*). (*Right*) Maximum orthogonal diameters (D2 and D1) are 17 and 11 mm, and area measured by full volume is 1.5 cm^2.

contrast enhancement, the sensitivity of TTE has improved to approximately 85% on the basis of recent data from Cecconi et al.[145] and Evangelista et al.[146] Therefore, TTE may be of some use as the initial imaging modality, especially in the emergency room (Figure 27). In addition, TTE provides assessment of left ventricular contractility, pericardial effusion, aortic valve function, right ventricular size and function, and pulmonary artery pressure, which may facilitate the diagnosis of chest pain due to myocardial ischemia and/or infarction, pulmonary embolism, or pericardial disease and may identify dissection complications such as aortic regurgitation (AR) in an early fashion. Moreover, the use of contrast agents may further improve the accuracy, as illustrated in Figure 28.[146] Nevertheless, because of the potential catastrophic nature of type A aortic dissection, negative results on TTE should not be considered definitive, and further imaging should follow.

Moreover, TTE is less sensitive for the diagnosis of type B dissection, because the descending thoracic aorta (located farther from the transducer) is imaged less easily and accurately. Therefore, although TTE may be diagnostic in many instances, its role is predom-inantly that of a screening procedure. TEE, on the other hand, is highly accurate for establishing the diagnosis of both type A and type B acute aortic dissection. Since the landmark multicenter European Cooperative Study,[119] several additional studies have demonstrated the high accuracy of TEE, with sensitivity approaching 100%.[42,147-150]

a. Echocardiographic Findings.—The diagnostic hallmark of aortic dissection is a mobile dissection flap that separates the true and false lumens (Figure 29). Important features of the dissection flap include oscillation or motion that is independent of the aorta itself, visualization in more than one view, and clear distinction from reverberations from other structures, such as a calcified aortic wall, catheter in the right ventricular outflow tract, pacemaker wire, or pericardial fluid in the transverse oblique sinus.

The true and false lumens can almost always be differentiated. In the descending thoracic aorta, the false lumen is usually larger than the true lumen. The dissection flap typically moves toward the false lumen in systole (systolic expansion of the true lumen) and toward the true lumen in diastole (diastolic expansion of the false lumen),

Table 8 Mechanisms of AR in type A aortic dissection

1. Dilatation of the aortic root leading to incomplete aortic leaflet coaptation
2. Cusp prolapse (asymmetric dissection depressing cusp[s] below annulus)
3. Disruption of aortic annular support resulting in flail leaflet
4. Invagination/prolapse of dissection flap through the aortic valve in diastole
5. Preexisting aortic valve disease (e.g., bicuspid valve)

sometimes causing compression of the true lumen. Moreover, the characteristics of blood flow vary in the true and false lumens. In the true lumen, antegrade systolic flow is rapid enough to create brighter shades of red or blue on color Doppler. In contrast, flow in the false lumen is generally slower, producing duller colors. In fact, flow in the false lumen may be absent or in the opposite direction (retrograde) to that of the true lumen. The sluggish flow in the false lumen may result in the presence of spontaneous echo contrast, sometimes referred to as "smoke." The false lumen may also contain variable degrees of thrombus. Additional findings in patients with aortic dissection include dilatation of the aorta, compression of the left atrium, AR, pericardial and/or pleural effusion, and involvement of the coronary arteries. Table 7 summarizes the main echocardiographic findings in aortic dissection. Three-dimensional TEE may provide information beyond what can be obtained with 2D TEE.[151] For example, the size of the entry tear size and its relationship to surrounding structures may be shown in greater detail, allowing better morphologic and dynamic evaluation of aortic dissection (Figure 30). Such information may be particularly helpful when the flap spirals around the long axis of the aorta. Moreover, 3D TEE demonstrates the dissection flap not as a linear structure but as a sheet of tissue of variable thickness in the long, short, or oblique axis. This may make it possible to distinguish a true dissection flap from an artifact when it is relatively immobile. In addition, multiplane 3D TEE provides a more rapid and accurate evaluation of the aortic arch than 2D TEE.

b. Detection of Complications.—AR occurs in approximately 50% of patients with type A aortic dissection. The presence, severity, and mechanism(s) of AR may influence surgical decision making and aid the surgeon in deciding whether to spare, repair, or replace the aortic valve.[148,152,153] The mechanisms of AR are listed in Table 8, and several of these are illustrated in Figure 31. These mechanisms will be discussed in greater detail in section III.B.6, "Use of TEE to Guide Surgery for Type A Aortic Dissection."

A pericardial effusion in an ascending aortic dissection is an indicator of poor prognosis and suggests rupture of the false lumen in the pericardium. Echocardiography is the best diagnostic technique for estimating the presence and severity of tamponade. Periaortic hematoma and pleural effusion are best diagnosed by CT. The presence of periaortic hematoma has also been related to increased mortality.[154,155]

TEE is capable of imaging the ostia and proximal segments of the coronary arteries in nearly all patients and may demonstrate coronary involvement due to dissection (flap invagination into the coronary ostium and origin of coronary ostium from the false lumen).[148] Color Doppler is useful for verifying normal or abnormal or absent flow into the proximal coronary arteries. Detection of segmental wall motion abnormalities of the left ventricle by TTE or TEE may

also help identify this complication. Color Doppler also reveals reentry sites (often multiple, as in Figure 32), which explain why the false lumen often remains patent over time.

c. Limitations of TEE.—The limitations of TEE for evaluating patients with aortic dissection are few but deserve mention. Interposition of the trachea between the ascending aorta and the esophagus limits visualization of the distal ascending aorta and proximal arch. In a small number of patients, the dissection may be limited to this area, making detection more difficult. In addition, the cerebral vessels (especially the brachiocephalic and left common carotid arteries) can be difficult to image by TEE. Moreover, the celiac trunk and superior mesenteric artery cannot be consistently imaged by TEE, and CT is considered the gold standard for detecting complications below the diaphragm. Last, TEE depends largely on operator skill for image acquisition and interpretation. Reverberation artifacts, especially in the ascending aorta, can mimic a dissection flap and result in a false-positive diagnosis.[156-159] Knowledge of mediastinal and para-aortic tissues (e.g., the hemiazygos sheath, the thoracic venous anatomy and common anatomic variants) is essential.

3. CT. Data from the IRAD published in 2000 showed that among 464 patients with acute aortic dissections (62% with type A), nearly two-thirds underwent CTA as the initial diagnostic imaging. The computed tomographic data in this study were acquired on older generation scanners, which may explain the fact that most patients underwent several imaging tests (average, 1.8 tests).[129]

A more recent IRAD publication, now including 894 patients, showed that the "quickest diagnostic times" were achieved when the initial test was CT, whereas the initial use of MRI or catheter-based aortography resulted in significantly longer diagnostic times.[160]

Today, newer generation modern multidetector computed tomographic scanners are ubiquitous even in remote-area hospitals throughout the United States and Europe and are usually staffed and readily available 24 hours a day. In 2007, according to 2011 health data from the Organisation for Economic Co-operation and Development, there existed 34.3 computed tomographic scanners per million population in the United States, and 185 computed tomographic examinations were performed per 1,000 patients in US hospitals.

Computed tomographic angiographic protocols are robust and relatively operator independent. Computed tomographic angiographic protocols that are designed to exclude dissections typically begin with low-dose noncontrast CT to exclude the possibility of IMH, followed by contrast-enhanced computed tomographic angiography. The coverage includes the entire thorax, abdomen, and pelvis to allow delineation of the extent of a flap and its extension into branch vessels and to evaluate for end-organ ischemia (e.g., bowel or kidneys), and possible extravasation.[1] Examples of computed tomographic angiography are illustrated in Figures 33 and 34.

Diagnostic accuracy is extremely high for the exclusion of aortic dissection (98%–100%).[122,161,162] However, false positives for the detection of type A dissection near the aortic arch may infrequently occur with older generation computed tomographic scanners, which may lead to unnecessary operations.[163-166] Single-slice spiral computed tomographic scanners and early-generation multidetector computed tomographic scanners frequently demonstrate pulsation artifact in the ascending aorta, which occasionally may mimic type A dissection (pseudoflaps).[80,164,165] However, aortic pulsation artifact and pseudoflaps can be completely eliminated with the use
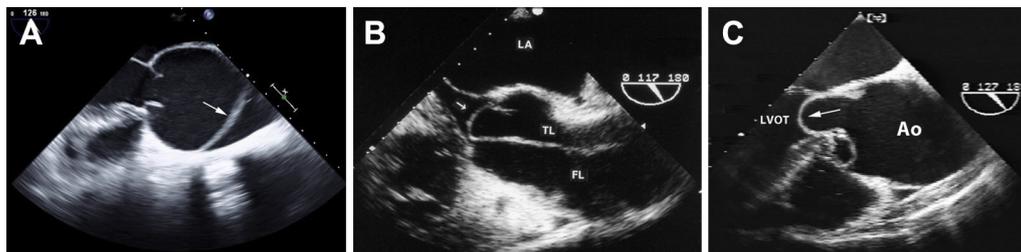
Figure 31 Mechanisms of AR in the setting of aortic dissection. **(A)** Transesophageal echocardiogram demonstrating absence of coaptation of aortic leaflets due to dilatation of the aortic root (the most common mechanism of aortic insufficiency associated with type A dissection). Arrow designates the dissection flap. **(B)** Transesophageal echocardiogram of the aortic root illustrating prolapse of the aortic valve (*small arrow*) due to extension of the dissection to the annulus causing AR (not shown). *FL*, False lumen; *LA*, left atrium; *TL*, true lumen. **(C)** Transesophageal echocardiogram of the aortic root and ascending aorta (Ao) illustrating a dissection flap (*arrow*) prolapsing through the aortic valve into the left ventricular outflow tract (LVOT), resulting in AR in this patient.
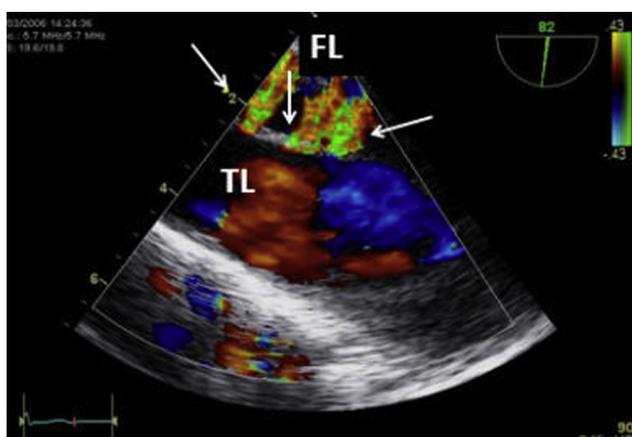
Figure 32 Longitudinal view of a transesophageal echocardiogram with color Doppler illustrates multiple reentry sites (*arrows*) demonstrating flow from true lumen (TL) to false lumen (FL). Reentry sites are the major reason the false lumen remains patent over time.

of electrocardiographically gated computed tomographic angiographic acquisitions.[167,168] Therefore, it is advisable to use electrocardiographic gating or triggering if ascending aortic pathology is suspected.[80,167,169,170] False-positive results on CT leading to unnecessary surgery for aortic dissection have not been reported to date with the use of newer generation electrocardiographically gated multidetector computed tomographic angiographic scans.

Surgery or transcatheter intervention in type B dissection may be indicated if there is occlusion of major aortic branches leading to end-organ ischemia or expansion of the aortic diameter or interval extension of the dissection flap.[171] MDCT allows imaging of the entire aorta and iliac system within seconds and allows delineating the intimal flap extension into aortic arch vessels and the abdominal aorta and its branches as well as the iliac system, which may determine the feasibility of stent-graft repair.[170,172] Entry and reentry sites, aortic diameters, and the relationships between true and false lumen can be defined using multiplanar multidetector computed tomographic reformations. MDCT also allows the determination of end-organ perfusion, such as asymmetric or absent enhancement of kidneys in case of renal artery occlusion.[72,167]

Given the multiplanar reformation capabilities that, unlike MRI, can be applied post hoc, and 3D imaging capabilities, CT has

extremely high retest reliability for measurement of aortic diameters on follow-up scans. The multiplanar reconstruction capabilities facilitate endovascular treatment planning and may allow the determination of proximal fenestrations that may be amenable to endovascular repair.[173] Because determination of these features is important, reporting of the extension of dissection and aneurysms into branch vessels and secondary end-organ hypoperfusion are considered "essential elements" of aortic imaging reports.[1] Gated MDCT may determine proximal extent of the flap into coronary artery ostia, or the aortic valve, as well as presence of pericardial effusion or hemopericardium.[168]

Gated MDCT may simultaneously exclude the presence of obstructive coronary artery disease in acute dissections,[174] as well as coronary artery dissection and aortic valve tears.[167,170,175] In addition, combination of a gated or triggered thoracic computed tomographic angiographic acquisition with a nongated abdominal and pelvic acquisition is feasible at low radiation doses.[172,176-178]

Further dose reduction using axial prospective electrocardiographic triggering (compared with spiral retrospective gating) computed tomographic angiography at a tube potential of 100 kV allows the further reduction of radiation doses without impairment of image quality of the aorta or coronary arteries.[179]

The "triple rule-out" protocol for assessing acute chest pain in the emergency room is rarely needed and is neither technically suitable nor medically necessary on a routine basis. Optimal protocols for coronary CT angiography, for pulmonary embolism, and for aortic dissection differ, and "triple rule-out" CT is not optimal for all three. Given the increased radiation and contrast exposure and the lack of accurate diagnostic data for aortic dissection, there are no grounds to recommend triple rule-out CT for this condition. If there is a reasonable clinical suspicion for aortic dissection, then the highest quality study for this specific indication should be performed.[180,181]

In summary, CT angiography is readily available throughout the United States and Europe; is most often the first imaging test when acute aortic dissection is suspected; has extremely high diagnostic accuracy; allows the evaluation of the entire aorta and its branches, the coronary arteries, the aortic valve, and the pericardium; and results in the shortest time to diagnosis compared with other imaging modalities, therefore allowing rapid initiation of therapy. Disadvantages of CT include the need for iodinated contrast material and ionizing radiation, although substantial dose reductions have recently been achieved with newer hardware technology and imaging protocols, and this issue may be of less concern in the setting of AAS.
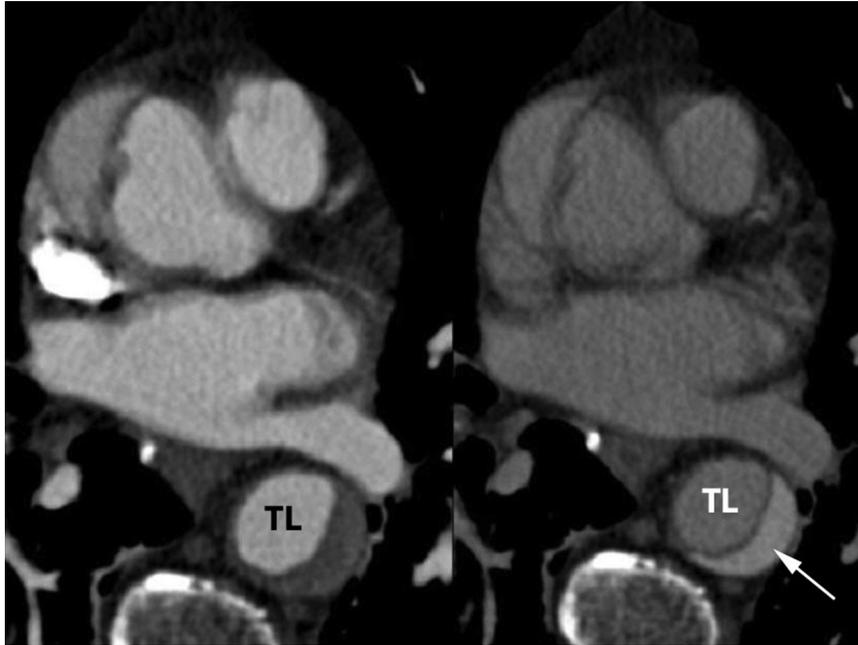
Figure 33 Axial source images from the computed tomographic aortogram (*left*) and the late-phase computed tomographic study (*right*) performed in a patient with AAS. The additional late acquisition rules out false lumen thrombosis, showing late enhancement and retention of contrast-enhanced blood in the false lumen.
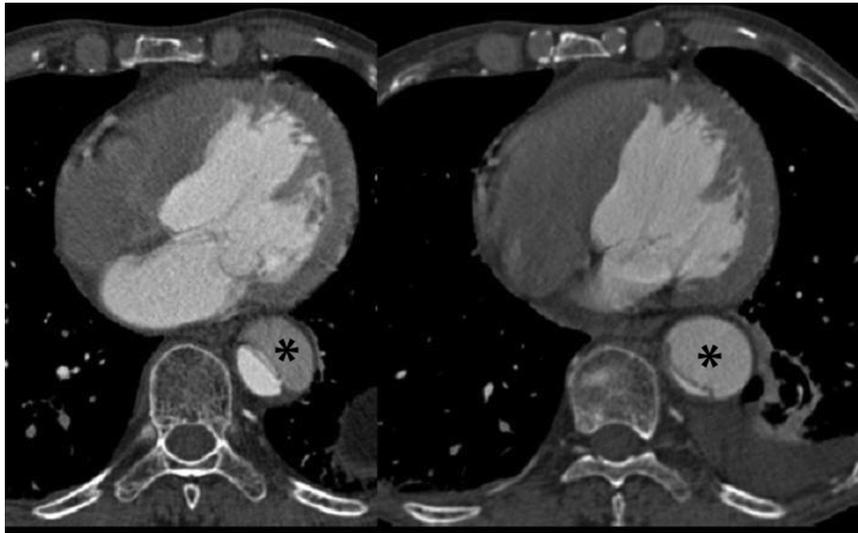
Figure 34 Evolutive changes in a type B chronic aortic dissection. The comparison is performed by synchronizing thin (0.75-mm) axial images of the baseline and follow-up computed tomographic aortograms. The images show an expansion of the false lumen (*asterisk*) with compression of the true lumen, with an overall mild external expansion of the dissected descending thoracic aorta. Note the similarity of mediastinal and posterior thoracic wall anatomic markers.

4. MRI of Aortic Dissection. Early identification of aortic dissection and precise characterization of anatomic details are critical for clinical and surgical management of this condition.[182] Imaging of suspected dissection should address not only the presence of a dissection flap and its extent but also the entry and reentry points, presence and severity of aortic insufficiency, and flow into arch and visceral branch vessels. MRI, which can address all of these issues noninvasively, provides high spatial and contrast resolution and functional assessment with an imaging time of 20 to 30 min. Specifically, MRI has very high sensitivity (97%–100%) and specificity (94%–100%) for diagnosing dissection.[161,183,184] MRI also provides imaging without the burden of ionizing radiation, an important consideration for patients who undergo serial assessments of a known aortic dissection.

MRI does have potential limitations in this patient population. Although the scan times for MRI are relatively short, they are significantly longer than the scan times for CT angiography. Additionally, physiologic waveforms are challenging to obtain within the MRI scanner environment.[185,186] Although cardiac rhythm, blood pressure, and oximetry can be monitored with MRI-appropriate equipment, caring for patients within an MRI scanning area can be difficult in
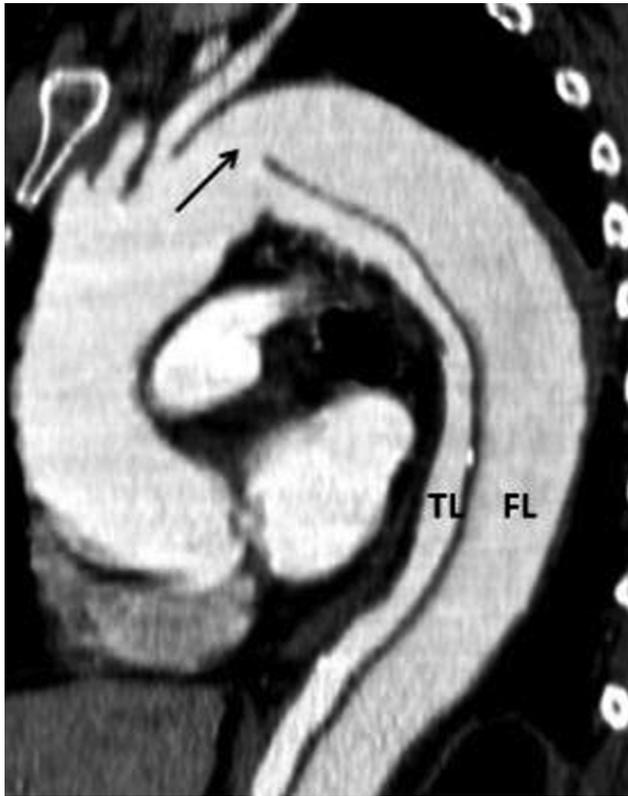
Figure 35 MR image extracted from a dynamic cine steady-state free precession (SSFP) sequence in a patient with type B aortic dissection arising just after the origin of the left subclavian artery. The arrow shows the entry tear. *FL*, false lumen; *TL*, true lumen.

emergent or unstable clinical scenarios that may be associated with aortic dissection.

A combination of dark-blood and bright-blood images in axial and oblique planes oriented to the aorta allows the detection and characterization of intimal flaps. True and false lumens can be differentiated by patterns of flow and by anatomic features (Figures 35 and 36).[185] The false lumen can often be identified on spin-echo images by a higher intraluminal signal intensity attributable to slower flow and may be characterized by web-like remnants of dissected media.[187] Cine bright-blood imaging can also be used to directly visualize flow patterns within true and false lumens. Associated anatomic findings outside of the aorta on MRI may also be of interest, such as high signal intensity within pericardial effusion on dark-blood imaging, indicating the possibility of the ascending aorta rupturing into the pericardial space.[188] Phase-contrast imaging can provide flow quantification of aortic insufficiency associated with dissection and can also allow definition of entry and reentry sites and differentiation of slow flow and thrombus in the false lumen. Newer 3D phase-contrast approaches have shown promise in further defining the flow characteristics and associated parameters of aortic dissection, such as wall stress.[189]

Contrast-enhanced 3D MRA provides 3D data, results that allow postprocessing and detailed assessment of aortic and large-branch vessel anatomy in cases of dissection.[190] The dynamics of aortic flow can also be evaluated with time-resolved MRA.[191] Imaging with blood-pool contrast agents allows steady-state phase scanning, which can improve spatial resolution and better demonstrate the amount of thrombus within the false lumen.[192]

5. Imaging Algorithm. Aortic dissection is a life-threatening condition that is associated with high early mortality and therefore requires prompt and accurate diagnosis. Numerous publications have sought to establish the relative merits of CT, TEE, and MRI as first-line imaging modalities. In truth, each diagnostic method has its strengths and weakness, as previously discussed. The optimal choice of imaging modality at a given institution should depend not only on the proven accuracy (all three are highly accurate) but also on the availability of the techniques and on the experience and confidence of the physician performing and interpreting the technique. CT has become the most commonly used first-time imaging modality partly because it is more readily available on a 24-hour basis.[129] TEE may be the preferred imaging modality in the emergency room, if an experienced cardiologist is available, because it provides immediate and sufficient information to determine if emergency surgery will be required. Although CT may be less accurate for determining the degree and mechanism of AR, this can be evaluated by TTE and/or intraoperative TEE. The relative advantages and disadvantages of the various imaging modalities are summarized in Table 9.

There are situations in which a single imaging test is insufficient to confidently confirm or exclude the diagnosis of aortic dissection. A strong clinical suspicion accompanied by a negative initial imaging test should dictate a second test, as should a situation in which the first test is nondiagnostic. This may be due to technical limitations or interpretative difficulties (e.g., distinguishing an artifact from a true flap). Because of the importance of establishing a correct diagnosis in this potentially life-threatening condition, obtaining a second or even a third imaging modality should be considered.

In summary, CT is an excellent imaging modality for diagnosing aortic dissection and is most often the initial modality when aortic dissection is suspected because of its accuracy, widespread availability, and because it provides rapid evaluation of the entire aorta and its branches. TTE may be useful as the initial imaging modality in the emergency room, especially when the aortic root is involved. Contrast may improve its accuracy. TTE may also complement CT by adding information about the presence, severity, and mechanism(s) of AR, pericardial effusion, and left ventricular function. TEE may be a second-line diagnostic procedure when information from CT is limited (sometimes not certain if the ascending aorta is involved). TEE can define entry tear location and size, mechanism(s) and severity of AR, and involvement of coronary arteries. TEE should be performed immediately before surgery in the operating room and should be used to monitor the operative results. All of these modalities may be helpful for identifying associated lesions at the aortic valve level (e.g., bicuspid aortic valve [BAV]) that may require a specific surgical strategy.

6. Use of TEE to Guide Surgery for Type A Aortic Dissection. TEE should be performed in the operating room in all patients during repair of type A aortic dissection. Even if the diagnosis has been "established" with a preoperative imaging modality, confirmation by intraoperative TEE before initiating cardiopulmonary bypass will minimize the possibility of a false-positive diagnosis. Once the diagnosis of aortic dissection has been confirmed, the primary purpose of the intraoperative TEE is to detail the anatomy of the dissection and to better define its physiologic consequences. The origin and proximal extent of the dissection flap and the dimensions of the aorta at the annulus, sinuses of Valsalva, and STJ are important
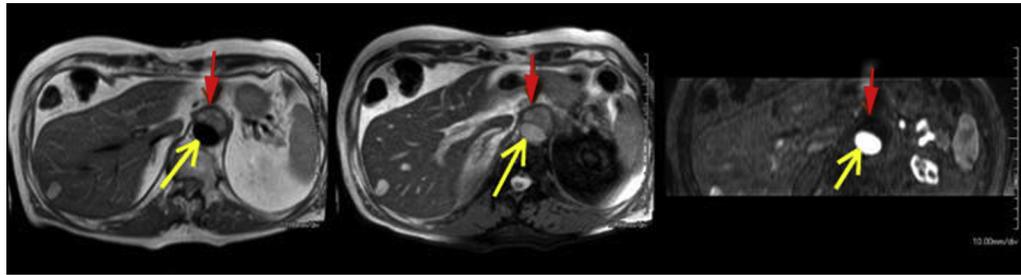
Figure 36 Images from a 55-year-old woman with chronic type B aortic dissection. The true lumen (*yellow arrow*) is characterized by lack of signal in the dark blood image (*left*), bright signal in the single-shot steady-state free precession (SSFP) image (*middle*), and bright signal (caused by contrast filling) in the MR angiographic image (*right*). False lumen (*red arrow*) is notable for intermediate signal on dark blood and single-shot SSFP sequences, and lack of signal is noted in the thrombosed false lumen on MRA.

Table 9 Recommendation for choice of imaging modality for aortic dissection

Modality	Recommendation	Advantages	Disadvantages
CT	First-line	• Initial test in >70% of patients* • Widely available, quickest diagnostic times • Very high diagnostic accuracy • Relatively operator independent • Allows evaluation of entire aorta, including arch vessels, mesenteric vessels and renal arteries	• Ionizing radiation exposure • Requires iodinated contrast material • Pulsation artifact in ascending aorta (can be improved with ECG gating)
TEE	First- and second-line	• Very high diagnostic accuracy in thoracic aorta • Widely available, portable, convenient, fast • Excellent for pericardial effusion, and presence, degree and mechanism(s) of AR and LV function • Can detect involvement of coronary arteries • Safely performed on critically ill patients, even those on ventilators • Optimal procedure for guidance in OR	• Operator dependent (depends on skill of operator) • "Blind spot" upper ascending aorta, proximal arch • Not reliable for cerebral vessels, celiac trunk, SMA, etc. • Reverberation artifacts can potentially mimic dissection flap (can be differentiated from flaps in vast majority) • Semi-invasive
TTE	Second-line	• Often initial imaging modality in ER • Provides assessment of LV contractility, pericardial effusion, RV size and function, PA pressure • Presence and severity of AR	• Sensitivity not sufficient distal to aortic root • Descending thoracic aorta imaged less easily and accurately • Misses IMH and PAU
MRI	Third-line	• 3D multiplanar, and high resolution • Very high diagnostic accuracy • Does not require ionizing radiation or iodinated contrast • Appropriate for serial imaging over many years	• Less widely available • Difficult monitoring critically ill patients • Not feasible in emergent or unstable clinical situations • Longer examination time • Caution with use of gadolinium in renal failure
Angiography	Fourth-line	• Rarely necessary	• Often misses IMH (up to 10%–20% of ADs) • Long diagnostic time • Requires ICM • Morbidity • Less sensitivity than CT, TEE, and MRI

AD, Aortic dissection; *ECG*, electrocardiographic; *ER*, emergency room; *ICM*, iodinated contrast media; *IMH*, intramural hematoma; *LV*, left ventricular; *OR*, operating room; *PA*, pulmonary artery; *PAU*, penetrating atherosclerotic ulcer; *RV*, right ventricular; *SMA*, superior mesenteric artery.
*In IRAD.

for determining whether to replace the ascending aorta alone or to also replace the root.

Up to 50% of type A aortic dissections are complicated by moderate or severe AR, and there are several mechanisms by which this may occur.[193] Most commonly, aortic dilatation, be it acute or chronic, leads to aortic leaflet tethering that, in turn, results in incomplete aortic valve closure and secondary AR.[194] When the dissection flap extends proximally into the sinuses of Valsalva (i.e., below the level of the STJ), it can effectively detach one or more of the aortic valve commissures from the outer aortic wall; the aortic valve leaflets are then no longer

suspended from the STJ and therefore prolapse in diastole, causing significant AR. Less commonly, the dissection process is extensive and results in a long, complex dissection flap, a piece of which may itself prolapse through the aortic valve into the left ventricular outflow tract in diastole, preventing normal leaflet coaptation and causing AR.[195] Remarkably, in some patients, the dissection causes prolapse of the aortic leaflets, which would otherwise produce severe AR, yet a lengthy piece of the dissection flap falls back against the aortic valve in early diastole and essentially smothers the orifice and prevents regurgitation. In such cases, Doppler may reveal only mild AR
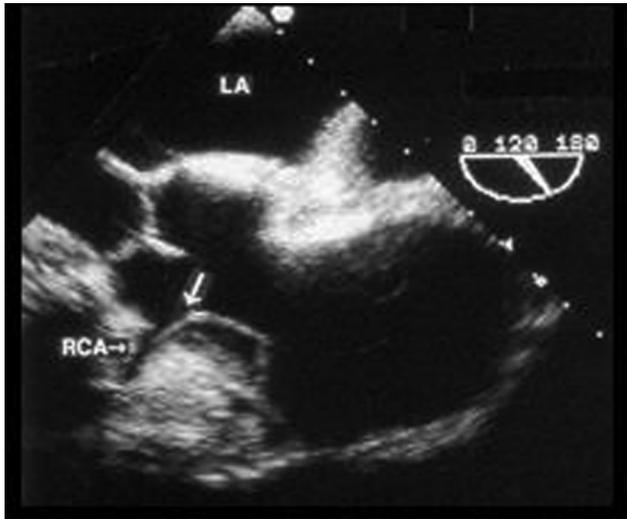
Figure 37 Transesophageal echocardiogram from a patient with type A aortic dissection that illustrates the dissection flap (*arrow*) entering the ostium of the right coronary artery (RCA). *LA*, Left atrium.

Table 10 Prevalence of IMH (as percentage of aortic dissection or nontraumatic AAS)

Author	Year	n	%	Source
Mohr-Kahaly	1994	27/114	23%	420
Nienaber	1995	25/195	12.8%	421
Keren	1996	10/49	20%	422
Harris	1997	19/84	23%	423
Vilacosta	1997	15/88	17%	229
Nishigami	2000	59/130	45%	424
Ganaha	2002	66/725	9%	425
Evangelista	2003	68/302	22%	154
Attia (meta-analysis)	2009	—	17%	426
	Totals	289/1,687	17%	

despite significant disruption of the aortic valve. Alternatively, a circumferential dissection of the ascending aorta can tear away and produce a tubular proximal dissection flap that prolapses the aortic valve in diastole, essentially akin to "intussusception," producing severe AR.[196] These patients may not require repair or replacement of the aortic valve.

Some patients with aortic dissection have more than one of these anatomic processes occurring simultaneously. Fortunately, most of these anatomic causes of AR are correctable during surgery, so informing the surgeon in detail about the anatomic findings and mechanisms of AR may permit successful repair rather than replacement of the aortic valve. Type A aortic dissection can sometimes compromise flow to one of the coronary arteries, the right coronary artery more often than the left. Although coronary involvement may be evident preoperatively with ischemic changes on electrocardiography, the process may be dynamic, so the echocardiographer should examine both coronary ostia to determine if they are compromised (Figure 37). Color Doppler is useful to document normal or disturbed or absent flow in each coronary artery.

The emergent surgical treatment of type A dissection is limited to proximal aortic segments in the majority of patients. However, when the dissection extends into the abdominal aorta, patients are at risk for malperfusion, which occurs from either of two mechanisms: static obstruction occurs when the dissection flap extends into a branch artery and limits antegrade arterial flow, and dynamic obstruction occurs because of marked compression of the true lumen by a distended false lumen, resulting in impaired forward flow through the true lumen to feed the otherwise patent branch arteries. Because TEE is usually unable to visualize the abdominal branch arteries themselves, the presence of static obstruction cannot be readily assessed. However, TEE can identify true luminal compression in the distal descending thoracic aorta and confirm impaired systolic flow by Doppler. Although such findings do not necessarily indicate clinical malperfusion, at the very least they represent the substrate for dynamic malperfusion, and it is therefore important to bring this to the attention of the surgeon.

On occasion, distension of the false lumen will compress the true lumen and produce malperfusion of organs or limbs.[197] Usually, stan-

dard surgical repair of the ascending aorta restores flow to the true lumen partially or fully. If the true lumen remains compressed and is associated with malperfusion, further intervention (e.g., endovascular stent grafting or percutaneous fenestration of the dissection flap to decompress the false lumen) may be necessary.[198] On occasion, in patients with organ malperfusion, endovascular stent grafts may be placed before repair of the ascending aorta.

Preoperative TEE should also evaluate the pericardial space for the presence of an associated pericardial effusion. In some cases, aortic dissection may be accompanied by a small serous effusion, but more often, the presence of an effusion is due to bleeding into the pericardial space. In such cases, the blood pooling acutely in the pericardial space will typically clot and appear echocardiographically as a mass sliding back and forth within a layer of pericardial fluid. This finding of a clot within the pericardial fluid heralds potential catastrophic aortic rupture and should therefore be communicated promptly to the surgeon.

After the repair of a type A aortic dissection, the echocardiographer should systematically reexamine the anatomic features of the aortic valve and proximal aorta to make sure that the surgical correction has been adequate (including exclusion of the entry tear and exclusion of all proximal communications) and that the aortic valve is competent. In addition, when the dissection has extended to the distal aorta, the echocardiographer should reexamine the descending thoracic aorta to determine the presence of adequate flow through the true lumen.

7. Use of Imaging Procedures to Guide Endovascular Therapy. The success of TEVAR is critically dependent on high-quality, accurate imaging before, during, and after stent-graft placement.[199] Although invasive catheter-based angiography (Figure 14) is the method of first choice for the guidance of aortic stent-graft placement,[42] TEE offers definite advantages in the hands of an experienced examiner.[59,60,62,200,201] TEE is particularly useful in the operating room and provides contributions at various phases of the procedure. In patients with type B aortic dissection, guidewire advancement and positioning can be guided by both fluoroscopy and TEE. However, unlike fluoroscopy, TEE can differentiate between true and false lumens and can confirm correct guidewire placement in the true lumen and prevent misplacement of a catheter or wire before deploying any device. In atherosclerotic aneurysms, protruding aortic plaques at the
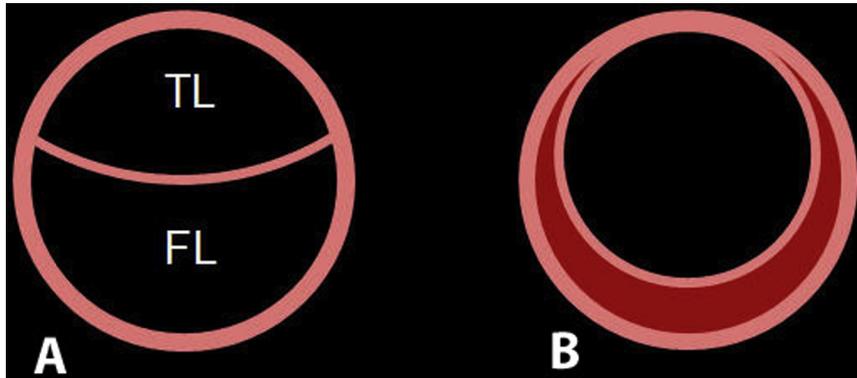
Figure 38 **(A)** Diagram of classic aortic dissection on the left illustrating a dissection flap separating a true lumen (TL) from a false lumen (FL). **(B)** An IMH lacks a dissection flap and true and false lumens and instead appears as a thickened aortic wall, typically with crescentic thickening as in this diagram. Notice that the aortic lumen is preserved (remains round and smooth walled).

proximal neck may impede tight adhesion between the stent-graft and aortic wall, leading to dangerous proximal leaks. These plaques are easily detected by TEE and not by angiography or fluoroscopy. Therefore, just before proximal stent-graft deployment, TEE is essential for selecting an aortic wall segment without protruding plaques and confirming selection of the stent-graft diameter.[59,60,62]

Orientation and navigation as guided by TEE can be complemented by the use of IVUS (usually with 10-MHz transducers) over a guidewire, thereby confirming or correcting navigation in the true lumen even at the level of the abdominal aorta and iliac arteries. In addition, intraprocedural IVUS may clarify the mechanism of branch vessel compromise when malperfusion is suspected (e.g., dynamic vs static obstruction of a branch vessel).[125,126] Thrombus formation within the false lumen can also be visualized by spontaneous echo contrast, and IMH is easily depicted as crescent-shaped or circular wall thickening. Device sizing can be very challenging with aortic dissections because of the possibility of compromising the true lumen. After endovascular stent graft implantation, IVUS also enables dynamic evaluation of the success of the procedure.[200,202-204]

Angiography, TEE, and IVUS are used for evaluating the expansion of stent grafts, verification of branch anastomosis and the beginning of false lumen thrombosis, and reevaluation of improved malperfusion. During a procedure, TEE may be superior for assessing retrograde type A dissection and can provide immediate information on left ventricular function. With the use of color Doppler, TEE is superior to angiography, and especially to IVUS, in the detection of endoleaks after stent graft implantation.[59,62,125] In several studies, TEE provided decisive additional information to angiography and fluoroscopy, leading to successful procedural changes in up to 40% to 50% of patients.[59,60,62] After stent-graft deployment, color Doppler TEE is highly useful for detecting persistent leaks that can be promptly resolved by balloon dilatation or further stent-graft implantations.[205] Most of these leaks are not visible on angiography. To maximize sensitivity for persistent leaks, reduced Doppler scale (25 cm/sec) can improve color signal detection. However, by itself, this can lead to false-positive diagnoses of leaks, because immediately after implantation, Dacron porosity can create temporary low blood flow through the stent (and seen with low-velocity color flow Doppler), especially when systolic blood pressure is >120 mm Hg. To prevent false-positive diagnosis of leaks, pulsed Doppler velocity assessment permits distinction between Dacron porosity (usually with velocity <50 cm/sec) and the faster flow of true persistent leaks

(usually >100 cm/sec) with higher sensitivity than angiography.[126] In aortic dissection, TEE is also useful for detecting small distal reentry tears not visible on angiography; thoracic reentry tears can subsequently be resolved by additional stent-graft deployment.[59,62,125] TEE is partially limited for visualizing the brachiocephalic and left common carotid artery ostia, and this information may be crucial to proximal positioning of the stent graft. It should be noted that TEE is useful when a Dacron stent graft is used, whereas it is not useful with polytetrafluoroethylene or Gore-Tex prostheses because polytetrafluoroethylene acts as a barrier to ultrasound.

In a recent small study, intraluminal phased-array ultrasound imaging proved to be superior to IVUS and to TEE in detecting communications between the true and false lumens of aortic dissection.[200] However, IVUS and intraluminal phased-array ultrasound imaging catheters are disposable and therefore more expensive than TEE and cannot be performed simultaneously with stent-graft placement, whereas TEE is suited to parallel imaging and intraprocedural monitoring.

In summary, TEE and IVUS are particularly useful for guiding endovascular procedures requiring hybrid monitoring techniques, such as a combination of stent-graft placement and open visceral bypass grafting.[59,62,206] TEE is crucial for selecting and monitoring surgical treatment and detecting complications that may require intervention. Thus, intraoperative TEE should be considered mandatory. TEE may also be useful during endovascular procedures in patients with descending aortic dissections by differentiating true and false lumens, permitting correct guidewire placement in the true lumen, helping guide correct stent-graft positioning, and identifying suboptimal results and presence of leaks.

8. Serial Follow-Up of Aortic Dissection (Choice of Tests). After the diagnosis and management of acute aortic dissection, imaging techniques play a major role in prognosis assessment and in the diagnosis of complications during follow-up. Morphologic and dynamic information may be useful for predicting aortic dissection evolution and identifying the subgroup of patients with a greater tendency to severe aortic enlargement. Regular assessment of the aorta should be made 1, 3, 6 and 12 months after the acute event, followed by yearly examinations.

After discharge, variables related to greater aortic dilatation were entry tear size, maximum descending aorta diameter in the subacute phase, and the high-pressure pattern in false lumen. Maximum aortic

Table 11 Imaging features of IMH
1. Focal aortic wall thickening (crescentic > concentric)
2. Preserved luminal shape with smooth luminal border
3. Absence of dissection flap and false lumen
4. Echolucent regions may be present in the aortic wall
5. Central displacement of intimal calcium

diameter in the subacute phase was a significant predictor of progressive dilatation because, according to the law of Laplace, larger aortic diameters are associated with increased wall stress.

TEE provides prognostic information in acute type A dissection beyond that provided by clinical risk variables. A flap confined to ascending aorta or a completely thrombosed false lumen has proved to have a protective role.[207] Finally, increased false luminal pressure is another important factor predictive of future false luminal enlargement. In the majority of cases, high false luminal pressure relates to a large entry tear without distal emptying flow or reentry site of similar size. It may be difficult to identify the distal reentry communication; thus, in the presence of a large entry tear, indirect signs of high false luminal pressure such as true luminal compression, partial false luminal thrombosis, or the velocity pattern of the echocardiographic contrast in the false lumen should be considered.

CT is the technique most frequently used for serial follow-up of aortic dissection. The large field of view of CT permits identification of anatomic landmarks that allow measurements to be obtained at identical levels as previous measurements. CT has excellent reproducibility for aortic size measurement, has excellent accuracy for identifying entry tears and distal reentry sites, and allows the assessment of vessel malperfusion. MRI appears to be an excellent alternative technique for following patients treated medically or surgically in AAS. MRI avoids exposure to ionizing radiation and the nephrotoxic contrast agents used for computed tomographic angiography and is less invasive than TEE. Furthermore, the integrated study of anatomy and physiology of blood flow can provide information that may explain the mechanism(s) responsible for aortic dilatation. Time-resolved MRA can provide additional dynamic information on blood flow in entry tears. Velocity-encoded cine MR sequences have a promising role in the functional assessment of aortic dissection by virtue of quantification of flow in both lumens and the possibility of identifying hemodynamic patterns of progressive dilatation risk. For planning surgery or endovascular repair, it is very useful to demonstrate the course of the flap, entry tear location, false luminal thrombosis, aortic diameter, and main arterial trunk involvement. Both computed tomographic angiography and MRA take advantage of postprocessing software capabilities that allow multiplane reconstructions, maximum-intensity projection (MIP) and volume-rendering reconstructions.

9. Predictors of Complications by Imaging Techniques. a. Maximum Aortic Diameter.–Maximum aortic dilatation after the acute phase is a major predictor of complications during follow-up. Both CT and MRI are superior to TEE for measuring the aortic size distal to the aortic root. Aneurysmal dilatation of the dissected aorta will occur in 25% to 40% of patients surviving acute type B aortic dissection. Secondary dilatation of the aorta during follow-up of aortic dissection has been considered a significant predictor of aortic rupture. A descending thoracic aortic diameter > 45 mm after the acute phase and the presence of a patent false lumen have been related to aneurysm development of the false lumen (>60 mm)
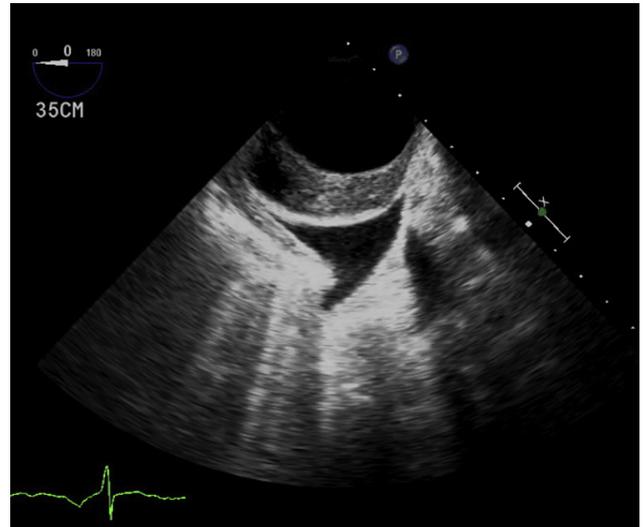
Figure 39 Transesophageal echocardiogram of a cross-sectional view of the descending thoracic aorta at 35 cm from the incisors illustrates a crescentic-shaped IMH.
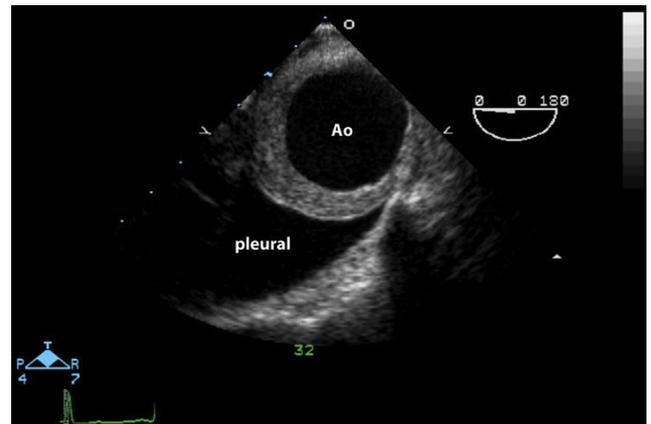
Figure 40 Transesophageal echocardiogram of a cross-sectional view of the descending thoracic aorta (Ao) illustrating a concentric IMH. There is a small right pleural effusion.

and surgical reintervention. A diameter > 60 mm or annual growth > 5 mm implies a high risk for aortic rupture.[208] Other studies have shown maximum false luminal diameter in the proximal part of descending aorta to be a predictor of complications.[209] However, this diameter has low reproducibility, mainly due to movement of the intimal flap.

b. Patent False Lumen.–In addition to aortic diameter, a consistent predictor of outcomes in acute type B aortic dissection has been the hemodynamic status of the false lumen, classically divided into either a thrombosed false lumen or a patent false lumen. Persistence of patent false lumen in the descending aorta is common in both dissection types and has been strongly associated with poor prognosis. Total thrombosis of the false lumen, considered a precursor of spontaneous healing, is a rare event, even after surgical repair of a type A aortic dissection. A persistently patent false lumen can be found in most type B aortic dissections during follow-up and in >70% of type A

Figure 41 This diagram illustrates the different appearances of the hemiazygos sheath (a normal structure), atherosclerotic plaque, and an aneurysm containing a mural thrombus from an IMH.

aortic dissections after surgical repair.[197] After type A dissection repair, patent false lumen in the descending aorta is linked to survival at 5 years. Thus, use of intraoperative TEE to direct elimination of the entry tear, not just repairing the ascending aorta, is of great importance.

c. Partial False Luminal Thrombosis.—Studies have shown that completely thrombosed false lumens have improved outcomes, whereas patent false lumens carry an increased risk for aortic expansion and death.[197,210] However, in the IRAD series, partial thrombosis of the false lumen, defined as the concurrent presence of both flow and thrombus and present in a third of patients, was the strongest independent predictor of follow-up mortality, with a 2.7-fold increased risk for death compared to patients with patent false lumen without thrombus formation.[199] Prospective studies using CT or MR for assessing the whole aorta are required to confirm these results.

d. Entry Tear Size.—The prognostic value of entry tear size was evaluated by Evangelista *et al.*,[211] who documented that a large entry tear is a strong predictor of late mortality and of the need for aortic surgical treatment. An entry tear size ≥ 10 mm was an optimal cutoff value for predicting dissection-related adverse events, with sensitivity of 85% and specificity of 87%. TEE and CT are superior to MRI in the assessment of entry tear size and location. Recently it has been shown that agreement between entry tear area by 3D TEE and CT is excellent.[151] When the entry tear is small, the flow volume that enters the false lumen is low, and thus the false luminal pressures will be low. Therefore, the combination of a large entry tear and indirect signs of high pressure of the false lumen, distinguishable by imaging techniques, should be considered a predictor of aortic enlargement and adverse events and warrants close follow-up.

e. True Luminal Compression.—True luminal compression is an indirect sign of high false luminal pressure. However, true luminal compression assessment may be limited by intimal flap movement during the cardiac cycle, as well as local factors such as in spiral dissection, that may reduce reproducibility of this finding. Patients with clear overall true luminal compression have a higher risk for rapid false luminal enlargement and further aortic complications.

10. Follow-Up Strategy. After discharge, follow-up by CT or MRI is indicated depending on technique availability, preferential information sought, and patient characteristics such as age, renal function, and test tolerance at 3, 6, 12 months and annually thereafter.
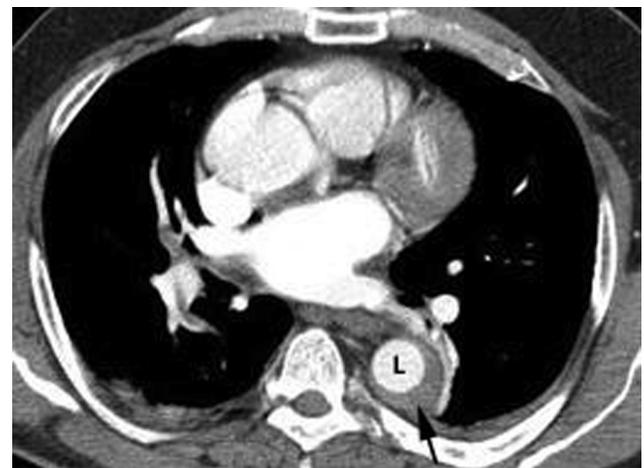
Figure 42 CTA illustrating an IMH. The arrow points to the crescent-shaped thickened wall due to the IMH. Note the lumen (L) is preserved.

C. IMH

1. Introduction. Advances in aortic imaging technology, including TEE, CT, and MRI, have led to increasing recognition of aortic IMH among patients with AAS. IMH, generally considered to be a variant of aortic dissection, accounts for approximately 10% to 25% of AAS (Table 10). IMH was first described in 1920 as "dissection without intimal tear"[212] and was believed to result from rupture of the vasa vasorum, allowing bleeding between the elastic lamina of the aortic media.[79,212,213] However, recent findings suggest that at least some IMHs may be initiated by small intimal tears that are undetectable by current aortic imaging modalities and are often overlooked on gross inspection of the aorta at the time of surgery or autopsy.[214-217] IMH is not a single entity but can be associated with several conditions, including spontaneous ("typical") aortic dissection, penetrating ulcer, aortic trauma, and iatrogenic dissection (cardiac catheterization, cardiac surgery).

2. Imaging Hallmarks and Features. The imaging hallmarks of classic aortic dissection—the presence of a dissection flap and the presence of a double channel aorta—are both absent in IMH (Figure 38) In addition, there is usually no reentry site. General imaging features of IMH are listed in Table 11. Typically, IMH appears as thickening of the

Table 12 IMH: key points

- IMH represents hemorrhage into medial layer of aorta
- Absence of dissection flap between a double-channel aorta
- Crescentic or concentric thickening of aortic wall
- Can progress to localized or frank dissection or rupture
- IMH thickness and maximal aortic diameter predict risk for progression
- CT appearance is high-attenuation eccentric or concentric wall thickening on noncontrast image
- Subtle wall thickening can be missed at inexperienced centers

Figure 43 Diagram illustrating the characteristic features of a penetrating atherosclerotic ulcer: presence of severe atherosclerosis and penetration of the ulcer or "outpouching" into the media.

Figure 44 Gross pathology specimen from a patient with a ruptured penetrating atherosclerotic ulcer (*small arrow*) associated with IMH and blood external to the aortic wall (*large arrow*).

aortic wall > 0.5 cm in a crescentic or concentric pattern (Figures 39 and 40). As mentioned, a mobile dissection flap is absent. The aortic lumen's shape is preserved, and the luminal wall is curvilinear and usually smooth, as opposed to a rough, irregular border seen with aortic atherosclerosis and penetrating ulcer, although both may coexist. There is no Doppler evidence of communication between the hematoma and the true lumen, but there may be some color Doppler flow within the hematoma. There may also be areas of echolucency within the aortic wall hematoma. IMH is generally a more localized process than classic aortic dissection, which typically propagates along the entire aorta to the iliac arteries. IMH may weaken the aortic wall and either progress outward with aortic expansion and/or rupture or inward with disruption of the intima-media, resulting in typical aortic dissection. Evangelista et al. described seven evolution patterns: regression, progression to classical dissection with longitudinal propagation, progression to localized dissection, development of fusiform aneurysm, development of saccular aneurysm, development of pseudoaneurysm, and persistence of IMH. Therefore, serial imaging is necessary to rule out progression in patients who receive only medical treatment, because clinical signs and symptoms cannot predict progression. Although there are no established guidelines for the optimal frequency and longitudinal duration for surveillance imaging of patients with IMH, Evangelista et al.,[154] on the basis of the significant dynamic evolution of IMH, recommended imaging at 1, 3, 6, 9, and 12 months from the time of diagnosis. Once stability has been documented, surveillance imaging may be annual.

IMHs present a more difficult diagnostic challenge than typical aortic dissections because of the lack of both flow and an oscillating dissection flap. Because IMH thickness may be progressive, establishing the diagnosis of IMH may require observation time and repeat imaging. Evangelista et al.[218] demonstrated that the initial imaging test results were negative in >12% of patients and that a repeat study was required hours to several days later. IMH can be difficult to distinguish from a thrombosed false lumen of classic aortic dissection, because they can both appear as a crescent-shaped thickening of the aortic wall. However, in aortic dissection, the diameter of the thrombosed false lumen is usually larger than that of most, but not all, IMHs. Conversely, the circumferential extent of an IMH is usually larger than that of an aortic dissection. The appearance of a crescent-shaped thickening of the aortic wall can be mimicked by a normal structure, the hemiazygos sheath, which is a periaortic fat pad.[219] This fat pad is typically present on TEE when the tip of the probe is 30 to 35 cm from the incisors. Aortic atherosclerosis results in thickening of the aortic wall but produces an irregular intraluminal surface that differentiates it from IMH, which has a smooth luminal surface. Moreover, the "lumpy-bumpy" appearance of atherosclerosis tends to vary along each centimeter of the aorta, unlike IMH, which tends to be smooth over a greater length of the aorta. Mural thrombus
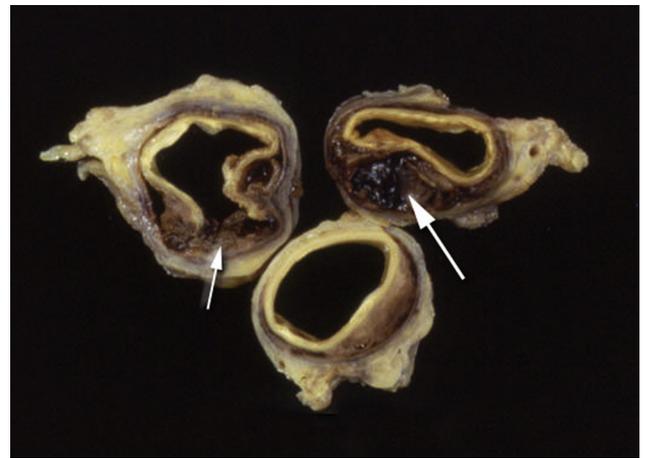
may appear lining a TAA, most often in the descending aorta, but typically has an irregular luminal surface, narrows the lumen and does not extend longitudinally as much as IMH. Figure 41 illustrates the different features of several of these entities from IMH. Aortitis causes thickening of the aortic wall that is typically concentric and typically has normal segments interspersed between the involved sites.

Detection of IMH by CT shows thickening of the aortic wall with higher attenuation than intraluminal blood (from 40 to 70 Hounsfield units) on contrast-enhanced CT (Figure 42). It is vitally important to perform unenhanced CT as the first step in the computed tomographic imaging evaluation of a suspected AAS, because contrast material within the lumen may obscure the IMH. On imaging follow-up of IMH, the appearance of ulcerlike projections (ULPs) is frequently observed, likely representing intimal ruptures that allow communication between the aortic lumen and the medial wall hematoma.[220] MRI offers the possibility of diagnosing intramural bleeding in the hyperacute phase because the hematoma shows an isointense signal on T1-weighted images and a hyperintense signal on T2-weighted images. From the first 24 hours, the change from oxyhemoglobin to methemoglobin determines a hyperintense signal on both T1- and T2-weighted images that together with fat suppression is useful for differentiating periaortic fat from IMH. Although greater availability and shorter examination duration favor the use of

Figure 45 Transesophageal echocardiogram from a patient with a penetrating atherosclerotic ulcer (*arrow*). Note the prominent aortic atheroma (not labeled).

Table 13 PAUs: imaging parameters to report
Lesion Location
Lesion width, length, depth
Aortic diameter at the level of the lesion
Presence/absence/extent of IMH
Contrast extension beyond/outside aortic wall
Mediastinal hematoma
Pleural effusion
Presence and length of false lumen

exudate believed to be inflammatory in origin owing to the proximity of the IMH to the adventitia.[210,230] The likely different prognostic significance of the two pathogenic theories proposed may explain the discordance in the medical literature.

Key points related to IMH are listed in Table 12.

D. PAU

1. Introduction. The term *penetrating aortic ulcer* describes the condition in which ulceration of an atherosclerotic lesion penetrates the aortic internal elastic lamina into the aortic media (Figure 43).[231] Although the clinical presentation of PAU is similar to that of classic aortic dissection, PAU is considered to be a disease of the intima (i.e., atherosclerosis), whereas aortic dissection and its variant (IMH) are fundamentally diseases of the media (degenerative changes of the elastic fibers and smooth muscle cells are paramount), and most patients with aortic dissection typically have little atherosclerotic disease. PAUs may occur anywhere along the length of the aorta but appear most often in the mid and distal portions of the descending thoracic aorta, and they are uncommon in the ascending aorta, arch, and abdominal aorta.[232] PAUs are sometimes multifocal, which is to be expected because aortic atherosclerosis is a diffuse process. They may occur in an aorta of normal caliber but are more often present in aortas of increased diameter.[232-235]

Typically, when an ulcer penetrates into the media, a localized IMH develops (Figure 44). In most patients, this IMH is localized, but occasionally it can involve the entire descending aorta.[223] Rarely, the medial hematoma ruptures back into the aortic lumen, resulting in a classic-appearing dissection with flow in both lumens. Once formed, PAUs may remain quiescent, but the weakened aortic wall may provide a basis for saccular, fusiform, or false aneurysm formation.[231,233,224-227] External rupture into the mediastinum or right or left pleural space may occur but is uncommon.[233,234] Embolization of thrombus or atherosclerotic debris from the ulcer to the distal arterial circulation may also occur.

2. Imaging Features. The diagnosis of PAU requires demonstration of an "ulcerlike" or "craterlike" out-pouching in the aortic wall (the internal elastic lamina is not visible on imaging studies), as seen in Figure 45. Because protrusion through the internal elastic lamina cannot be identified, PAUs can be detected only when they protrude outside the contour of the aortic lumen. Atheromatous ulcers that do not enter the media may be hard to distinguish from PAUs. Therefore, a diagnosis of PAU must be made with caution, especially if the suspected aortic defect has been detected incidentally.

Another entity that may be mistaken for a PAU is a ULP that may evolve from an IMH, as described above. These are localized,

CT in the acute setting, MRI may be complementary for the diagnosis of IMH. The greater contrast among tissues can allow MRI to detect even small IMHs that may go unnoticed by CT. In addition, mural thrombi in TAAs are easier to distinguish from IMH by MRI because mural thrombus shows a hypo- or isointense signal in both T1- and T2-weighted sequences.

3. Imaging Algorithm. CT may be considered the first-line diagnostic imaging modality for IMH, particularly in the acute setting. Detection is based on the high-attenuation signal of acute bleeding by noncontrast enhancement. When findings on CT or TEE are equivocal, MRI may be valuable, as the hyperintense signal in the aortic wall can facilitate a correct diagnosis.

4. Serial Follow-Up of IMH (Choice of Tests). As above, IMH may evolve by reabsorption, aneurysm formation, or conversion to classic dissection.[154] In one series, IMH regressed completely in 34%, led to aneurysm in 20% and pseudoaneurysm in 24%, and progressed to aortic dissection in 12%. Because of their wide field of vision allowing the identification of landmarks, MRI and CT are superior to TEE for defining this dynamic evolution. On surveillance imaging of IMH, the appearance of ULP is frequently observed, and such ulcers may rupture and allow communication between the medial hematoma and the aortic lumen.[221,222] MRI offers the possibility of diagnosing the intramural bleeding evolution and new asymptomatic intramural rebleeding episodes.

5. Predictors of Complications. Most of these predictors may be defined by imaging techniques:

1. Maximum aortic diameter in the acute phase is one of the major predictors of progression in type B IMH and therefore should be reported. Patients with maximum aortic diameters > 40 to 50 mm have a higher risk for dissection, regardless of the location within the descending aorta.[216,223-229]
2. Wall thickness has been described as a predictor of progression; however, not all studies have supported this finding. The thickness threshold for predicting progression has been variably reported to be 10, 12, or 15 mm.[228]
3. The incidence of periaortic hemorrhage or pleural effusion is higher in IMH than in aortic dissection; in some studies, this incidence reaches to 40%. Some series related pleural effusion to worse prognosis in IMH; however, this remains controversial. Two mechanisms have been described: leakage of blood from the aorta through microperforations or a nonhemorrhagic

Table 14 Recommendations for choice of imaging modality for PAU

Modality	Recommendation	Advantages	Disadvantages
CT	First-line	• Superior to TEE for detecting PAU, especially small PAUs • Permits assessment of entire aorta and other thoracic structures • Detects extraluminal abnormalities better than TEE (e.g., pseudoaneurysm, mediastinal fluid) • Follow-up by CT recommended	• Ionizing radiation exposure and iodinated contrast material
MRI	Second-line	• Provides multiple images without contrast • Excellent for detecting associated IMH complicating PAU • Excellent for differentiating primary IMH from atherosclerotic plaque and intraluminal thrombus	• Less widely available than CT • Operator dependent
TEE	Third-line	• Differential diagnosis between PAU and ULP	• Less well studied than CT or MRI • Semi-invasive • Operator dependent

Table 15 Etiologies of TAAs

1. Marfan syndrome
2. BAV-related aortopathy
3. Familial TAA syndrome
4. Ehlers-Danlos syndrome type IV (vascular type)
5. Loeys-Dietz syndrome
6. Turner syndrome
7. Shprintzen-Goldberg (marfanoid-craniosynostosis) syndrome
8. Noninfectious aortitis (e.g., GCA, TA, nonspecific arteritis)
9. Infectious aortitis (mycotic syndrome)
10. Syphilitic aortitis
11. Trauma
12. Idiopathic

Saccular   **Fusiform**

Figure 46 Diagram illustrating the two morphologic types of aortic aneurysms: saccular and fusiform.

blood-filled pouches that protrude into the IMH, with a wide communicating orifice of >3 mm. ULPs are felt to be the consequence of a focal dissection and a short intimal flap resulting in a small pseudoaneurysm. Differentiation from a PAU may be difficult. Generally, a PAU has jagged edges, is accompanied by multiple irregularities in the intimal layer, and may be accompanied by localized hematoma.

TEE, CT, and MRI may all detect PAU and its complications. Once identified, attention should be directed to assessing (1) the maximum depth of penetration of the ulcer, measured from the aortic lumen; (2) its maximum width at the entry site; and (3) the axial length of the associated medial hematoma. Observations that should be reported are listed in Table 13.

3. Imaging Modalities. *a. CT.*—The typical computed tomographic finding of a PAU is a localized contrastlike out-pouching of the aortic wall communicating with the lumen. Its appearance has been likened to a "collar button."[228] As mentioned above, PAUs are most often found in the mid or distal descending thoracic aorta.[226] Thickening (enhancement) of the aortic wall external to sites of intimal calcification suggests localized IMH. These findings are usually in conjunction with severe atherosclerosis. CT has certain advantages over TEE. It can examine areas of the aorta not covered by TEE, allowing more complete identification of the out-pouching produced by PAUs. Moreover, it can also identify calcified atherosclerotic plaques surrounding the ulcer. Computed tomographic angiography is also more likely than TEE to demonstrate extraluminal abnormalities, including pseudoaneurysm or fluid in the mediastinum or pleural space.

b. MRI.—MRI is excellent for detecting focal or extensive IMHs, which appear as areas of high signal intensity within the aortic wall on T1-weighted images.[79,229] Yucel *et al.*[236] demonstrated that MRI is superior to conventional CT for differentiating acute IMH from atherosclerotic plaque and chronic intraluminal thrombus. MRI has the additional advantage of providing multiplane images without the use of contrast material.

c. TEE.—TEE has been less well studied than CT and MRI for the diagnosis of PAU but may be of value when the results of CT and MRI are inconclusive. The characteristic finding, similar to what is seen on CT and MRI, is a craterlike out-pouching of the aortic wall, often with jagged edges, usually associated with extensive aortic atheroma. Although uncommon, a localized aortic dissection may occur, but the dissection flap, if present, tends to be thick, irregular, nonoscillating, and usually of limited length.[237] The reason for the limited length of the dissection may be that the dissection plane is lost because of scarring or atrophy of the media and secondary to the atherosclerotic process.

d. Aortography.—Catheter-based aortography is rarely performed to diagnose PAU because of the superiority of current axial imaging modalities and the high definition of TEE. These modalities also
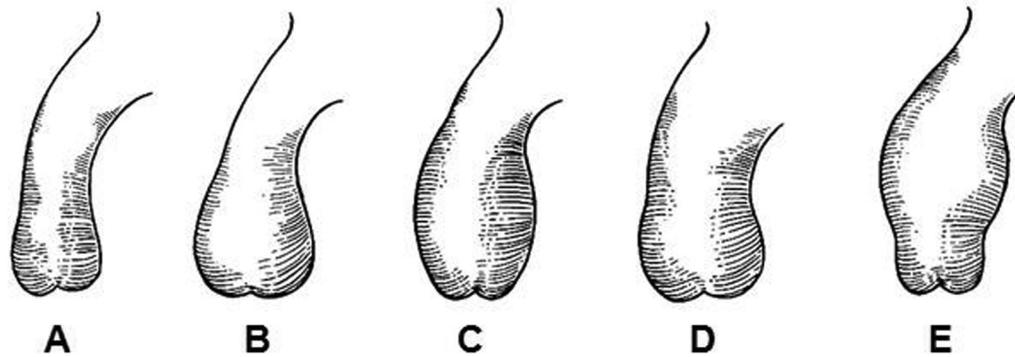
Figure 47 Diagram of some of the various shapes of aortic root and ascending aortic aneurysms. **(A)** Normal. **(B)** Characteristic "marfanoid" or "pear-shaped" aortic root with dilatation localized to the annulus and sinuses of Valsalva. **(C, D)** Two patterns of dilatation involving the annulus, sinuses of Valsalva, and ascending aorta. **(E)** Dilatation beginning at the STJ, but sparing the aortic annulus and sinuses of Valsalva.

provide superior definition of the surrounding wall, making identification of associated IMH easier. The characteristic aortography finding, a contrast medium–filled out-pouching resembling an ulcer of the gastrointestinal tract, is typically associated with "cobblestoning" of the aortic wall in the region of the ulcer consistent with diffuse atherosclerosis, in the absence of a dissection flap or false lumen.

4. Imaging Algorithm. CTA is considered the first-line diagnostic imaging modality.[226,234,238-240] It is widely available, permits assessment of other thoracic structures, and provides 3D reconstructed images that are essential in planning surgery or TEVAR. Moreover, CT is superior to TEE for detecting small ulcers. It is also efficient for the evaluation of the degree of ulcer penetration and bleeding into or outside the aortic wall. MRI is excellent for differentiating PAUs from IMH, atherosclerotic plaque, and intraluminal chronic mural thrombus.[241,242] However, MRI is less widely available than CT and is unable to detect displacement of intimal calcification, which frequently accompanies PAU. Recommendations for choice of imaging modalities for PAUs are summarized in Table 14.

Despite differences in opinion regarding the natural history and management of PAUs, there is agreement that all PAUs, even those found incidentally, warrant close clinical and imaging follow-up, usually by CTA. Findings concerning for progression include an increase in aortic diameter or wall thickening or the appearance of a thin-walled saccular aneurysm. Rupture is indicated by the presence of extra-aortic blood.

5. Serial Follow-Up of PAU (Choice of Tests). The natural history of PAU is unknown. As with IMH, several outcomes have been described. Many patients with PAUs do not need immediate aortic repair but do require close follow-up with serial imaging studies, by CT or MRI, to document disease progression. Although many authors have documented the propensity for aortic ulcers to develop progressive aneurysmal dilatation, the progression is usually slow. Spontaneous complete aortic rupture is uncommon but may occur. Some PAUs are found incidentally, in which case size and progressive enlargement are the only predictors of complications. Both CT and MRI provide superior assessment to TEE in the follow-up of PAU. Surveillance imaging should be performed at intervals similar to what is recommended for aortic dissection.

Table 16 Goal of imaging of TAAs

1 Confirm diagnosis
2 Measure maximal diameter of the aneurysm
3 Define longitudinal extent of the aneurysm
4 Measure the diameters of the proximal and distal margins of the aneurysm
5 Determine involvement of the aortic valve
6 Determine involvement of the arch vessel(s)
7 Detect periaortic hematoma or other sign of leakage
8 Differentiate from aortic dissection
9 Detect mural thrombus

IV. THORACIC AORTIC ANEURYSM

A. Definitions and Terminology

Aortic aneurysm is a pathologic entity that is distinct from aortic dissection. The vast majority of aortic dissections (longitudinal splitting of the media) occur without preceding aneurysms. True aneurysms result from stretching of the entire thickness of the aortic wall; thus, the wall of an aneurysm contains all three of its layers (intima, media, and adventitia). TAAs may involve one or more aortic segments (the aortic root, ascending aorta, arch, or descending thoracic aorta). Sixty percent of TAAs involve the aortic root and/or ascending tubular aorta, 40% involve the descending aorta, 10% involve the arch, and 10% involve the thoracoabdominal aorta.[243] In 1991, the joint councils of the Society of Vascular Surgery and the North American Chapter of the International Society for Cardiovascular Surgery appointed an ad hoc committee to define the standards for reporting on arterial aneurysm.[244] Aneurysm was defined as a permanent focal dilatation of an artery having a ≥50% increase in diameter compared with the expected normal diameter of the artery in question. This definition was also adopted by the 2010 American College of Cardiology Foundation, American Heart Association, American Association for Thoracic Surgery, American College of Radiology, American Surgical Association, Society for Cardiac Angiography and Interventions, Society of Interventional Radiology, Society of Thoracic Surgeons, and Society for Vascular Medicine guidelines for the diagnosis and management of patients with thoracic aortic disease.[1]

Table 17 Recommendations for choice of imaging modality for TAA

Modality	Recommendation	Advantages	Disadvantages
CT	First-line	• First-line technique for staging, surveillance • Contrast: enhanced CT and MRI very accurate for measuring size of all TAAs (superior to echocardiography for distal ascending aorta, arch, and descending aorta) • All segments of aorta and aortic branches well visualized	• Use of ionizing radiation and ICM • Cardiac motion can cause imaging artifacts
MRI	Second-line	• Ideal technique for comparative follow-up studies • Excellent modality in stable patients • Preferred for follow-up for younger patients • Avoids ionizing radiation • Can image entire aorta	• Examination times longer than CT • Benefits from patient cooperation (breath hold) • Limited in emergency situations in unstable patients and patients with implantable metallic devices • Benefits from gadolinium
TTE	Second-line	• Usually diagnostic for aneurysms effecting aortic root • Useful for family screening • Useful for following aortic root disease • Excellent reproducibility of measurements • Excellent for AR, LV function	• Distal ascending aorta, arch, and descending aorta not reliably imaged
TEE	Third-line	• Excellent for assessment of AR mechanisms • Excellent images of aortic root, ascending aorta, arch, and descending thoracic aorta	• Less valuable for routine screening or serial follow-up (semi-invasive) • Distal ascending aorta may be poorly imaged • Does not permit full visualization of arch vessels • Limited landmarks for serial examinations
Aortography	Third-line	• Reserved for therapeutic intervention • Useful to guide endovascular procedures	• Invasive; risk for contrast-induced nephropathy • Visualizes only aortic lumen • Does not permit accurate measurements

LV, Left ventricular.

Although our writing committee endorses this definition in general, we would like to point out some practical considerations. First, the current definition lacks an outcomes correlate; second, many publications use the term *aortic dilatation* with different arbitrary cutoff values to define the significance of dilatation.[245-248] Last, if a common echocardiographic upper limit of 37 mm is considered for the ascending aorta (see the section on normal anatomy and reference values), then the ascending aorta is dilated at a diameter of >55.5 mm (37 + 18.5 mm), which seems excessive given that it is larger than the typical threshold for surgery. General descriptions, such as "there is an ascending aortic aneurysm," are inadequate.[243] It is preferable to state that "there is a 5-cm ascending thoracic aortic aneurysm," because it conveys prognostic, follow-up, and management implications. Descriptive terms such as *small, large*, and *giant* to describe aneurysms should also be avoided.

Other commonly used terms are included in the 2010 guidelines[1]: ectasia is arterial dilatation < 150% of normal arterial diameter. Arteriomegaly is diffuse arterial dilatation involving several arterial segments, with an increase in diameter > 50% in comparison with the expected normal arterial diameter.

Aortic dilatation is an acceptable nonspecific term that encompasses both ectasia and aneurysm. Again, imaging reports must include the diameters of the affected aortic segments. Moreover, it is ideal to perform serial imaging studies at the same center with the same technique, so that direct comparisons can be made.[243] When this is not practical, direct comparison with previous examinations should be made to confirm that serial changes are genuine.

B. Classification of Aneurysms

Aortic aneurysms can be classified according to morphology, location (as above), and etiology. The etiologies of TAAs are listed in Table 15. These are discussed in other sections of this document.

C. Morphology

Aneurysms of the aorta can be classified into two morphologic types: fusiform and saccular (Figure 46). Fusiform aneurysms, which are more common than saccular aneurysms, result from diffuse weakening of the aortic wall. This process leads to dilatation of the entire circumference of the aorta, producing a spindle-shaped deformity with a tapered beginning and end. Saccular aneurysms result when only a portion of the aortic circumference is weakened, producing an asymmetric, relatively focal balloon-shaped out-pouching. There are also various morphologic shapes of the aortic root and ascending aorta, some of which suggest specific etiologies (Figure 47).

The major goals of imaging TAAs are listed in Table 16, and recommendations for choice of imaging modalities are listed in Table 17.

D. Serial Follow-Up of Aortic Aneurysms (Choice of Tests)

Aortic diameter is the principal predictor of aortic rupture or dissection.[249] The risk for rupture or dissection of TAAs from different etiologies increases significantly at sizes > 60 mm. The mean rupture rate is only 2% per year for aneurysms <50 mm in diameter, rising slightly to 3% for aneurysms with diameters of 50 to 59 mm, but increasing sharply to 7% per year for aneurysms ≥60 mm in

diameter.[250] The rate of growth is significantly greater for aneurysms of the descending aorta, at 1.9 mm per year, than those of the ascending aorta, at 0.07 mm per year.[249]

The clinical importance of the maximum aortic diameter for determining the timing of prophylactic surgical repair implies makes it critical that measurements be made as accurately as possible. It is essential for the same observer to compare measurements side by side using the same anatomic references. Tomographic scans in a situation for which the aorta does not lie perpendicular to the plane of the scan produce an elliptical image with major (maximum) and minor (minimum) diameters. Because the major diameter is typically an overestimate, in most natural history studies of aneurysm expansion, the minimum diameter has been reported to avoid the effect of obliquity.

Aortic root dilatation can be followed by TTE in most cases. Diameter expansion, severity of AR, and left ventricular function may be accurately evaluated when the echocardiographic window is adequate. However, when dilatation involves the ascending aorta above the STJ, TTE does not always adequately visualize the affected segment, in which case CT or MRI should be performed. TEE may be warranted when the type of surgical treatment (repair or valve replacement) is being considered. Both TTE and TEE have limitations for adequate measurement of distal ascending aorta, aortic arch, and descending aorta diameters. In addition, if the aorta is tortuous, transesophageal echocardiographic images may be difficult to measure accurately. The multiplanar capacity of MDCT, together with its submillimeter spatial resolution, renders it an excellent technique for interval surveillance of both thoracic and abdominal aortic aneurysms. Measurements must adhere to a strict protocol that permits comparison between different imaging techniques as well as follow-up of the patient. MDCT permits one to choose an imaging plane in any arbitrary space orientation; thus, it is possible to easily find the maximum aortic diameter plane, which must be perpendicular to the longitudinal plane of the aortic segment. When the axial data are reconstructed into 3D images (computed tomographic angiography), one can measure the tortuous aorta in true cross-section and obtain an accurate diameter. Measurements should be taken on multiplane reconstruction images. A further common presentation of data is a parasagittal, oblique MIP plane that passes through the aortic root, ascending aorta, aortic arch, and descending aorta. The MIP plane must have a thickness proportional to the aortic tortuosity to make sure that the maximum diameter is included in the image. This plane is easily reproducible and comparable in follow-up studies.

MRI accurately defines aortic diameter, aneurysm extent, and the aneurysm's relationship with the main arterial branches. It is recommended to combine MR angiographic images with black-blood spin-echo sequences, which are useful for detecting pathology of the wall and adjacent structures that could go unnoticed if only MR angiographic images are acquired. In mycotic aneurysm, postcontrast T1-weighted images permit the identification of inflammatory changes in the aortic wall and adjacent fat, secondary to bacterial infection. The information provided by MRA in aortic aneurysm assessment is similar to that offered by current MDCT. Both methods permit accurate determinations of aortic diameters in sagittal plane. Furthermore, postprocessing techniques (MIP, multiplane reconstruction, and volume rendering) facilitate visualization of the aorta in its entirety, together with the relationship of its principal branches, and are highly useful when planning treatment. The sagittal plane makes it possible to obtain more reproducible measurements. In asymptomatic patients with aortic aneurysms and those approaching the need for surgery, imaging techniques should be performed at 6-month intervals until aortic size remains stable, in which case imaging may be annual.

1. Algorithm for Follow-Up. TTE can be used for serial imaging of the dilated aortic root and proximal ascending aorta when agreement between the dimensions measured by TTE and CT or MRI has been established. When the aneurysm is located in the mid or upper portion of the ascending aorta, aortic arch, or descending thoracic aorta, CT or MRI is recommended for follow-up. Measurements should be made on multiplane reconstruction images or in parasagittal, oblique MIP plane that passes through the involved aortic segments. Although annual surveillance MDCT has been recommended, the strategy is not well established and should be individualized from annually to every 2 to 3 years depending on the abnormalities present, history of complications among family members, the present size, and the degree of change in size over time.

E. Use of TEE to Guide Surgery for TAAs

When patients with aortic root or ascending TAAs undergo aortic repair, the anatomy of the aorta and aortic valve has usually been defined preoperatively. Nevertheless, it is always wise to use intraoperative TEE to confirm the prior imaging findings. The initial intraoperative transesophageal echocardiographic examination should begin before the initiation of cardiopulmonary bypass, so the physiology of the aortic valve can be assessed. If the valve is bicuspid, one should determine the presence and severity of associated valvular aortic stenosis, regurgitation, or both. If there is significant AR, one should determine the mechanism, looking specifically for prolapse and/or retraction of the conjoined leaflet, as this is a common cause of bicuspid AR and may be correctable with BAV repair. One should also assess the degree of leaflet thickening, calcification, and restriction, because in the setting of significant valve dysfunction, these findings may influence the surgeon's decision regarding the need for valve repair or replacement.

Even when the aortic valve is tricuspid with otherwise normal leaflets, the presence of an ascending aortic aneurysm can result in AR. The commissures of the aortic leaflets are located just below the STJ; dilatation of the aorta at that level may tether the leaflets, leaving insufficient slack for the three leaflets to coapt properly in the middle, resulting in a jet of central AR.[32,194,251] AR due to leaflet tethering can occur with aneurysms of both the aortic root and the ascending aorta. Fortunately, with repair of the aneurysm and restoration of normal aortic geometry, normal leaflet coaptation is often restored, which in turn leads to resolution of the valvular regurgitation. Therefore, in a patient with an aneurysm with significant AR, identifying such aortic leaflet tethering on preoperative TEE may reassure the surgeon that aortic valve replacement is not necessary.

The ascending aorta, aortic arch, and descending aorta should each be inspected for the presence of associated pathology, such as an unrecognized aortic dissection, IMH, PAU, or protruding atheromas. Large atheromas in the ascending aorta or arch may prompt additional imaging of the aorta using intraoperative epiaortic echocardiography and influence decisions regarding the site of aortic cannulation and perfusion.

Postoperative TEE should begin as soon as the patient comes off cardiopulmonary bypass. The examination should begin with inspection of the aortic valve, as unanticipated valve dysfunction may necessitate a return to bypass. If preoperatively there had been significant AR due to leaflet tethering, one should confirm appropriate leaflet coaptation and alleviation of AR after repair. If repair of bicuspid valve prolapse was performed, one should confirm that the prolapse has resolved and that the AR is no longer significant. If a valve-sparing root repair was performed, one should confirm that the three aortic valve leaflets coapt normally and that there is little or no AR. If the
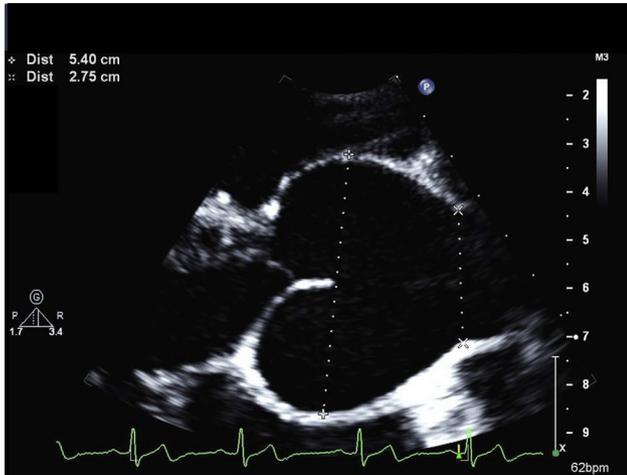
Figure 48 Transthoracic long-axis image demonstrating marked dilatation of the aortic root (*sinuses*) in a patient with Marfan syndrome. Note the normal dimension at the STJ.

aortic valve had been replaced, one should confirm that the prosthetic leaflet or disk motion is normal, that there is no more than physiologic AR, and that there are no paravalvular leaks.

After aortic valve replacement or aortic root replacement, it is typical to see focal thickening around the aortic root. It is important to document this so as not to confuse this finding with pathology on subsequent imaging. For more detailed information, readers are referred to the recently published Society of Thoracic Surgeons aortic valve and ascending aorta guidelines for management and quality measures.[252]

F. Specific Conditions

1. Marfan Syndrome. Marfan syndrome is an inherited disorder of connective tissue that occurs as a result of a mutation in the *FBN1* gene, which encodes fibrillin. One of the hallmark features of this disorder is dilatation or dissection of the proximal ascending aorta (aortic root).[253] The remaining portions of the aorta may also dilate and dissect, but involvement of the aortic root is expected when there is associated vascular disease. Noninvasive aortic imaging with subsequent elective aortic replacement has contributed to the dramatic improvement in survival noted in patients with Marfan syndrome over the past few decades.[254]

a. Aortic Imaging in Unoperated Patients with Marfan Syndrome.–TTE is generally the initial imaging tool used for the identification and serial follow-up of ascending aortic enlargement in patients with known or suspected Marfan syndrome, because of its availability, noninvasive nature, reliability, and lack of need for radiation or contrast material. Characteristic aortic features include dilatation of the aortic root, whereas the STJ and remaining portions of the ascending aorta generally are normal in size (Figure 48). Normative values are used to determine the presence and extent of aortic enlargement on the basis of age and BSA.[9] The leading edge–to–leading edge measurement technique is generally performed in patients with Marfan syndrome <18 years of age, and the size of the aorta is reported along with the Z score.[255] Although there is dispute regarding the best echocardiographic aortic measurement method, the most important concept is that serial measurements for each individual patient are performed using the same method to determine aortic dimension change over time.
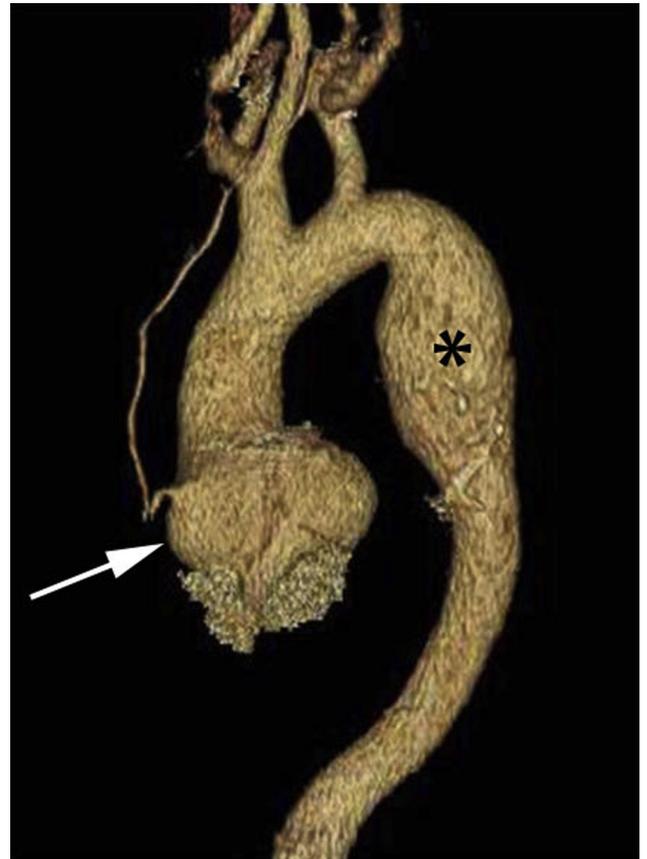
Figure 49 Computed tomographic 3D volume-rendered reconstruction of the thoracic aorta demonstrating aortic root dilatation (*arrow*) and proximal descending thoracic aorta dilatation (*asterisk*). The descending thoracic aortic dilatation was not noted on TTE.

Some patients with Marfan syndrome have suboptimal transthoracic echocardiographic images, and in these patients, serial CT or MRI is required to monitor aortic diameter.

At the time of initial diagnosis of aortopathy in Marfan syndrome by TTE, additional imaging with CT or MRI is generally recommended to confirm that the size of the aorta measured by TTE is accurate and correlates with the computed tomographic or MRI measurement and to document the diameters of the distal ascending aorta, aortic arch, and descending aortic segments, which may also be enlarged but are often incompletely visualized by TTE (Figure 49).

For the follow-up of aortic root enlargement in patients with Marfan syndrome, follow-up imaging in 6 months is recommended. If at that time the aortic diameter remains stable, is <45 mm, and there is no family or personal history of aortic dissection, then annual aortic imaging is reasonable. Patients with Marfan syndrome who do not meet these criteria should undergo repeat aortic imaging every 6 months.

TTE can be used for serial imaging follow-up of the dilated ascending aorta when correlation between the dimensions measured by TTE and CT or MRI has been documented. Occasionally, patients with Marfan syndrome do not demonstrate aortic enlargement until well into adulthood. These patients can be referred for transthoracic echocardiographic screening at 2- to 3-year intervals.

Repeat CT or MRI is suggested at least every 3 years in patients with Marfan syndrome to reassess the aortic arch and descending

Table 18 Genetic conditions associated with aortic disease

BAV
Marfan syndrome
Loeys-Dietz syndrome
Turner syndrome
Ehlers-Danlos vascular type (type IV)
Familial TAA
Shprintzen-Goldberg (craniosynostosis) syndrome

aorta and to reconfirm that TTE remains reliable in its measurement of the ascending aorta. Patients with Marfan syndrome with aneurysmal dilatation of the proximal descending thoracic aorta require regular CT or MRI to monitor aortic stability, because TTE does not provide reliable imaging of this region.

TEE is generally not used for the initial diagnosis or follow-up of aortic dilatation in patients with Marfan syndrome because of its semi-invasive nature and the difficulty directly comparing dimensions over time.

b. Postoperative Aortic Imaging in Marfan Syndrome.–After elective aortic root replacement, dismissal or early (within 6 months) TTE and CT or MRI are generally performed to establish a baseline aortic assessment for patients with Marfan syndrome. Annual TTE and CT or MRI of the aorta are generally recommended after aortic root replacement. The frequency of aortic imaging is individualized depending on patient characteristics, such as the type of operation performed and the extent of aortic dilatation elsewhere. Serial postoperative follow-up imaging should focus on progression of disease affecting the native aorta, and common postoperative complications, including the development of pseudoaneurysm and coronary anastomotic aneurysms.

c. Postdissection Aortic Imaging in Marfan Syndrome.–Patients with Marfan syndrome with repaired type A aortic dissection should undergo serial aortic imaging with CT or MRI; the imaging frequency depends on the extent of aortic dissection and the type of repair. Patients with Marfan syndrome with type B aortic dissection that has not been repaired require regular follow-up imaging (see section III.B, "Aortic Dissection").

d. Family Screening.–Marfan syndrome is inherited in an autosomal-dominant fashion, so transthoracic echocardiographic screening is recommended for the first-degree relatives of an affected individual unless a gene mutation has been identified and genetic testing can be used to identify affected family members.[1] All affected family members should undergo regular aortic imaging. Although there are no specific guideline recommendations for "regular" imaging, serial imaging should depend on the age and specific features of a given individual.

2. Other Genetic Diseases of the Aorta in Adults. Two genetic conditions associated with thoracic aortic disease, BAV and Marfan syndrome, are relatively common and are discussed elsewhere in this review. Many additional predisposing conditions for aortic aneurysm formation and dissection are listed in Table 18. The scope of this document does not permit a detailed discussion of these less common entities, but a few pertinent details are mentioned. Importantly, awareness of these disorders and their potential risk is critical not only to presenting patients but also to their close relatives.

a. Turner Syndrome.–Women with Turner syndrome are at risk for BAV, aortic coarctation, and aortic dilatation or dissection. Aortic dilatation in patients with Turner syndrome has been reported to occur in up to 40% of cases. Imaging of the aorta in these patients must include the ascending aorta, aortic arch, and proximal descending aorta. As in other cases, aortic dilatation coexists with a BAV and/or coarctation.[256-258] Patients with Turner syndrome have a small stature compared with same-age individuals in the general population, so all aortic measurements should be indexed to BSA. An indexed aortic diameter of >2 cm/m^2 in the ascending aorta should be followed annually, as the risk for aortic dissection is increased.[258]

b. Loeys-Dietz Syndrome.–Loeys-Dietz syndrome results from a gene mutation of transforming growth factor β receptor 1 or 2 and is inherited in an autosomal-dominant fashion.[259] Aortic root aneurysms are present in the majority of patients with Loeys-Dietz syndrome. Involvement of other aortic segments and smaller arteries in the form of aneurysms or marked tortuosity are characteristic in this population.[259,260] Dissection can occur at dimensions smaller than in other inherited disorders of connective tissue. Although an annual comprehensive arterial imaging protocol with MDCT or MRI has been recommended,[261] the strategy for follow-up is not well established and should be individualized from annually to every 2 to 3 years depending on abnormalities present, family risk of complications, and degree of evolution. Interpretation should include information about the caliber of the aortic root, the ascending and descending aorta, and the pulmonary artery (pulmonary artery dilatation may also occur). If progression of aortic disease has occurred, it should be monitored every 6 months (every 12 months for other arteries) given the markedly increased risk for dissection or rupture.

c. Familial TAAs.–Different gene mutations have been identified in familial TAAs, predominantly with an autosomal-dominant inheritance. Aneurysms in relatives may be seen in the thoracic aorta, the abdominal aorta, or the cerebral circulation. Therefore, comprehensive imaging for screening of first-order relatives of probands with TAA is advisable.[262] The frequency and modality of vascular imaging in affected persons is similar to that outlined for Marfan syndrome but should be individualized.[263]

d. Ehlers-Danlos Syndrome.–The vascular form of Ehlers-Danlos syndrome (type IV) is a rare autosomal-dominant disorder with vascular involvement characterized by arterial dilatation and rupture. The role of aortic imaging in this population is less clear. Elective surgical repair of aortic aneurysms or other vascular involvement carries a high risk because of due to tissue fragility, so the impact of serial aortic imaging is unclear.[264]

3. BAV-Related Aortopathy. *a. Bicuspid Valve–Related Aortopathy.*–BAVs affect 1% to 2% of the population and are often associated with aortopathy.[265-269] Nearly 50% of patients with BAVs have dilatation of either the aortic root or ascending aorta.[247,268,270] Dilatation of the aortic arch and descending thoracic aorta can also occur but is less common. Recently, it has been reported that patients with BAVs also are at increased risk for intracranial aneurysms compared with the normal population,[271] although the clinical significance of this is unknown. Progressive dilatation of the aorta may occur irrespective of the functional status of the BAV and places patients at increased risk for aortic dissection or rupture.[272,273] Patients with BAVs may also have coexisting coronary artery anomalies, including reversal of dominance, short left main coronary artery (<10 mm), and anomalous origin of the left circumflex artery from the right coronary
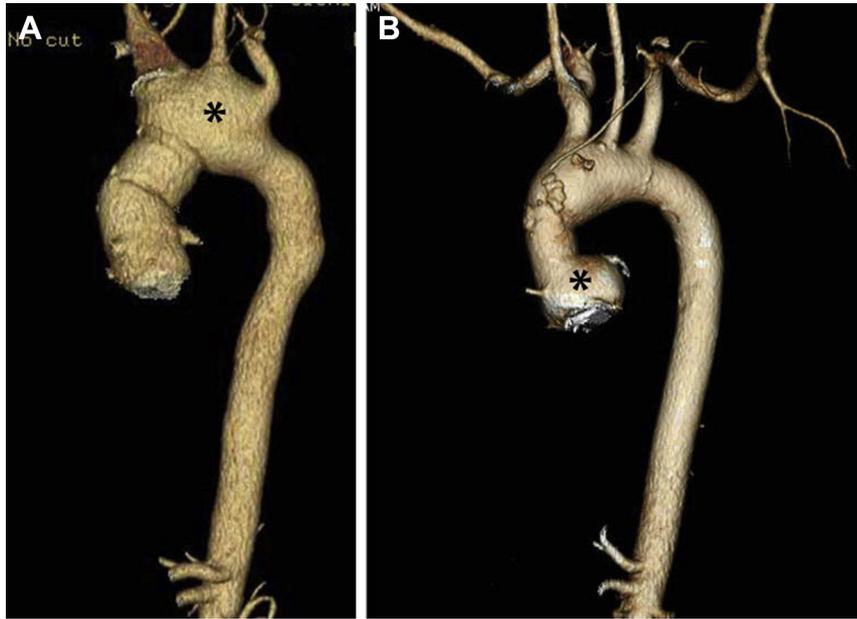
Figure 50 (A) Computed tomographic 3D volume-rendered reconstruction of the thoracic aorta in a patient with prior aortic valve and ascending aorta replacement due to bicuspid valve–related aortopathy; the image demonstrates aortic arch dilatation (*asterisk*). **(B)** Computed tomographic 3D volume-rendered reconstruction of the thoracic aorta in a patient with BAV and aortopathy with prior aortic valve and supracoronary aortic replacement; the image demonstrates features of asymmetric aortic root dilatation (*asterisk*).

cusp.[250,270,274-278] Failure to recognize these anomalies may result in risk for coronary artery injury during aortic valve repair or replacement.

b. Imaging of the Aorta in Patients with Unoperated BAVs.–TTE is the primary imaging tool for the initial diagnosis and screening as well as serial follow-up of patients with known or suspected BAVs with or without aortopathy. The aortic root or ascending aorta may be dilated. The pattern of dilatation may be associated with BAV morphology.[269] At the time of initial diagnosis of aortopathy in patients with BAVs, imaging with CT or MRI is generally recommended to confirm that the size of the aorta measured by TTE is accurate. Eccentric dilatation of the aortic sinus adjacent to the conjoined cusp increases the chance of underestimation of the aortic root measurement by TTE, particularly when the measurement is obtained only in the long-axis format. CT and MRI also provide important information about the size of the aortic arch and descending aortic segments, which are often incompletely visualized by TTE (Figure 49). Although BAV occurs in >50% of patients with coarctation, coarctation is noted in <10% of patients with BAVs. Nevertheless, whenever a BAV is detected, coarctation should always be sought.

c. Follow-Up Imaging of the Aorta in Patients with Unoperated BAVs.–All patients with BAVs and associated aortopathy should undergo annual surveillance imaging of the ascending aorta to monitor growth over time. TTE can be used to monitor the aortic root and ascending aorta when correlation between the dimensions measured by TTE and CT or MRI has been confirmed. After the identification of ascending aortic enlargement in a patient with BAV, repeat imaging after 6 months is recommended. If the aorta remains stable at 6-month follow-up and is <45 mm in size, and there is no family or personal history of aortic dissection, annual aortic imaging is recommended. Patients who do not meet these criteria should undergo repeat aortic imaging using TTE every 6 months. Occasionally, patients with BAV-related aortopathy have demon-

strated stable dilatation of the ascending aorta over several years; the frequency of aortic follow-up in these patients should be individualized. Patients with BAVs and no demonstrable aortopathy should be screened every 3 to 5 years with TTE for the development of aortic enlargement.

Repeat CT or MRI is suggested at least every 3 to 5 years to reassess the aortic arch and descending aorta and reconfirm that transthoracic echocardiographic measurements of the aortic root remain reliable for serial measurements.

TEE is generally not used for initial diagnosis and follow-up of BAV-related aortopathy, because of its semi-invasive nature and difficulty comparing dimensions over time.

Patients with BAVs with aneurysmal dilatation of the aortic arch or descending thoracic aorta or those with remote histories of type B aortic dissection require regular computed tomographic angiography or MRI to monitor aortic stability. In such cases, imaging should be repeated annually. TTE does not provide reliable imaging for serial follow-up of the dimensions of these portions of the aorta.

d. Postoperative Aortic Imaging in Patients with BAV-Related Aortopathy.–After elective aortic root replacement, early (dismissal or within 6 months) TTE and CT or MRI are generally performed to establish a baseline aortic and valve assessment. During the imaging study, it is critical to know what surgical procedure was performed to identify potential residua or sequelae (Figure 50). Annual aortic imaging is generally recommended after aortic root replacement or replacement of the aorta above the coronary arteries; however, the frequency is individualized depending on patient characteristics, type of operation performed, and duration of follow-up. Dilatation of the remaining ascending aorta, aortic arch, or descending thoracic aorta may continue after the ascending aorta has been replaced. Serial postoperative follow-up imaging should also focus on common postoperative complications, including the development of coronary button pseudoaneurysm formation, anastomotic site pseudoaneurysm formation, and progressive dilatation of other aortic segments.

Table 19 Genetic TAAs: key points	
Etiology	**Key features**
Marfan syndrome	• Aortic root most common location for aneurysm • Characteristic pear-shaped appearance • STJ diameter relatively normal • TTE initial imaging tool for detecting and serial follow-up • First-degree relatives require screening
BAV	• TTE primary imaging tool for diagnosis, screening, and follow-up • May involve ascending aorta or aortic root • Aneurysms occur even in absence of significant valve dysfunction • Screening of aortic valve and ascending aorta recommended even for first-degree relatives
Familial thoracic aortic syndrome	• Ascending aorta more commonly affected • Relatively fast growth rate
Vascular Ehlers-Danlos syndrome	• Aortic complications at a young age
Loeys-Dietz syndrome	• Widespread, aggressive vasculopathy • Aortic root aneurysms in up to 48% • Dissection can occur at dimensions smaller than in other inherited aortic disorders such as Marfan syndrome and BAV
Turner syndrome	• Associated with BAV • Aneurysms most commonly occur in ascending aorta

e. Family Screening.—Because aortopathy has been demonstrated in first-degree relatives of patients with BAV syndrome, screening first-degree relatives with TTE is recommended to identify dilatation of the aortic root or ascending aorta.[279]

Key points of imaging related to genetic diseases of the aorta are listed in Table 19.

V. TRAUMATIC INJURY TO THE THORACIC AORTA

Traumatic injuries to the aorta may result from either blunt (nonpenetrating, indirect) or sharp (penetrating, direct) trauma. Penetrating trauma is usually caused by stab or bullet wounds that puncture the aortic wall. Rare causes include misplacement of spinal fixation screws and lacerations from spinal fractures.[280,281] Penetrating aortic trauma injures the aorta from outside to inside, does not have a predilection for site, and is usually fatal.[280,282-284] Blunt aortic injuries (BAIs) are far more common and are therefore the focus of this review.

In BAI, the aortic wall is damaged from the inside to the outside, from the intima to the adventitia. The most common location of

Table 20 CXR findings associated with BAIs
Widened mediastinum (>8.0 cm or mediastinum-to-chest width ratio > 0.25)
Rightward deviation of the trachea or nasogastric tube
Obscured aortic knob
Opacification of the aortopulmonary window
Downward displacement of the left main stem bronchus
Widened right paratracheal stripe
Left apical pleural cap
First and/or second rib fracture
Clavicle, sternal, or thoracic spine fracture
Hemothorax
Intrathoracic free air

BAI is at the aortic isthmus just distal to the left subclavian artery.[284-287] The second most common location is the supravalvular portion of the ascending aorta.[285,286,288,289] Motor vehicle accidents (especially at speeds of >40 mph) account for 75% of cases in most series of BAI,[280,287,290,291] but falls from heights of >10 feet, crush injuries, explosions, motorcycle and aircraft crashes, pedestrian injuries, and direct blows to the chest are also known to produce similar injuries.[284,290-292]

A. Pathology

The aortic isthmus is the most common location for BAI (80%–95%), followed by the ascending aorta and then the diaphragmatic aorta.[284,286-289] Those regions represent transition points between relatively fixed and mobile aortic segments. These transition points have the greatest exposure to shear and hydrostatic forces generated by abrupt deceleration. Unfortunately, investigators in the field have not been consistent in the terms they use to describe the result of BAI. Pathologists have described these injuries as tears, lacerations, disruptions, transactions, ruptures, dissections, and pseudoaneurysms. Even modern imaging modalities may not be able to define an injury in terms that are precisely consistent with pathologic descriptions. In this text, descriptive terms are used for the pathologic abnormalities that correlate with various imaging methods. Descriptions of images should include the site of the lesion (i.e., ascending aorta, aortic arch, isthmus, descending thoracic aorta, or abdominal aorta), as well as an estimate of the distance of the lesion from a reference anatomic structure (e.g., the aortic valve, the origin of the left subclavian artery, and the diaphragm). The description should also include the length of the aortic injury (in millimeters) and the total circumference of the aorta at the site of its injury.

A variety of aortic lesions can result from blunt aortic trauma.

1. Subadventitial aortic rupture involving the intima and media with incomplete circumferential extension: In this most frequent lesion encountered by imaging physicians, there is a discrete tear involving the intima and underlying media. The disrupted aortic wall (intima and media) usually protrudes into the aortic lumen, and through the disrupted wall, the aortic lumen communicates with a cavity (saccular false aneurysm) whose wall is composed only of adventitia. The inner surface of the aorta presents an abrupt discontinuation, and the outer contour is deformed by the false aneurysm. The protrusion of the torn aortic wall into the aortic lumen may produce "stenosis" with flow acceleration and a gradient (pseudocoarctation).

2. Subadventitial aortic rupture involving the intima and media with complete circumferential extension (aortic transection): This lesion results in a fusiform

Table 21 CT findings in blunt traumatic thoracic aortic injury

Direct signs
Contrast extravasation
Intimal flaps
Pseudoaneurysm formation
Filling defects (e.g., mural thrombus)
Indirect signs
Periaortic hematomas
Mediastinal hematomas

Table 22 Advantage of TEE in blunt traumatic thoracic aortic injury

1. Highly accurate in region of aortic isthmus (most common region for BAI)
2. Can be performed at bedside or in OR
3. Can be performed in unstable patients who need emergency OR and when there is not time for CT
4. No radiation exposure
5. Does not require contrast; safe in renal insufficiency
6. Can assess other cardiac injuries and cardiac function

OR, Operating room.

Table 23 Disadvantages of TEE in blunt traumatic thoracic aortic injury

Difficulty imaging distal ascending aorta
Difficulty evaluating arch vessels
Operator dependent (requires skilled operator)
●Training and experience required
●Availability
Not always safe in patients with facial, cervical, spine, oropharynx, or esophageal injuries
Reverberation artifact

pseudoaneurysm. Because the intima and media tear is circumferential, protrusion into the lumen does not occur. The inner surface of the aneurysm is smooth, formed solely by adventitia. As a consequence, the aortic wall is extremely thin and fragile. Imaging typically reveals abrupt change in aortic diameter.

3. IMH: Accumulation of blood within the media may result from blunt aortic trauma because of disruption of the vasa vasorum or the development of small intimal tears. The aortic wall shows a localized, usually crescentic thickening (usually >5 mm). The inner aortic surface is smooth, the aortic lumen is partially reduced, and the outer aortic contour is unaltered. There is no flap and no flow signals within the hematoma.

4. Traumatic aortic dissection: The elastic and collagen fibers of the aortic wall are remarkably strong radially but may relatively easily be split when exposed to transaxial stress. As is true of spontaneous aortic dissection, aortic trauma may produce separation of the media. This lesion is uncommon and can mimic spontaneous aortic dissection but has significant differences. It is usually localized to the area of the aortic injury and does not propagate distally toward the iliac arteries. It typically fails to create two channels and may have a direction transverse to the longitudinal axis of the aorta. Consequently, the resulting "flap" is usually thicker and less mobile than the classical intimal flap. The aorta is usually symmetrically enlarged.

5. Lesion of the aortic branches: Partial or total avulsion, pseudoaneurysm, dissection, and thrombosis may occur as isolated injuries to branch arteries or in association with BAI.

6. Superficial lesions involving only the intima: With improvements in imaging technology, ever more subtle lesions are being identified. The term *minimal aortic injury* is often used to describe a lesion that carries a relatively low risk for rupture. Ten percent of BAIs diagnosed with high-resolution techniques have minimal aortic injuries.[293] Although most of these intimal injuries heal spontaneously and hence may not require surgical repair, the natural history of these injuries is unknown.[294,295] Frank tears produced by BAI but limited to the intima appear as thin, linear mobile intraluminal projections from the aortic wall. No alterations of the diameter or external contour of the aorta are present. Thrombi, often mobile, may be present within the aortic lumen, presumably in areas of exposed collagen. Minimal aortic injury from an imaging standpoint is an injury with the intimal flap <10 mm, accompanied by minimal or no periaortic mediastinal hematoma.[293]

B. Imaging Modalities

On the basis of a landmark study by Parmley *et al.*,[284] aortography was considered the best study to identify BAI for >40 years. However, aortography is invasive, requires a special team for its performance, and is prone to both false-positive and false-negative results, rendering it a poor choice for screening.[296-299] CT is now the diagnostic test of choice.[285,287,300-304] Other options for the diagnosis of blunt traumatic aortic injury include CXR, TEE, IVUS, and MRI. Each of the imaging techniques has relative advantages and disadvantages.

1. CXR. Although a plain CXR is often an initial study in emergency departments and can sometimes suggest aortic injury, even when the image is not of diagnostic quality, no single or combination of radiographic signs demonstrates sufficient sensitivity or specificity to reliably detect or exclude traumatic aortic rupture.[241,280,305] Therefore, further imaging should be performed whenever an abnormality is suspected on clinical presentation or on CXR or when the mechanism of injury is compatible with aortic injury. The most significant CXR findings include, but are not limited to, widened mediastinum, an obscured aortic knob, rightward deviation of the trachea or nasogastric tube, and opacification of the aortopulmonary window. A more complete list of CXR findings seen in BAI is shown in Table 20.

2. Aortography. As mentioned, selective contrast aortography was long considered to be the reference standard examination for the diagnosis of traumatic aortic injury. Compared with necropsy, prior reports claimed sensitivity, specificity, and accuracy approaching 100%,[296,299,306] but with the introduction of CT and TEE, the failings of aortography became readily apparent. Indeed, modern CT and TEE are able to identify minimal injuries such as intimal tears, which constitute up to 10% of BAIs, whereas such injuries cannot be detected by contrast aortography. Moreover, significant interobserver variability in the interpretation of aortographic images has been reported. On an aortogram, the diagnosis of an intimal injury requires the demonstration of an intimal irregularity or filling defect caused by an intimal flap.[307] The presence of contrast media outside the lumen of the aorta is an important sign of transmural laceration: when the leak is contained, it may be termed a pseudoaneurysm, whereas free extravasation indicates frank rupture.[307] Diagnostic pitfalls of aortography for blunt thoracic aortic injury include the ductus diverticulum, the aortic spindle (a short segment of fusiform dilatation of the aorta just distal to the isthmus), atherosclerotic disease, artifacts from streaming or mixing of contrast media, and motion artifacts.

3. CT. The introduction of multidetector computed tomographic angiography, with up to eightfold reduction in scan times, made whole-body CT technically feasible,[308,309] and over the past decade, CT has almost completely replaced aortography and TEE as the first-line imaging test for BAI.[300-304] Some of the advantages of MDCT include

Table 24 Recommendations for choice of imaging modality for aortic trauma

Modality	Recommendation	Advantages	Disadvantages
CT	First-line	• Diagnostic test of choice • Sensitivity for detecting aortic trauma approaches 100%; negative predictive value approaches 100% • Patients with multiple injuries; whole-body CT feasible ("trauma panscan") • Images lumen, aortic wall, and periaortic structures	• False-positive results based on presence of mediastinal blood alone is substantial • Contrast streaming artifact and motion artifact
TEE	Second-line	• Wide availability, portability, rapid • May be first-line in some hemodynamically unstable patients • Can be performed during laparotomy, other procedures • Can detect minimal injuries (up to 10% of BAIs)	• Failure to image distal ascending aorta/proximal arch in some patients • Requires immediate presence of skilled operator
Aortography	Second-line	• May be useful when CT is uninterpretable or inconclusive	• Invasive, time consuming, requires specialized team, and transfer to catheterization laboratory • False-positive and false-negative results • Interobserver variability in interpretation
IVUS	Third-line	• Can image lumen, aortic wall, periaortic structures • Can be performed by the operating team	• Accuracy not yet proved in large clinical series
MRI	Third-line	• Useful primarily for chronic phase and serial examinations	• Examination times relatively long • Not suitable for unstable patients • Limited data available

superb diagnostic accuracy, availability, and speed. Importantly, at most trauma centers, CT of the thorax in patients at risk for BAI is not performed as a sole examination but is rather integrated into a whole-body CT—the so-called trauma panscan—with unique ability to identify associated injuries in the same diagnostic sitting (brain, facial bones, neck, chest, abdomen, pelvis). This latter technique has been shown to improve survival and reduce imaging time.[307,310,311]

Computed tomographic findings (both direct and indirect signs) in BAI are listed in Table 21. Nonaxial reconstructions of thin-section slices and careful evaluation of the aortic wall as well as exclusion of periaortic hemorrhage or hematomas may help in making an accurate diagnosis.[303,310] Although the presence of periaortic hemorrhage should lead to careful evaluation of the aorta for evidence of injury, conversely, the absence of a hematoma does not exclude aortic injury. Therefore, both aortography and TEE still have a role, especially in difficult cases and instances in which CT findings are equivocal.[280,303,310] In addition, there is still a role for aortography in some patients in whom branch-vessel injury is suspected, when there is a need to evaluate and manage active bleeding at other sites and in the planning of endovascular management.[304]

4. TEE. Because of its wide availability, portability, and accuracy, as well as the fact that no contrast medium is required, TEE is also a powerful diagnostic tool that gained popularity as a first-line study in the 1990s,[312-319] with reported sensitivities and specificities as high as 100% and 98%, respectively.[315] However, subsequent studies failed to confirm such high accuracy of TEE in suspected BAI.[320-322] Thus, its use as a first-line diagnostic tool is controversial. Furthermore, TEE may fail to adequately image the distal ascending aorta (TEE's known blind spot) and may not identify all of the branches of the aortic arch.[317-320] TEE is heavily operator dependent, and inexperience can lead to both false-positive and false-negative results.

Moreover, a skilled operator may not be available at night and on weekends. Additionally, patients with craniofacial trauma, cervical spine injuries, and airway concerns may not be suitable candidates for TEE. Last, as described above, patients with multiple traumatic injuries are likely to better served by a comprehensive computed tomographic scan rather than multiple individual diagnostic examinations.

One important role for TEE may be its ability to follow small or questionable intimal injuries that may not be seen well with either aortography or CT. In addition, TEE may be the only modality suitable for patients who require immediate laparotomy to control ongoing hemorrhage before CT. Tables 22 and 23 list some of the relative advantages and disadvantages of TEE for evaluating BAI.

Transesophageal echocardiographic findings in patients with BAIs include (1) dilatation in the region of the isthmus, (2) an abnormal aortic contour, (3) an intraluminal medial flap, (4) a pseudoaneurysm, (5) a crescentic or circumferential thickening of the aortic wall (IMH), and (6) mobile linear echodensities attached to the aortic wall consistent with an intimal tear or a thrombus. Similar findings are seen in patients with spontaneous aortic dissection, but there are some important differences. With traumatic aortic injury, the medial flap tends to be thicker, has greater mobility, and is typically perpendicular (rather than parallel) to the aortic wall so that there is an absence of two channels. The aortic contour is usually deformed because of the presence of a localized pseudoaneurysm. Last, with traumatic aortic injury, the findings are confined to the isthmus region, rather than propagating distally all the way to the iliac arteries.

5. IVUS. There is limited information on the role of IVUS for evaluating BAI. IVUS, like helical CT but unlike aortography, can visualize the lumen and both the aortic wall and the periaortic structures. Although limited by the absence of a reference-standard technique, a recent study found that IVUS performed better than catheter
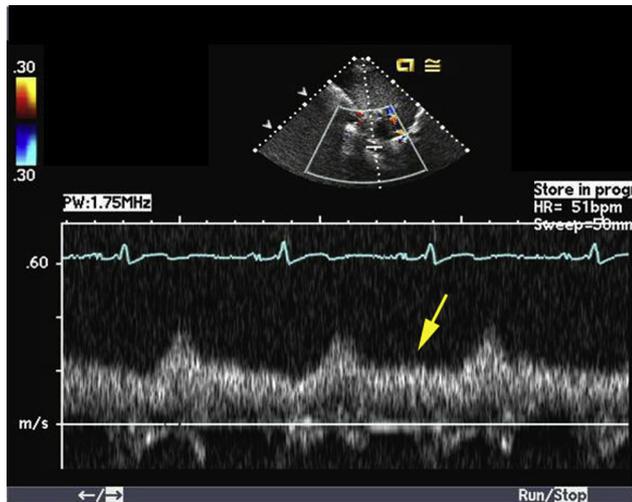
Figure 51 Abdominal aortic pulsed-wave Doppler examination in a patient with severe aortic coarctation demonstrates reduced and delayed systolic forward flow and persistent forward flow during diastole (*yellow arrow*). This "diastolic tail" is a pathognomonic sign of a hemodynamically significant coarctation.
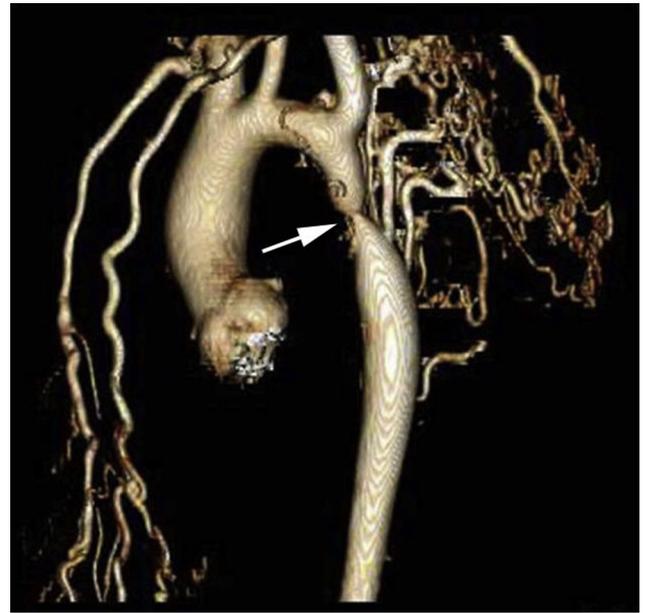
Figure 52 Computed tomographic 3D volume-rendered reconstruction of the thoracic aorta demonstrating severe aortic coarctation (*arrow*) and extensive collateral formation.

aortography in patients who had equivocal computed tomographic findings.[323] A decided disadvantage of IVUS is its limited field of view. In addition, the high cost of disposable transducers and the invasive nature limit IVUS to a problem-solving tool at present.[323]

6. MRI.   Until very recently, MRI has had limited applicability in the evaluation of acute aortic trauma. Its examination times are long, and access to patients is limited while they are in the magnet. MRI is not commonly used to evaluate injury to the thoracic great vessels in the acute phase, and few data are available in this setting. It can, however, be particularly useful for detecting the hemorrhagic component of a traumatic lesion. MRI is also an excellent method in the chronic phase of aortic trauma when serial examinations are required.[324,325] This is especially true if there is a contraindication to computed tomographic angiography. Modern MRI sequences allow both contrast and noncontrast techniques. Although these noncontrast techniques may be more time consuming, they may be of particular benefit in more stable patients with renal insufficiency, in whom iodinated contrast may be relatively contraindicated.

C. Imaging Algorithm

Contrast-enhanced MDCT is currently the preferred first-line imaging technique for suspected BAI, especially for patients with multiple injuries. Injuries to several organ systems (e.g., the brain, cervical spine, and abdomen and pelvis) can be detected in a matter of minutes, and diagnostic accuracy in both the detection and exclusion of acute traumatic aortic injury with both single-detector CT and MDCT is quite high.[302-304] Very importantly, the negative predictive value approaches 100% in some studies.[302] Although in most cases aortography is not necessary, there may be a role when branch-vessel injury is suspected and in the planning of endovascular therapy.[325] TEE and aortography are reserved for instances in which computed tomographic findings are equivocal. In some hemodynamically unstable patients, TEE may be a first-line technique, especially if CT requires transportation to a remote area. Recommendations for choice of imaging modality are listed in Table 24.

D. Imaging in Endovascular Repair

TEVAR is increasingly being used for acute aortic injury.[326,327] In the past, TEVAR was used selectively in high-risk patients with significant comorbidities. However, as experience with the technique has increased, in many institutions TEVAR has become the preferred interventional approach for BAI.

Imaging plays a key role when TEVAR is used to treat BAI. Measurements of aortic diameter should be based on aortic measurements obtained preoperatively by computed tomographic angiography or by IVUS. Length of graft coverage should be based on intraoperative aortography or IVUS measurements. Postprocedurally, aortography of the grafted segment is usually performed. Follow-up imaging is based on guidelines for evaluating endografting for nontraumatic aortic aneurysms, with computed tomographic angiography performed at 48 hours, at the time of discharge, and at 1, 6, and 12 months postprocedurally.[280]

VI. AORTIC COARCTATION

Aortic coarctation is a relatively uncommon congenital cardiovascular disorder. It is most commonly located just distal to the left subclavian artery. Aortic coarctation causes reduced blood flow to the lower body, which can present as hypertension and congestive heart failure early in life, or may be identified when a search for a cause of hypertension is performed later in life.

Patients with aortic coarctation also have a form of vasculopathy with increased risk for aneurysm formation in the ascending aorta, at the site of coarctation repair, and in the intracranial vasculature.[328] A BAV is present in >50% of patients with aortic coarctation.

The diagnosis of aortic coarctation can usually be made using TTE with Doppler imaging. The area of coarctation is often identified by 2D transthoracic echocardiographic techniques with color-flow imaging. Pulsed-wave Doppler assessment of the abdominal aorta in patients with severe aortic coarctation demonstrates reduced and
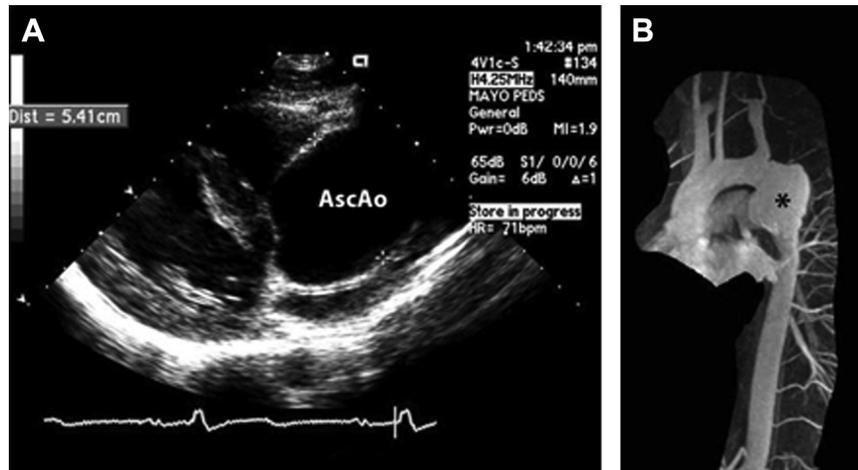
Figure 53 (A) Parasternal long-axis transthoracic echocardiogram in a patient with coarctation demonstrates marked dilatation of the ascending aorta (AscAo). **(B)** Three-dimensional reconstruction of the thoracic aorta using MR angiography in a different patient after coarctation repair demonstrating dilation of the proximal descending aorta, at the site of the prior repair (*asterisk*).

Table 25 Coarctation of aorta: key points
• Discrete narrowing of aortic lumen just distal to left subclavian artery
• Approximately 50% of patients with coarctation have BAVs
• <10% of patients with BAVs have coarctation
• Direct imaging of arch/proximal descending aorta often limited by TTE
• CT and MRI can best determine exact site, degree of obstruction, and extent of collaterals
• Doppler detects systolic flow acceleration/gradient with persistence of gradient into diastole
• Doppler gradients difficult to obtain by TEE because Doppler beam is relatively perpendicular to flow
• MRI can quantify gradient and collateral flow through velocity-encoded phase-contrast sequences
• Pseudocoarctation can be differentiated from true coarctation by identifying high, elongated arch, kinking that lacks luminal narrowing, and absence of enlarged collateral arteries

delayed forward flow in systole as well as continuation of forward flow in diastole (Figure 51) compared with the normal pattern of brisk forward flow in systole followed by early reversal of flow in diastole in persons without coarctation. Pulsed-wave Doppler is also used to measure the velocity in the descending aorta proximal to the region of obstruction. The peak and mean velocities and peak, mean, and maximum instantaneous gradients across the region of coarctation are measured by continuous-wave Doppler techniques and are used to help determine the severity of obstruction. It can be difficult to determine the severity of aortic coarctation obstruction by Doppler echocardiographic techniques alone when extensive collateral vessels are present. The exact site, length, degree of obstruction, and presence and extent of collateral vessels are best confirmed by CT or MRI (Figure 52).

Dilatation of the ascending aorta in patients with aortic coarctation is generally easily visualized by TTE, but dilatation of the coarctation repair site in the descending thoracic aorta is not well seen by TTE (Figure 53). These associated aortic complications emphasize the importance of multimodality imaging in patients with both unoperated and repaired aortic coarctation. Some key points related to multimodality imaging of coarctation are listed in Table 25.

Figure 54 Computed tomographic 3D volume-rendered reconstruction of the thoracic aorta demonstrating features of prior aortic coarctation repair, aortic arch hypoplasia, and an ascending-to-descending bypass graft (*asterisk*).

A. Aortic Imaging in Patients with Unoperated Aortic Coarctation

TTE can usually confirm the clinical diagnosis of aortic coarctation and is used to identify associated cardiovascular disorders such as BAV (present in >50% of patients with coarctation) and aortic dilatation. CT or MRI is recommended at the time of initial evaluation to determine the site and degree of obstruction and assess the aortic
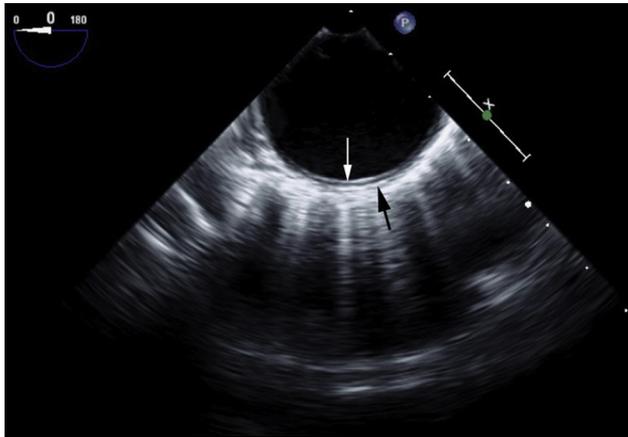
Figure 55 Transesophageal echocardiogram with a cross-section of a normal mid-descending thoracic aortic wall, which appears as two parallel echogenic lines separated by a relatively hypoechoic space. The inner line (*white arrow*) represents the luminal-intimal interface, and the outer line (*black arrow*) represents the medial-adventitial interface.

segments incompletely visualized by TTE. Patients with mild degrees of coarctation who do not require intervention should undergo annual TTE and periodic (every 3–5 years) CT or MRI to monitor for changes in the aorta. TEE is generally not used for initial diagnosis or follow-up of coarctation, because of its semi-invasive nature and difficulty comparing degree of obstruction over time.

B. Postoperative Aortic Imaging in Coarctation

Patients with prior coarctation repair require regular informed cardiovascular follow-up and imaging to evaluate for clinical and cardiovascular complications such as recurrent coarctation, ascending and descending thoracic aortic dilatation, and aortic dissection.[329]

Patients with complex recoarctation or coarctation and associated cardiovascular disease that requires operative intervention, such as coronary artery disease or aortic stenosis, may have an ascending-to-descending aortic bypass graft placed. These grafts can be partially visualized by TTE but require comprehensive imaging with CT or MRI to determine patency (Figure 54).

VII. ATHEROSCLEROSIS

Various terms have been used to describe the appearance of atherosclerotic lesions of the aorta on imaging. The simplest lesions are usually reported as "atheroma" or "atheromatous plaque." When mobile components are seen attached to these plaques, the terms *ruptured plaque, mobile plaque, mobile debris,* and *superimposed thrombi* are used. Some believe that mobile echodensities represent fibrous caps of ruptured plaques,[330] but autopsy and surgically examined specimens indicate that they are most often superimposed thrombi.[331-335] Supporting the latter conclusion, mobile lesions have been shown to disappear after anticoagulant therapy.[336] Both necropsy[337] and TEE[338,339] have demonstrated that the frequency and severity of atherosclerotic plaque is lowest in the ascending aorta, greater in the arch, and greatest in the descending thoracic aorta.

A growing body of evidence has established an association between echocardiographically demonstrated aortic atheroma and

Table 26 Grading system for severity of aortic atherosclerosis

Grade	Severity (atheroma thickness)	Description
1	Normal	Intimal thickness < 2 mm
2	Mild	Mild (focal or diffuse) intimal thickening of 2–3 mm
3	Moderate	Atheroma >3–5 mm (no mobile/ ulcerated components)
4	Severe	Atheroma >5 mm (no mobile/ ulcerated components)
5	Complex	Grade 2, 3, or 4 atheroma plus mobile or ulcerated components

embolic events, both cerebral and peripheral.[331,335,338,340-347] In addition, thoracic aortic atherosclerosis has been identified as a stronger predictor of significant coronary artery disease than are conventional risk factors[348] and as a marker of increased mortality.[349] Aortic atherosclerosis has also been associated with cholesterol embolization (blue-toe syndrome), stroke after coronary artery bypass surgery, and catheter-related embolism after cardiac catheterization and intra-aortic balloon pump insertion. Therefore, the detection of aortic atherosclerosis on imaging has prognostic implications.

A. Plaque Morphology and Classification

On ultrasound examination, the normal aortic wall is seen as two parallel echogenic lines separated by a relatively hypoechoic space (Figure 55). The inner line represents the luminal-intimal interface, whereas the outer line represents the medial-adventitial border. Thus, the distance between the lines reflects the combined thickness of the intima and media, the "intimal-medial thickness,"[350] which is normally ≤1 mm. Moreover, the normal aortic wall has a smooth, continuous surface. Any irregular thickening of ≥2 mm on TEE is therefore considered to be an atheroma.[331]

Aortic atherosclerosis has been classified on the basis of plaque characteristics of thickness, presence or absence of mobile components, and presence or absence of ulceration. Plaque thickness is considered to be a more objective and reliable measure of atheroma severity than is plaque morphology. Therefore, most grading systems are based on the maximal plaque thickness in the most diseased segment. Because there is currently no standard or universal grading system for reporting the severity of atherosclerosis, the grading system outlined in Table 26 and illustrated in Figure 56 was devised. This classification scheme, based on a review of multiple existing schemes,[344,351-363] represents a unanimous consensus of the writing committee. In this scheme, grades 1 to 4 represent progressive increases in maximum atheroma thickness from none to severe. Instead of the terms *mild, moderate,* and *severe,* some imagers may prefer the terms *small, moderate,* and *large.* Until any of these grading systems has been correlated with outcomes in a large prospective study, we recommend classifying aortic atheroma as simple or complex on the basis of the presence or absence of mobile components or ulceration(s). Although semiquantitative, the observations used in this simple classification (atheroma thickness,
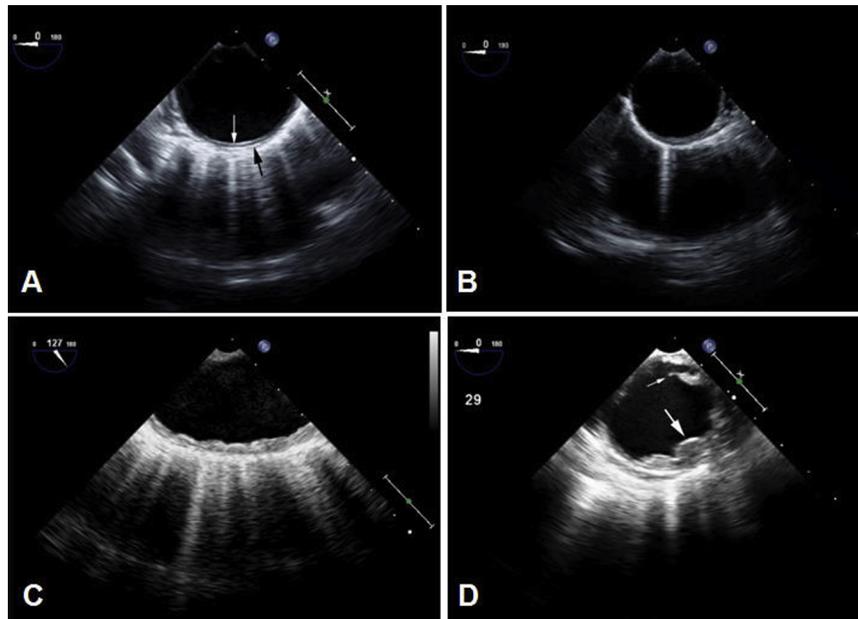
Figure 56 Four transesophageal echocardiographic images demonstrating different degrees of aortic atherosclerosis: **(A)** Normal (see Figure 54). **(B)** Mild atherosclerosis. **(C)** Moderate atherosclerosis, with a plaque thickness of <4 mm. **(D)** Severe/complex atherosclerosis with a plaque thickness that is >5 mm (*large arrow*). *Small arrow* indicates a mobile component of the plaque.

presence or absence of mobile components, and presence or absence of ulceration) are relatively objective and reproducible.

Furthermore, we, like most authors, designate any plaque, regardless of thickness, to be complex if there are mobile components or ulcerations. One group subdivided mobile lesions as (1) discrete 1- to 2-mm mobile lesions; (2) long, slender lesions that move freely in the pulsatile flow of the aorta; and (3) large masses that rock in place with aortic blood flow.[330] However, a simpler and more widely used classification has also been proposed by Thenappan *et al.*[362] In this scheme, plaques are considered "stable" when they are calcified, immobile, echodense, and homogeneous and lack signs of ulceration. They are considered "unstable" if they are mobile, nonhomogeneous, ulcerated, or spongiform. Another group derived a "total plaque burden score" from the addition of the circumferential extent of the plaque to its thickness.[360]

The major limitation of the existing classification systems, including ours, is the failure to account for the overall plaque burden in terms of its extent over the length of the thoracic aorta or a segment of the aorta. Therefore, it is recommended to report whether the atheromas are localized or diffuse.

B. Imaging Modalities

1. Echocardiography. Until the advent of TEE, the aorta was an underrecognized source of systemic embolism. Now, because of its ability to obtain high-resolution images of the aortic intima-lumen interface and detect mobile components, calcification, and ulceration,[364] TEE has become the procedure of choice for both detecting aortic atheroma and assessing atheroma size and morphology.

Important plaque features associated with an increased risk for embolization are protrusion of the plaque into the aortic lumen ≥4 mm, often with an irregular plaque surface (sometimes resembling a "seabed," especially using 3D echocardiography),[365] ulceration, and superimposed mobile components. Additionally,

hypoechoic atheromas may represent noncalcified, lipid-laden plaques that are prone to rupture and thrombosis, although ultrasound is not a reliable discriminator of plaque composition. To define the location of plaques accurately and reproducibly, the distance of the probe tip from the teeth (incisors) should be noted.

Nevertheless, TEE has several shortcomings. Its resolution may be compromised by near-field distortion, a limitation inherent in any ultrasound technique: the anterior third of the aorta in cross-section is often less well imaged because it is adjacent to the esophagus and thus in the near field of the transducer. In addition, air in the trachea and right main stem bronchus often creates a blind spot that may limit visualization of the distal ascending aorta and proximal aortic arch. In addition, determination of plaque extent and/or complexity may be limited when using (2D TEE), because only one plane can be visualized or measured at a time. Single-plane views may not appreciate an asymptomatic plaque and may mistake a single lobulated plaque for two separate plaques. Piazzese *et al.*[366] demonstrated that 3D TEE provides superior visualization of the number, morphology, volume, and spatial extent of aortic atheromas compared with 2D TEE.

Although atherosclerosis of the aorta is occasionally detected on TTE from the suprasternal view, TTE is not a reliable technique for the detection or characterization of atheroma.

2. Epiaortic Ultrasound (EAU). Because atherosclerosis of the ascending aorta is associated with an increased risk for perioperative stroke,[360,365,367-371] some centers use intraoperative measures to try to reduce the incidence of cerebral injury and neurocognitive deficits.[367,370,372,373] Three approaches have been used: digital palpation of the aorta, TEE, and EAU.[353,368,374,375] Several investigators have demonstrated that EAU is superior to both manual palpation and TEE for detecting atheroma in the ascending aorta and arch.[368,375,376] Its high sensitivity and excellent reproducibility make it a clinically useful tool.[377] Compared with TEE, EAU has better resolution, less artifact, no blind spot, and

Table 27 Choice of imaging modality for aortic atherosclerosis

Modality	Recommendation	Advantages	Disadvantages
TEE	First-line	• Most frequently used method • Procedure of choice for detecting atheroma, atheroma size and mobility • High resolution of aortic intima-lumen interface • Very reproducible	• Near-field distortion • Not reliable for plaque composition • Distal ascending aorta, proximal arch may be limited
CT	Second-line	• Sensitivity, specificity, accuracy for identifying atheroma approaches that of TEE • Able to image entire aorta, assess overall plaque burden	• Cannot be used in OR during surgery • Radiation exposure • Requires contrast agent • Limited utility for assessing mobile thrombi
MRI	Second-line	• Provides information about plaque composition • Can image the entire aorta	• Limited utility for assessing mobile thrombi • Spatial resolution inferior to CT • Overestimates plaque thickness compared with TEE • Limited use • No generally accepted protocol for aortic imaging
Epiaortic echocardiography	Third-line	• Superior to TEE for detecting atheroma in ascending aorta and arch in OR • Compared with TEE, better resolution, fewer artifacts, no blind spot	• Not widely or routinely used in cardiac surgery • Experience of surgeons and anesthesiologists is less than with TEE

OR, Operating room.

superior detection of disease in the mid and distal ascending aorta. Moreover, EAU also appears to be superior to preoperative CT for this purpose.[378] For a more detailed discussion of EAU, the reader is referred to the excellent guidelines on this topic.[379]

Nevertheless, despite the strengths of EAU, intraoperative TEE is still used more often than EAU for several reasons. First, at many centers TEE is routinely used in cardiac surgery to monitor volume and ventricular function and to evaluate the adequacy of the surgical procedure, so it has become the most common way aortic atheromas are detected. Second, despite its potential superiority, EAU is less widely available in most operating rooms than is TEE, and therefore surgeons and anesthesiologists have less experience working with it than with TEE. Nevertheless, EAU should be available in instances in which TEE is contraindicated or the rare instances in which the TEE probe cannot be inserted. In addition, some groups perform EAU before nonaortic surgery (e.g., coronary bypass grafting) in select "high-risk" patients (for atherosclerosis), including those aged > 75 years, with peripheral vascular disease, with histories of cerebrovascular disease, with palpable calcifications on the ascending aorta, and with findings on TEE. The finding of prominent atheromas may lead to modifications of surgical techniques.

During an epiaortic scan, mapping of the distribution of aortic atheromas should be performed. The ascending aorta may be divided into proximal, middle, and distal thirds. Each segment may have atheroma in its anterior, posterior, lateral, and medial walls, and details of plaque location should be conveyed to the surgeon.[380]

3. CT. Multidetector computed tomographic angiography of the aorta can also be used to detect aortic atheroma. Its sensitivity, specificity, and overall accuracy for identifying severe aortic atheroma approaches that of TEE.[381,382] The degree of x-ray attenuation may be used to estimate the composition of atherosclerotic plaque.[383] Calcified plaque appears as a light, high-attenuation signal, whereas lipid-rich or fibrous plaque appears as hypoattenuated dark signals within the vessel wall. However, quantification is limited by calcium-provoked "blooming ar-

tifacts," which may lead to overestimation of calcified plaques.[381] One potential advantage of MDCT is its ability to image the entire aorta in a continuous manner, which is not possible by TEE (including areas poorly visualized by TEE), allowing the assessment of aortic plaque burden in the entire thoracic aorta in a semiquantitative fashion.[384] Although MDCT can identify high-risk atherosclerotic features before cardiac surgery, unlike TEE and EAU, it cannot be used in the operating room during surgery. Other limitations of MDCT are the relatively high radiation dose associated with its use and the requirement for contrast agents for aortic imaging. However, newer computed tomographic imaging techniques may require lower radiation doses in the evaluation of the aorta.

4. MRI. MRI, another alternative for detecting and evaluating aortic atherosclerosis, can supply information about plaque characteristics.[385,386] However, MRI has limited utility for assessing the mobile thrombi that are often superimposed on plaques. Moreover, its spatial resolution is inferior to that of CT.[387] Compared with TEE, MRI overestimates plaque thickness and consequently classifies more patients as at high risk (≥4-mm plaque thickness).[388] In addition, whereas transesophageal echocardiographic measurements of aortic plaque are very reproducible, the reproducibility of MRI measurements is less well established. Thus, this technology has not yet gained wide clinical acceptance and is a less cost-effective method for detection of aortic atherosclerosis. Nevertheless, MRI remains promising because of unique potential to characterize plaque composition,[383] which is more reliable than TEE for this purpose. Both contrast-enhanced and noncontrast MRI techniques have been developed, but most remain in the nonclinical realm at this time.

C. Imaging Algorithm

TEE, CT, and MRI are powerful diagnostic tools for visualizing aortic atheromas. In patients with stroke or peripheral embolism, TEE is the technique of choice because it affords excellent assessment of the size
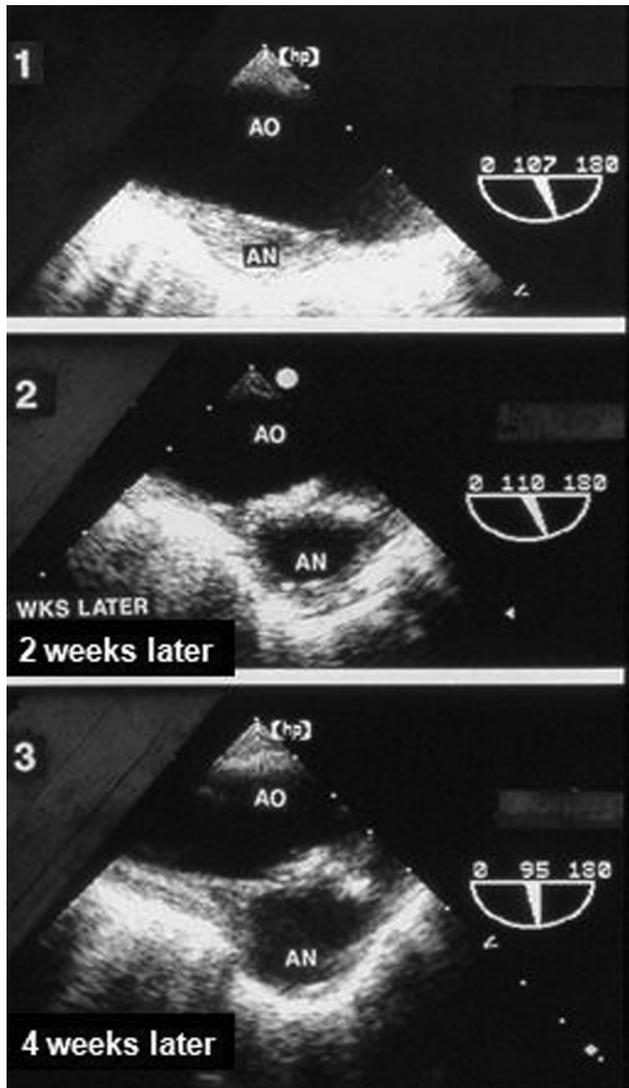
Figure 57 This transesophageal echocardiogram of the proximal descending thoracic aorta obtained in a patient with aortic valve endocarditis demonstrates an early incipient aneurysm (frame 1) and rapid enlargement. Frame 2 was taken 2 weeks later, at the time of aortic valve replacement, and frame 3 was taken at the time of staged aortic surgery 4 weeks after the initial TEE. *AN*, Aneurysm; *AO*, aorta.

and mobility of complicated plaques. CT can image the entire aorta (including areas poorly visualized by TEE) but requires exposure to radiation and the use of contrast agents. MRI can noninvasively distinguish various components of the plaque, such as fibrous cap, lipid core, and thrombus thereby assessing plaque stability. Serial MRI or CT can be used to monitor progression or regression of atheromatous plaques after therapy with lipid-lowering agents. The relative advantages and disadvantages of the various imaging techniques for atherosclerosis are summarized in Table 27.

D. Serial Follow-Up of Atherosclerosis (Choice of Tests)

In clinical practice, TEE is the technique of choice for the follow-up of thoracic aortic atherosclerosis because it affords excellent assessment of the size and mobility of complicated plaques. MRI can noninva-

Table 28 Mycotic aneurysm: key points

- Aorta should be evaluated in all patients with infective endocarditis
- Can lead to saccular (more common) or fusiform aneurysm
- Normal appearance of adjacent regions of aorta
- Echocardiography, CT, and MR all preferable to aortography
- PET may be useful
- Requires close follow-up because progression is often rapid

PET, Positron emission tomography.

Table 29 Noninfectious aortitis: etiologies

TA
GCA (temporal arteritis)
Spondyloarthropathies (ankylosing spondylitis and Reiter syndrome)
ANCA associated (Wegener's disease, polyarteritis nodosum, microscopic polyangiitis)
Systemic lupus erythematosus
Rheumatoid arthritis
Behçet syndrome
Cogan syndrome
Relapsing polychondritis
Sarcoidosis
Idiopathic aortitis

ANCA, Antineutrophil cytoplasmic antibody; *GCA*, giant cell arteritis; *TA*, takayasu arteritis.

sively distinguish various components of the plaque, such as fibrous cap, lipid core, and thrombus, thereby assessing plaque stability. In T2-weighted images, fibrous cap and thrombus are seen as a high-intensity signal, and lipid core is seen as a low-intensity signal. Although CT can distinguish calcified plaque from fibrolipid plaque, this method is less efficient than MRI for the characterization of atherosclerotic plaque composition, and standard MDCT without electrocardiographic gating does not assess plaque mobility.

TEE is the imaging modality of choice for diagnosing aortic atherosclerosis and atheromas. Advantages of TEE over other noninvasive modalities (CT and MRI) include the ability to accurately measure the size and mobility of plaque and overlying thrombi in real time. When atherosclerosis is present, the severity and location of the most severe atheromas should be reported. In patients in whom the suprasternal window is optimal, plaques in the aortic arch may be detected by TTE.

VIII. AORTITIS

A. Mycotic Aneurysms of the Aorta

Mycotic aneurysms of the thoracic aorta are extremely uncommon, but they are important because they are potentially life threatening. Untreated, a mycotic aneurysm may lead to septic thromboembolism, rupture, or death. Osler[389] coined the term *mycotic aneurysm* in 1885, describing a mushroom-shaped aneurysm that resembled a fungal growth. However, this term is a misnomer, because the vast majority of infected aneurysms are bacterial and not fungal. So the term has since been broadened to include all aneurysms with an infectious component.
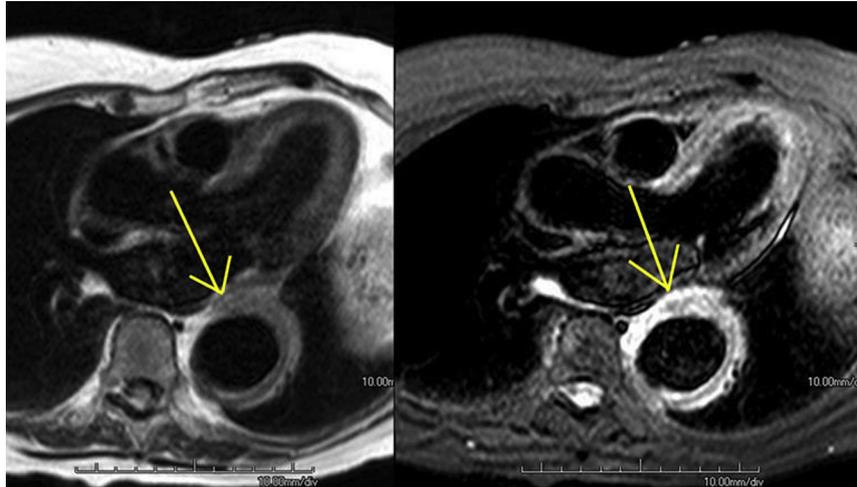
Figure 58 MR images from a 54-year-old woman with elevated sedimentation rate and dilation of the descending aorta. Wall thickening is well depicted in dark blood images (*left, yellow arrow*). Short tau inversion recovery (STIR) images (*right*) demonstrate bright signals in the aortic wall (*yellow arrow*), a result consistent with edema. Surgical repair was performed in this patient, and histology was consistent with GCA.

Mycotic aortic aneurysms most often result from septic emboli in patients with left-sided endocarditis, so one should consider imaging the thoracic aorta to exclude mycotic aneurysms in patients with mitral or aortic valve endocarditis. Aortic seeding may also result from bloodborne dissemination from an infection anywhere in the body. Mycotic aneurysms may also be associated with aortic trauma caused by accidents, surgical manipulation, or invasive diagnostic procedures.[390,391]

The classical triad of fever, abdominal, back, or chest pain, and leukocytosis is present in the majority of patients.[392,393] Aortic infections should be considered when such classic signs and symptoms cannot otherwise be explained. Therefore, suspicion must be heightened in immunosuppressed patients and in those with open or endovascular implants.[394,395] Once suspected, the diagnosis should be pursued vigorously because progression is the rule. Figure 57 illustrates such a case and also emphasizes the potential for rapid progression.

Aortography is no longer the diagnostic modality of choice, but characteristic aortographic features include either saccular or fusiform aortic aneurysm with a normal appearance of the adjacent regions of the aorta.[396,397] However, these findings are nonspecific and unreliable. Moreover, aortography images only the aortic lumen (and not the aortic wall) and could potentially induce an aortic rupture when the wall is fragile.

Echocardiography, CT, and MRI are now the preferred imaging techniques. Contrast-enhanced CT may reveal a change in aortic size, saccular aneurysm formation, periaortic nodularity, and/or air in the aortic wall. However, milder degrees of inflammation or aortic wall edema may be missed.[394,398,399] MRI with gadolinium contrast enhancement is another useful imaging modality. In addition to detection of an aneurysm, associated aortitis may appear as vessel wall edema, enhancement, or wall thickening. Specific protocols have been developed, such as the "edema-weighted" technique, that may detect even small changes within and around the aortic wall.[394] In addition, these noninvasive imaging techniques may allow rapid exclusion of other aortic pathologies that may resemble aortic infection, such as aortic dissection, IMH, and PAU.

Recently, ^{18}F fluorodeoxyglucose positron emission tomography appears to hold promise for diagnosing mycotic aneurysms and graft infections by detecting hypermetabolic activity, as elevated ^{18}F fluorodeoxyglucose uptake within the aortic wall is suggestive of active vascular infection.[379] Response to antibiotic therapy can also be monitored as a decrease in ^{18}F fluorodeoxyglucose uptake within the aortic wall suggests improvement.[400]

Table 28 lists several key points concerning mycotic aneurysms.

B. Noninfectious Aortitis

TA and GCA, although rare, are the most common of a group of disorders that can be categorized as noninfectious aortitis (Table 29).[394] A detailed discussion of the imaging features of each of these is beyond the scope of this document, but a brief discussion of TA and GCA follows.

TA is a rare, large-vessel vasculitis of unknown etiology, predominantly affecting young women (age < 40 years). The thoracic aorta and its major branches are most often affected,[401] but the pulmonary arteries and abdominal aorta may also be affected. TA is characterized by a nonspecific inflammatory process that can progress to stenotic, even occlusive lesions secondary to intimal thickening.[401,402] Progression of the disease can lead to destruction of the media, leading to aneurysm formation or rupture.

Digital subtraction angiography of the aorta and its branches, previously the gold standard, only provides information relating to luminal changes (ranging from smooth tapering stenosis to frank occlusion), which are a late feature. MRI, CT, and echocardiography can demonstrate homogeneous circumferential thickening of the aortic wall with a uniform smooth internal surface, which is different from the appearance of atherosclerosis[403,404] but may be misdiagnosed as IMH. CT and MRI provide a more generalized survey of the aorta and its proximal branches than echocardiography, including the abdominal aorta and distal pulmonary arteries, which are sometimes affected.[405] MRI may show arterial wall edema, a marker of active disease.[406] In chronic TA, the aortic wall may become calcified, which is best appreciated by CT. Positron emission tomography is a promising technique that may reveal the level of vascular inflammatory activity.[407]

GCA is a systemic panarteritis that characteristically affects middle-aged and elderly patients (age > 50 years).[408,409]

Table 30 Common aortic surgical procedures

1. Valveless ascending grafts
   a. Interposition technique
   b. Inclusion technique
2. Composite aortic grafts
3. Aortic arch grafts
4. Descending aortic grafts
5. Endovascular stent grafts
6. Resuspension of the aortic valve
7. Valve-sparing root replacement
8. Use of biologic adhesives and sealants
9. Coronary artery (button) reimplantation

Table 31 Less common aortic surgical procedures

1. "Elephant trunk" procedure
2. Cabrol shunt procedure
3. Cabrol coronary graft procedure
4. Aortic tailoring (aortoplasty)
5. Fenestration
6. Obliteration of false lumen (primary repair)
   a. Glue aortoplasty
   b. Insertion of foreign material
   c. Thromboexclusion
7. Aortic girdling (wrapping the aorta with Dacron mesh)

Although classically the temporal and/or other cranial arteries are involved, the aorta and its major branches are affected in approximately 10% to 18% of patients.[410,411] Dilatation of the aortic root and ascending aorta are common and can lead to aortic dissection or rupture, usually several years after the initial diagnosis. If a diagnosis of extracranial GCA is suspected, echocardiography, CT, or MRI is recommended. The finding of a thickened aortic wall on CT or MRI indicates inflammation of the aortic wall (Figure 58) and thus active disease.[412] Studies with positron emission tomography have suggested that subclinical aortic inflammation is often present in patients with GCA.[413]

IX. POSTSURGICAL IMAGING OF THE AORTIC ROOT AND AORTA

Advances in diagnostic imaging techniques have allowed earlier diagnosis of and more prompt surgical intervention for thoracic aortic disease, which in turn has likely improved outcomes for both emergency and elective surgery of the aorta. As a consequence increasing numbers of patients are presenting for follow-up care.

For both aortic dissections and aneurysms involving the ascending aorta, the surgeon usually replaces the ascending aorta with an interposition Dacron graft but leaves the native aortic root, arch, and descending aorta behind. Thus, survivors of the initial repair may remain at considerable risk for future aneurysmal dilatation and eventual rupture. Consequently, appropriate follow-up requires long-term clinical monitoring and follow-up imaging to detect such complications and to allow timely surgical or percutaneous reintervention. The foundation for such follow-up imaging is obtaining adequate baseline imaging that provides a reliable reference for future comparisons of aortic size and appearance. Moreover, baseline imaging will detect technical failures and improper or incomplete repairs with the potential for subsequent complications.

A. What the Imager Needs to Know

To evaluate postoperative findings accurately, the imaging physician must possess a general understanding of the surgical techniques available to treat thoracic aortic diseases and awareness of the details of the surgical procedure that was used in the individual patient. In most instances, the postoperative image may differ in important ways from that seen before the surgical intervention. It follows that the expected postoperative image and any possible variations as presented by the relevant imaging modality must be understood. Only then can the spectrum of potential postsurgical complications

be accurately recognized and distinguished from the expected postoperative appearance.

B. Common Aortic Surgical Techniques

Listed in Tables 30 and 31 are some of the more common aortic procedures and some of the alternative or less common procedures. A brief discussion of some of the more common procedures follows. The scope of this review does not permit detailed discussion of modifications of standard procedures or of less commonly used techniques.

1. Interposition Technique. This currently standard technique includes excision of the diseased segment of the native ascending aorta and its replacement with a polyester (Dacron) graft. The proximal anastomotic site is often supracoronary, and the distal anastomotic site is immediately proximal to the brachiocephalic artery. The anastomotic sites are often reinforced with externally placed circumferential strips of Teflon felt.

2. Inclusion Technique. The inclusion technique consists of an aortotomy, placement of an artificial graft within the diseased native aorta, and enclosing or "wrapping" the graft with the native aorta, which is sutured around the graft. This procedure creates a potential space between the graft and the native aortic wall, which has important imaging implications. The use of this technique has diminished significantly because improved graft materials have led to decreased bleeding (this technique was used to provide a space into which leakage through grafts could occur to minimize extensive bleeding into the mediastinum).

3. Composite Grafts. A composite graft, or conduit, is a synthetic (commonly Dacron) aortic graft that includes a directly attached mechanical valve or bioprosthetic valve. With composite graft replacement, the coronary ostia are dissected from the native aorta with a rim of surrounding aorta ("button technique"), and each button is then reanastomosed individually to the composite graft.

4. Aortic Arch Grafts. For select patients with aortic arch involvement, open surgery may range from partial to complete arch replacement with or without debranching and reattachment of one or more of the arch vessels.

5. Elephant Trunk Procedure. Surgery for treatment of diffuse thoracic aortic disease is commonly performed in a two-stage operation. The first stage consists of repair of the ascending aorta and aortic arch (with reconstruction of the great vessels); an extension of the aortic graft is inserted into the lumen of the proximal descending thoracic aorta,

where it floats freely and is referred to as the "elephant trunk." The second stage of the operation consists of repair of the descending aorta using the elephant trunk for the proximal anastomosis of an open surgical graft or as the proximal landing zone for an endovascular stent graft.

6. Cabrol Shunt Procedure. The Cabrol shunt procedure is an uncommon adjunct to the inclusion graft technique, performed to prevent progressive bleeding into the potential space between the graft and the native aortic wall, as described earlier. This procedure consists of a surgically created shunt between this potential space and the right atrium to alleviate any pressure in the perigraft space.

7. Technical Adjuncts. For all types of grafts, circumferential felt or pericardial rings are often used to buttress anastomoses. Felt pledgets are also used to reinforce the graft or the native aortic wall at sites of intraoperative cannula placement. These rings and pledgets have imaging implications for each of the imaging modalities, such as otherwise unexplained thickenings, reverberations, and acoustic shadowing.

A variety of adhesives, or biologic glues, have been used as an adjunct to standard methods of achieving anastomotic hemostasis (such as sutures and clips). These bioglues have also been used for re-approximating layers of the dissected aorta and for strengthening weakened aortic tissues by a "tanning" process. Although the value of these tissue adhesives is recognized, there are reports of tissue necrosis leading to false aneurysms.[414] Moreover, these substances may produce edema, inflammation, and fibrosis, leading to thickening of the aortic wall or adjacent tissues. Such thickening can be confused with leakage and hematoma by imaging techniques.

C. Normal Postoperative Features

The details of the surgery that has been performed will determine the appearance of the ascending aorta on prospective imaging studies. There are only a few descriptions of the echocardiographic appearance of the ascending aorta after reconstruction. More information is available on computed tomographic and MRI findings. An aortic interposition graft is visualized as a thin, corrugated tube with an echodensity greater than that of the native aorta. There is usually an abrupt change between the graft and the native aorta as felt strips that are used to reinforce the anastomoses provide visual markers of those borders. Occasionally there is angulation of the aortic graft, especially near the anastomoses. These points of angulation are not clinically significant but can mimic a dissection flap, especially on axial computed tomographic images.

A small amount of perigraft thickening (<10 mm) is a common postoperative finding. This presumably results from minor leakage at the anastomotic suture lines created by needle holes. The uniform and concentric distribution of this thickening helps differentiate it from more serious leakage. Another mimicker of pathology can be seen at the site of coronary anastomoses. When the coronary arteries are resected with a rim of native aortic tissue (button technique), a focal bulge at this site can be misinterpreted as an incipient pseudoaneurysm. Importantly, the inclusion graft technique creates a potential space between the graft and its wrap, the native aorta. This space often contains fluid and/or hematoma, which can be a normal finding with no clinical significance, especially when <10 mm in thickness.

After repair of a type A dissection, a persistent dissection flap is seen distal to the ascending aortic graft in 80% of patients.[40] This persistence of a double-channel aorta after surgery is not considered a complication, provided it does not increase in size. In chronic dissections, the residual dissection flap becomes thickened because of collagen deposition and becomes less oscillatory or even immobile.

Table 32 Potential postoperative complications of aortic surgery

1. Anastomotic leakage, disruption, dehiscence
2. Pseudoaneurysm (at proximal, distal, or coronary anastomotic site)
3. Progressive AR
4. Involvement of aortic branches
5. Perigraft infection
6. Compression of graft by hematoma (inclusion technique)
7. Aneurysmal dilatation of false lumen (status post dissection repair)
8. Compression or collapse of true lumen (by expanding false lumen)
9. Frank rupture
10. Anastomotic stenosis
11. Development of recurrent dissection or aneurysm proximal to a graft in patients in whom a supracoronary procedure has been performed.
12. Aortoesophageal or aortopulmonary fistula
13. Graft herniation into thoracotomy defect

Many early postoperative CT studies show pleural or pericardial effusions, mediastinal lymph node enlargement, and/or left lobe atelectasis. These findings diminish in frequency over time and presumably represent normal postoperative findings without adverse clinical consequences.

D. Complications after Aortic Repair

Total removal of the diseased aortic segment is seldom possible with surgical repair of aortic lesions such as aneurysm and dissection, and the anastomoses between graft and native aorta are potential sites for late complications. Therefore, periodic postoperative surveillance by cardiovascular imaging specialists who are familiar with aortic diseases and surgical procedures cannot be overemphasized. Early detection of complications can facilitate optimal management, including reoperation when appropriate. Potential postoperative complications are listed in Table 32. An awareness of such complications, and the ability to differentiate them from the spectrum of "normal" postoperative findings, is obviously important. Some of the more common complications are discussed.

1. Pseudoaneurysm. Pseudoaneurysm is an important early or late complication that can occur after surgery for aneurysm dissection. In the vast majority of patients, pseudoaneurysm is not associated with any clinical symptoms.[415] The silent nature of these potentially life-threatening complications emphasizes the need for surveillance imaging. Pseudoaneurysms usually occur at anastomoses. Although they can form at the site of needle holes even when the suture lines are intact, more often they originate from partial dehiscence of the proximal or distal suture lines or at the site of coronary reimplantation. The size of the pseudoaneurysm, its change over time, and the patient's symptoms and clinical status will determine management. Small, sterile pseudoaneurysms can remain stable for years without further intervention. Pseudoaneurysms are readily detectable by both CT and MRI. TEE is also reliable for detecting pseudoaneurysms of the aortic root and proximal ascending aorta but can miss lesions in the distal ascending aorta because of the interposition of the trachea.

2. False Luminal Dilatation. Surgery for type A aortic dissection is usually limited to the ascending aorta. Distal to the ascending aortic

graft, a dissection flap and a false lumen with demonstrable blood flow are present in approximately 80% of patients.[40] Strictly speaking, this is not a complication, but there is a potential for false luminal expansion. Typically, the median diameter of the aortic arch, descending thoracic aorta, and abdominal aorta are all mildly enlarged after type A aortic dissection repair.[416] Although expansion rates are low, progressive dilatation of the patent false lumen, facilitated by the poor condition of the weakened and thinned wall, often occurs. This may result in late aortic rupture or collapse of the true lumen. In the minority of patients, the false lumen can become thrombosed. Although the influence of thrombosis of the false lumen on long-term survival remains speculative, it may be associated with improved survival.

3. Involvement of Aortic Branches. Extension of a dissection flap and/or IMH into an aortic branch may result in luminal narrowing or total obstruction. In addition, dilatation of a patent false lumen and associated collapse of the true lumen may also affect the branch vessels. These complications may occur in the coronary arteries, supra-aortic vessels, or visceral vessels.

4. Infection. Early- or late-onset infection complicates prosthetic aortic graft insertion in 0.5% to 5% of patients. CT is considered the standard imaging method for aortic graft infection.[417] The role of TEE for detection for graft infection has not been thoroughly investigated.

E. Recommendations for Serial Imaging Techniques and Schedules

The imaging modality of choice for evaluating the postoperative aorta has not been clearly determined. Both CT and MRI are reasonable choices. These techniques provide precise and reproducible measurements of the native aorta diameter at any level and have the advantage compared with TEE of including the supra-aortic and visceral vessels in a single examination and providing reproducible landmarks for comparing images from serial studies.

We consider contrast-enhanced CT to be the optimal diagnostic tool for follow-up of patients after surgery for aortic disease. MRI is also valuable for serial follow-up because image resolution is comparable with that of CT. In some patients, MRI may be preferred because neither radiation nor contrast media are required. This is especially true in young patients (e.g., those with Marfan syndrome) because the radiation exposure from serial examinations may be considerable.

TTE, although a routine study for many cardiology patients, is limited in its utility to follow patients after aortic surgery. TTE provides an adequate assessment of the aortic valve, aortic root, and proximal ascending aorta but is limited in its ability to image the remainder of the thoracic aorta.

TEE has some advantages over CT and MRI. It is portable, provides excellent images of the aortic root, can precisely assess the morphology and function of the aortic valve, and provides information on left ventricular function. However, it may not be able to image the distal ascending aorta (which may be the site of the aortic graft's distal anastomosis), the proximal aortic arch, the proximal aortic arch vessels, and the distal abdominal aorta. Moreover, it cannot assess the relationship of aortic pseudoaneurysms to adjacent anatomic structures such as the lung or mediastinum. Last, TEE is semi-invasive, which is a drawback for serial, repeated examinations.

The plan for follow-up surveillance imaging should not be left to other practitioners alone. Primary responsibility lie with the aortic specialist (cardiac surgeon, cardiologist, or vascular surgeon) overseeing the evaluation and management of the patient. Ideally, there should be a computer database into which the relevant clinical, surgical, and imaging details of every patient with thoracic aortic disease are entered. The surveillance imaging modality and the frequency of follow-up should be decided on the basis of the individual patient's clinical history, prior intervention, and rate of progression of the disease, outlined in Table 5. In general, patients with small aortas or mild disease can be followed at less frequent intervals than are those with larger aortas. Although it is reasonable to permit surveillance imaging examinations to be performed at sites close to the patient's home, ideally the images should be reviewed and the patient followed by a provider or center with expertise and experience in the management of thoracic aortic disease.

X. SUMMARY

In conclusion, the considerable advances in diagnostic imaging techniques have greatly increased our understanding of thoracic aortic diseases. The availability, cost/benefit ratio, and additive value of each technique determine its indications. TTE continues to be the technique most used in clinical practice for aortic root assessment. CT has the advantage of its high-resolution assessment of the entire aorta and excellent accuracy on size measurements. MRI offers the greatest morphologic and dynamic information of the aorta without radiation, although in clinical practice it is less commonly available.

New advances such as time-resolved 3D phase-contrast velocity (four-dimensional flow) on MRI, electrocardiographically gated MDCT, and the use of contrast in echocardiographic studies, will permit further improvement in the definition of biomechanical properties of the diseased aorta wall, which can be expected to influence the prognostication and management of patients with aortic diseases.

NOTICE AND DISCLAIMER

This report is made available by ASE and the European Association of Cardiovascular Imaging (EACVI) as a courtesy reference source for members. This report contains recommendations only and should not be used as the sole basis to make medical practice decisions or for disciplinary action against any employee. The statements and recommendations contained in this report are based primarily on the opinions of experts, rather than on scientifically verified data. The ASE and EACVI make no express or implied warranties regarding the completeness or accuracy of the information in this report, including the warranty of merchantability or fitness for a particular purpose. In no event shall the ASE and EACVI be liable to you, your patients, or any other third parties for any decision made or action taken by you or such other parties in reliance on this information. Nor does your use of this information constitute the offering of medical advice by the ASE and EACVI or create any physician-patient relationship between the ASE and EACVI and your patients or anyone else.

REFERENCES

1. Hiratzka LF, Bakris GL, Beckman JA, Bersin RM, Carr VF, Casey DEJ, et al. 2010 ACCF/AHA/AATS/ACR/ASA/SCA/SCAI/SIR/STS/SVM guidelines for the diagnosis and management of patients with Thoracic

Aortic Disease: a report of the American College of Cardiology Foundation/American Heart Association Task Force on Practice Guidelines, American Association for Thoracic Surgery, American College of Radiology, American Stroke Association, Society of Cardiovascular Anesthesiologists, Society for Cardiovascular Angiography and Interventions, Society of Interventional Radiology, Society of Thoracic Surgeons, and Society for Vascular Medicine. Circulation 2010;121:e266-369.

2. Gott VL, Pyeritz RE, Magovern GJJ, Cameron DE, McKusick VA. Surgical treatment of aneurysms of the ascending aorta in the Marfan syndrome. Results of composite-graft repair in 50 patients. N Engl J Med 1986;314: 1070-4.

3. Roman MJ, Devereux RB, Niles NW, Hochreiter C, Kligfield P, Sato N, et al. Aortic root dilatation as a cause of isolated, severe aortic regurgitation. Prevalence, clinical and echocardiographic patterns, and relation to left ventricular hypertrophy and function. Ann Intern Med 1987;106:800-7.

4. Vriz O, Driussi C, Bettio M, Ferrara F, D'Andrea A, Bossone E. Aortic root dimensions and stiffness in healthy subjects. Am J Cardiol 2013;112: 1224-9.

5. Burman ED, Keegan J, Kilner PJ. Aortic root measurement by cardiovascular magnetic resonance: specification of planes and lines of measurement and corresponding normal values. Circ Cardiovasc Imaging 2008;1:104-13.

6. Devereux RB, de Simone G, Arnett DK, Best LG, Boerwinkle E, Howard BV, et al. Normal limits in relation to age, body size and gender of two-dimensional echocardiographic aortic root dimensions in persons >/=15 years of age. Am J Cardiol 2012;110:1189-94.

7. Hager A, Kaemmerer H, Rapp-Bernhardt U, Blucher S, Rapp K, Bernhardt TM, et al. Diameters of the thoracic aorta throughout life as measured with helical computed tomography. J Thorac Cardiovasc Surg 2002;123:1060-6.

8. Lin FY, Devereux RB, Roman MJ, Meng J, Jow VM, Jacobs A, et al. Assessment of the thoracic aorta by multidetector computed tomography: age- and sex-specific reference values in adults without evident cardiovascular disease. J Cardiovasc Comput Tomogr 2008;2:298-308.

9. Roman MJ, Devereux RB, Kramer-Fox R, O'Loughlin J. Two-dimensional echocardiographic aortic root dimensions in normal children and adults. Am J Cardiol 1989;64:507-12.

10. Vasan RS, Larson MG, Benjamin EJ, Levy D. Echocardiographic reference values for aortic root size: the Framingham Heart Study. J Am Soc Echocardiogr 1995;8:793-800.

11. Lam CS, Xanthakis V, Sullivan LM, Lieb W, Aragam J, Redfield MM, et al. Aortic root remodeling over the adult life course: longitudinal data from the Framingham Heart Study. Circulation 2010;122:884-90.

12. Daimon M, Watanabe H, Abe Y, Hirata K, Hozumi T, Ishii K, et al. Normal values of echocardiographic parameters in relation to age in a healthy Japanese population: the JAMP study. Circ J 2008;72:1859-66.

13. Vasan RS, Larson MG, Levy D. Determinants of echocardiographic aortic root size. The Framingham Heart Study. Circulation 1995;91:734-40.

14. Drexler M, Erbel R, Muller U, Wittlich N, Mohr-Kahaly S, Meyer J. Measurement of intracardiac dimensions and structures in normal young adult subjects by transesophageal echocardiography. Am J Cardiol 1990;65:1491-6.

15. Sheil ML, Jenkins O, Sholler GF. Echocardiographic assessment of aortic root dimensions in normal children based on measurement of a new ratio of aortic size independent of growth. Am J Cardiol 1995;75:711-5.

16. Lang RM, Bierig M, Devereux RB, Flachskampf FA, Foster E, Pellikka PA, et al. Recommendations for chamber quantification: a report from the American Society of Echocardiography's Guidelines and Standards Committee and the Chamber Quantification Writing Group, developed in conjunction with the European Association of Echocardiography, a branch of the European Society of Cardiology. J Am Soc Echocardiogr 2005;18:1440-63.

17. Iskandar A, Thompson PD. A meta-analysis of aortic root size in elite athletes. Circulation 2013;127:791-8.

18. Pelliccia A, Di Paolo FM, De Blasiis E, Quattrini FM, Pisicchio C, Guerra E, et al. Prevalence and clinical significance of aortic root dilation in highly trained competitive athletes. Circulation 2010;122:698-706. 3 p following 706.

19. Pelliccia A, Di Paolo FM, Quattrini FM. Aortic root dilatation in athletic population. Prog Cardiovasc Dis 2012;54:432-7.

20. Wolak A, Gransar H, Thomson LE, Friedman JD, Hachamovitch R, Gutstein A, et al. Aortic size assessment by noncontrast cardiac computed tomography: normal limits by age, gender, and body surface area. JACC Cardiovasc Imaging 2008;1:200-9.

21. Kalsch H, Lehmann N, Mohlenkamp S, Becker A, Moebus S, Schmermund A, et al. Body-surface adjusted aortic reference diameters for improved identification of patients with thoracic aortic aneurysms: results from the population-based Heinz Nixdorf Recall study. Int J Cardiol 2013;163:72-8.

22. De Backer J, Loeys B, Devos D, Dietz H, De Sutter J, De Paepe A. A critical analysis of minor cardiovascular criteria in the diagnostic evaluation of patients with Marfan syndrome. Genet Med 2006;8:401-8.

23. Lu TL, Huber CH, Rizzo E, Dehmeshki J, von Segesser LK, Qanadli SD. Ascending aorta measurements as assessed by ECG-gated multi-detector computed tomography: a pilot study to establish normative values for transcatheter therapies. Eur Radiol 2009;19:664-9.

24. Mao SS, Ahmadi N, Shah B, Beckmann D, Chen A, Ngo L, et al. Normal thoracic aorta diameter on cardiac computed tomography in healthy asymptomatic adults: impact of age and gender. Acad Radiol 2008;15: 827-34.

25. Tsang JF, Lytwyn M, Farag A, Zeglinski M, Wallace K, daSilva M, et al. Multimodality imaging of aortic dimensions: comparison of transthoracic echocardiography with multidetector row computed tomography. Echocardiography 2012;29:735-41.

26. Garcier JM, Petitcolin V, Filaire M, Mofid R, Azarnouch K, Ravel A, et al. Normal diameter of the thoracic aorta in adults: a magnetic resonance imaging study. Surg Radiol Anat 2003;25:322-9.

27. Muraru D, Maffessanti F, Kocabay G, Peluso D, Bianco LD, Piasentini E, et al. Ascending aorta diameters measured by echocardiography using both leading edge-to-leading edge and inner edge-to-inner edge conventions in healthy volunteers. Eur Heart J Cardiovasc Imaging 2014;15: 415-22.

28. Quint LE, Liu PS, Booher AM, Watcharotone K, Myles JD. Proximal thoracic aortic diameter measurements at CT: repeatability and reproducibility according to measurement method. Int J Cardiovasc Imaging 2013;29:479-88.

29. Sahn DJ, DeMaria A, Kisslo J, Weyman A. Recommendations regarding quantitation in M-mode echocardiography: results of a survey of echocardiographic measurements. Circulation 1978;58:1072-83.

30. Lee RT, Kamm RD. Vascular mechanics for the cardiologist. J Am Coll Cardiol 1994;23:1289-95.

31. Wilkinson IB, Franklin SS, Hall IR, Tyrrell S, Cockcroft JR. Pressure amplification explains why pulse pressure is unrelated to risk in young subjects. Hypertension 2001;38:1461-6.

32. Latham RD, Westerhof N, Sipkema P, Rubal BJ, Reuderink P, Murgo JP. Regional wave travel and reflections along the human aorta: a study with six simultaneous micromanometric pressures. Circulation 1985;72: 1257-69.

33. Laurent S, Cockcroft J, Van Bortel L, Boutouyrie P, Giannattasio C, Hayoz D, et al. Expert consensus document on arterial stiffness: methodological issues and clinical applications. Eur Heart J 2006;27: 2588-605.

34. Van Bortel LM, Laurent S, Boutouyrie P, Chowienczyk P, Cruickshank JK, De Backer T, et al. Expert consensus document on the measurement of aortic stiffness in daily practice using carotid-femoral pulse wave velocity. J Hypertens 2012;30:445-8.

35. Dogui A, Redheuil A, Lefort M, DeCesare A, Kachenoura N, Herment A, et al. Measurement of aortic arch pulse wave velocity in cardiovascular MR: comparison of transit time estimators and description of a new approach. J Magn Reson Imaging 2011;33:1321-9.

36. Earnest F 4th, Muhm JR, Sheedy PF 2nd. Roentgenographic findings in thoracic aortic dissection. Mayo Clin Proc 1979;54:43-50.

37. Jagannath AS, Sos TA, Lockhart SH, Saddekni S, Sniderman KW. Aortic dissection: a statistical analysis of the usefulness of plain chest radiographic findings. AJR Am J Roentgenol 1986;147:1123-6.

38. von Kodolitsch Y, Schwartz AG, Nienaber CA. Clinical prediction of acute aortic dissection. Arch Intern Med 2000;160:2977-82.

39. Evangelista A, Flachskampf FA, Erbel R, Antonini-Canterin F, Vlachopoulos C, Rocchi G, et al. Echocardiography in aortic diseases: EAE recommendations for clinical practice. Eur J Echocardiogr 2010; 11:645-58.

40. Goldstein SA, Mintz GS, Lindsay JJ. Aorta: comprehensive evaluation by echocardiography and transesophageal echocardiography. J Am Soc Echocardiogr 1993;6:634-59.

41. Goldstein SA, Lindsay JJ. Aortic Dissection: Noninvasive Evaluation. ACC Curr J Review 2001;10:18-20.

42. Nienaber CA, von Kodolitsch Y, Nicolas V, Siglow V, Piepho A, Brockhoff C, et al. The diagnosis of thoracic aortic dissection by noninvasive imaging procedures. N Engl J Med 1993;328:1-9.

43. Tamborini G, Galli CA, Maltagliati A, Andreini D, Pontone G, Quaglia C, et al. Comparison of feasibility and accuracy of transthoracic echocardiography versus computed tomography in patients with known ascending aortic aneurysm. Am J Cardiol 2006;98:966-9.

44. Weyman AE, Caldwell RL, Hurwitz RA, Girod DA, Dillon JC, Feigenbaum H, et al. Cross-sectional echocardiographic characterization of aortic obstruction. 1. Supravalvular aortic stenosis and aortic hypoplasia. Circulation 1978;57:491-7.

45. Weyman AE. Cross-sectional echocardiography. Philadelphia: Lea and Febiger; 1982.

46. Mintz GS, Kotler MN, Segal BL, Parry WR. Two dimensional echocardiographic recognition of the descending thoracic aorta. Am J Cardiol 1979; 44:232-8.

47. Steinberg CR, Archer M, Steinberg I. Measurement of the abdominal aorta after intravenous aortography in health and arteriosclerotic peripheral vascular disease. Am J Roentgenol Radium Ther Nucl Med 1965;95:703-8.

48. Fisher EA, Stahl JA, Budd JH, Goldman ME. Transesophageal echocardiography: procedures and clinical application. J Am Coll Cardiol 1991;18: 1333-48.

49. Seward JB, Khandheria BK, Oh JK, Abel MD, Hughes RWJ, Edwards WD, et al. Transesophageal echocardiography: technique, anatomic correlations, implementation, and clinical applications. Mayo Clin Proc 1988;63:649-80.

50. Taams MA, Gussenhoven WJ, Schippers LA, Roelandt J, van Herwerden LA, Bos E, et al. The value of transoesophageal echocardiography for diagnosis of thoracic aorta pathology. Eur Heart J 1988;9: 1308-16.

51. Seward JB, Khandheria BK, Freeman WK, Oh JK, Enriquez-Sarano M, Miller FA, et al. Multiplane transesophageal echocardiography: image orientation, examination technique, anatomic correlations, and clinical applications. Mayo Clin Proc 1993;68:523-51.

52. Hung J, Lang R, Flachskampf F, Shernan SK, McCulloch ML, Adams DB, et al. 3D echocardiography: a review of the current status and future directions. J Am Soc Echocardiogr 2007;20:213-33.

53. Lang RM, Badano LP, Tsang W, Adams DH, Agricola E, Buck T, et al. EAE/ASE recommendations for image acquisition and display using three-dimensional echocardiography. J Am Soc Echocardiogr 2012;25:3-46.

54. Monaghan MJ. Role of real time 3D echocardiography in evaluating the left ventricle. Heart 2006;92:131-6.

55. Schoenhagen P, Tuzcu EM, Kapadia SR, Desai MY, Svensson LG. Three-dimensional imaging of the aortic valve and aortic root with computed tomography: new standards in an era of transcatheter valve repair/implantation. Eur Heart J 2009;30:2079-86.

56. Wei J, Hsiung MC, Tsai SK, Ou CH, Chang CY, Chang YC, et al. The routine use of live three-dimensional transesophageal echocardiography in mitral valve surgery: clinical experience. Eur J Echocardiogr 2010;11: 14-8.

57. Scohy TV, Geniets B, McGhie J, Bogers AJ. Feasibility of real-time three-dimensional transesophageal echocardiography in type A aortic dissection. Interact Cardiovasc Thorac Surg 2010;11:112-3.

58. Erbel R, Alfonso F, Boileau C, Dirsch O, Eber B, Haverich A, et al. Diagnosis and management of aortic dissection. Eur Heart J 2001;22: 1642-81.

59. Fattori R, Caldarera I, Rapezzi C, Rocchi G, Napoli G, Parlapiano M, et al. Primary endoleakage in endovascular treatment of the thoracic aorta: importance of intraoperative transesophageal echocardiography. J Thorac Cardiovasc Surg 2000;120:490-5.

60. Koschyk DH, Nienaber CA, Knap M, Hofmann T, Kodolitsch YV, Skriabina V, et al. How to guide stent-graft implantation in type B aortic dissection? Comparison of angiography, transesophageal echocardiography, and intravascular ultrasound. Circulation 2005;112:I260-4.

61. Kpodonu J, Ramaiah VG, Diethrich EB. Intravascular ultrasound imaging as applied to the aorta: a new tool for the cardiovascular surgeon. Ann Thorac Surg 2008;86:1391-8.

62. Rocchi G, Lofiego C, Biagini E, Piva T, Bracchetti G, Lovato L, et al. Transesophageal echocardiography-guided algorithm for stent-graft implantation in aortic dissection. J Vasc Surg 2004;40:880-5.

63. Fernandez JD, Donovan S, Garrett HEJ, Burgar S. Endovascular thoracic aortic aneurysm repair: evaluating the utility of intravascular ultrasound measurements. J Endovasc Ther 2008;15:68-72.

64. Sebastia C, Pallisa E, Quiroga S, Alvarez-Castells A, Dominguez R, Evangelista A. Aortic dissection: diagnosis and follow-up with helical CT. Radiographics 1999;19:45-60. quiz 149-50.

65. Vernhet H, Serfaty JM, Serhal M, McFadden E, Bonnefoy E, Adeleine P, et al. Abdominal CT angiography before surgery as a predictor of postoperative death in acute aortic dissection. AJR Am J Roentgenol 2004;182:875-9.

66. Li Y, Fan Z, Xu L, Yang L, Xin H, Zhang N, et al. Prospective ECG-gated 320-row CT angiography of the whole aorta and coronary arteries. Eur Radiol 2012;22:2432-40.

67. Roos JE, Willmann JK, Weishaupt D, Lachat M, Marincek B, Hilfiker PR. Thoracic aorta: motion artifact reduction with retrospective and prospective electrocardiography-assisted multi-detector row CT. Radiology 2002;222:271-7.

68. Fleischmann D, Mitchell RS, Miller DC. Acute aortic syndromes: new insights from electrocardiographically gated computed tomography. Semin Thorac Cardiovasc Surg 2008;20:340-7.

69. Gao Y, Lu B, Hou Z, Yu F, Cao H, Han L, et al. Low dose dual-source CT angiography in infants with complex congenital heart disease: a randomized study. Eur J Radiol 2012;81:e789-95.

70. Schlosser FJ, Mojibian HR, Dardik A, Verhagen HJ, Moll FL, Muhs BE. Simultaneous sizing and preoperative risk stratification for thoracic endovascular aneurysm repair: role of gated computed tomography. J Vasc Surg 2008;48:561-70.

71. Runza G, Fattouch K, Cademartiri F, La Fata A, Damiani L, La Grutta L, et al. ECG-gated multidetector computed tomography for the assessment of the postoperative ascending aorta. Radiol Med 2009;114: 705-17.

72. Bolen MA, Mastracci TM, Schoenhagen P. Use of electrocardiographic-gated 4-dimensional CT to assess patency of abdominal aortic branch vessels in type B dissection. J Cardiovasc Comput Tomogr 2009;3:415-6.

73. Picano E, Vano E, Rehani MM, Cuocolo A, Mont L, Bodi V, et al. The appropriate and justified use of medical radiation in cardiovascular imaging: a position document of the ESC Associations of Cardiovascular Imaging, Percutaneous Cardiovascular Interventions and Electrophysiology. Eur Heart J 2014;35:665-72.

74. Katzberg RW, Lamba R. Contrast-induced nephropathy after intravenous administration: fact or fiction? Radiol Clin North Am 2009;47: 789-800, v.

75. Ellis JH, Cohan RH. Reducing the risk of contrast-induced nephropathy: a perspective on the controversies. AJR Am J Roentgenol 2009;192: 1544-9.

76. Hunt CH, Hartman RP, Hesley GK. Frequency and severity of adverse effects of iodinated and gadolinium contrast materials: retrospective review of 456,930 doses. AJR Am J Roentgenol 2009;193:1124-7.

77. Nakayama Y, Awai K, Funama Y, Liu D, Nakaura T, Tamura Y, et al. Lower tube voltage reduces contrast material and radiation doses on 16-MDCT aortography. AJR Am J Roentgenol 2006;187:W490-7.

78. Morita S, Ueno E, Masukawa A, Suzuki K, Machida H, Fujimura M. Hyperattenuating signs at unenhanced CT indicating acute vascular disease. Radiographics 2010;30:111-25.

79. Yamada T, Tada S, Harada J. Aortic dissection without intimal rupture: diagnosis with MR imaging and CT. Radiology 1988;168: 347-52.

80. Ko SF, Hsieh MJ, Chen MC, Ng SH, Fang FM, Huang CC, et al. Effects of heart rate on motion artifacts of the aorta on non-ECG-assisted 0.5-sec thoracic MDCT. AJR Am J Roentgenol 2005;184:1225-30.

81. van Prehn J, Vincken KL, Muhs BE, Barwegen GK, Bartels LW, Prokop M, et al. Toward endografting of the ascending aorta: insight into dynamics using dynamic cine-CTA. J Endovasc Ther 2007;14:551-60.

82. Hayter RG, Rhea JT, Small A, Tafazoli FS, Novelline RA. Suspected aortic dissection and other aortic disorders: multi-detector row CT in 373 cases in the emergency setting. Radiology 2006;238:841-52.

83. Wu W, Budovec J, Foley WD. Prospective and retrospective ECG gating for thoracic CT angiography: a comparative study. AJR Am J Roentgenol 2009;193:955-63.

84. Rozenblit AM, Patlas M, Rosenbaum AT, Okhi T, Veith FJ, Laks MP, et al. Detection of endoleaks after endovascular repair of abdominal aortic aneurysm: value of unenhanced and delayed helical CT acquisitions. Radiology 2003;227:426-33.

85. Evangelista A, Pineda V, Cuellar H. Aortic Atherosclerosis, Aneurysm and Dissection. In: M G, editor. Noninvasive Cardiovascular Imaging: A multimodality Approach. Philadelphia, PA: Lippincott Williams & Wilkins; 2010.

86. Agarwal PP, Chughtai A, Matzinger FR, Kazerooni EA. Multidetector CT of thoracic aortic aneurysms. Radiographics 2009;29:537-52.

87. Lell MM, Anders K, Uder M, Klotz E, Ditt H, Vega-Higuera F, et al. New techniques in CT angiography. Radiographics 2006;26(Suppl 1):S45-62.

88. Boll DT, Lewin JS, Duerk JL, Smith D, Subramanyan K, Merkle EM. Assessment of automatic vessel tracking techniques in preoperative planning of transluminal aortic stent graft implantation. J Comput Assist Tomogr 2004;28:278-85.

89. Lu TL, Rizzo E, Marques-Vidal PM, Segesser LK, Dehmeshki J, Qanadli SD. Variability of ascending aorta diameter measurements as assessed with electrocardiography-gated multidetector computerized tomography and computer assisted diagnosis software. Interact Cardiovasc Thorac Surg 2010;10:217-21.

90. Dillavou ED, Buck DG, Muluk SC, Makaroun MS. Two-dimensional versus three-dimensional CT scan for aortic measurement. J Endovasc Ther 2003;10:531-8.

91. Cayne NS, Veith FJ, Lipsitz EC, Ohki T, Mehta M, Gargiulo N, et al. Variability of maximal aortic aneurysm diameter measurements on CT scan: significance and methods to minimize. J Vasc Surg 2004;39:811-5.

92. Singh K, Jacobsen BK, Solberg S, Bonaa KH, Kumar S, Bajic R, et al. Intra- and interobserver variability in the measurements of abdominal aortic and common iliac artery diameter with computed tomography. The Tromso study. Eur J Vasc Endovasc Surg 2003;25:399-407.

93. Saini S, Frankel RB, Stark DD, Ferrucci JT. Magnetism: a primer and review. AJR Am J Roentgenol 1988;150:735-43.

94. Duerinckx AJ, Wexler L, Banerjee A, Higgins SS, Hardy CE, Helton G, et al. Postoperative evaluation of pulmonary arteries in congenital heart surgery by magnetic resonance imaging: comparison with echocardiography. Am Heart J 1994;128:1139-46.

95. Edelman RR, Chien D, Kim D. Fast selective black blood MR imaging. Radiology 1991;181:655-60.

96. Haddad JL, Rofsky NM, Ambrosino MM, Naidich DP, Weinreb JC. T2-weighted MR imaging of the chest: comparison of electrocardiograph-triggered conventional and turbo spin-echo and nontriggered turbo spin-echo sequences. J Magn Reson Imaging 1995;5:325-9.

97. Nienaber CA, Rehders TC, Fratz S. Detection and assessment of congenital heart disease with magnetic resonance techniques. J Cardiovasc Magn Reson 1999;1:169-84.

98. Corti R, Fuster V. Imaging of atherosclerosis: magnetic resonance imaging. Eur Heart J 2011;32:1709-19.

99. Flamm SD, White RD, Hoffman GS. The clinical application of 'edema-weighted' magnetic resonance imaging in the assessment of Takayasu's arteritis. Int J Cardiol 1998;66(Suppl 1):S151-9; discussion S161.

100. Krinsky GA, Rofsky NM, DeCorato DR, Weinreb JC, Earls JP, Flyer MA, et al. Thoracic aorta: comparison of gadolinium-enhanced three-dimensional MR angiography with conventional MR imaging. Radiology 1997;202:183-93.

101. Groves EM, Bireley W, Dill K, Carroll TJ, Carr JC. Quantitative analysis of ECG-gated high-resolution contrast-enhanced MR angiography of the thoracic aorta. AJR Am J Roentgenol 2007;188:522-8.

102. Setser RM, Kotys M, Bolen MA, Muthupillai R, Flamm SD. High resolution imaging of the right ventricle using ZOOM MRI. J Cardiovasc Magn Reson 2010;12:M8.

103. Utz JA, Herfkens RJ, Heinsimer JA, Shimakawa A, Glover G, Pelc N. Valvular regurgitation: dynamic MR imaging. Radiology 1988;168:91-4.

104. Hundley WG, Li HF, Hillis LD, Meshack BM, Lange RA, Willard JE, et al. Quantitation of cardiac output with velocity-encoded, phase-difference magnetic resonance imaging. Am J Cardiol 1995;75:1250-5.

105. Bolen MA, Popovic ZB, Rajiah P, Gabriel RS, Zurick AO, Lieber ML, et al. Cardiac MR assessment of aortic regurgitation: holodiastolic flow reversal in the descending aorta helps stratify severity. Radiology 2011;260:98-104.

106. O'Brien KR, Gabriel RS, Greiser A, Cowan BR, Young AA, Kerr AJ. Aortic valve stenotic area calculation from phase contrast cardiovascular magnetic resonance: the importance of short echo time. J Cardiovasc Magn Reson 2009;11:49.

107. Hundley WG, Li HF, Lange RA, Pfeifer DP, Meshack BM, Willard JE, et al. Assessment of left-to-right intracardiac shunting by velocity-encoded, phase-difference magnetic resonance imaging. A comparison with oximetric and indicator dilution techniques. Circulation 1995;91:2955-60.

108. Hope MD, Meadows AK, Hope TA, Ordovas KG, Saloner D, Reddy GP, et al. Clinical evaluation of aortic coarctation with 4D flow MR imaging. J Magn Reson Imaging 2010;31:711-8.

109. Hsiao A, Alley MT, Massaband P, Herfkens RJ, Chan FP, Vasanawala SS. Improved cardiovascular flow quantification with time-resolved volumetric phase-contrast MRI. Pediatr Radiol 2011;41:711-20.

110. Francois CJ, Tuite D, Deshpande V, Jerecic R, Weale P, Carr JC. Unenhanced MR angiography of the thoracic aorta: initial clinical evaluation. AJR Am J Roentgenol 2008;190:902-6.

111. Cohen EI, Weinreb DB, Siegelbaum RH, Honig S, Marin M, Weintraub JL, et al. Time-resolved MR angiography for the classification of endoleaks after endovascular aneurysm repair. J Magn Reson Imaging 2008;27:500-3.

112. Naehle CP, Kaestner M, Muller A, Willinek WW, Gieseke J, Schild HH, et al. First-pass and steady-state MR angiography of thoracic vasculature in children and adolescents. JACC Cardiovasc Imaging 2010;3:504-13.

113. Boonyasirinant T, Rajiah P, Setser RM, Lieber ML, Lever HM, Desai MY, et al. Aortic stiffness is increased in hypertrophic cardiomyopathy with myocardial fibrosis: novel insights in vascular function from magnetic resonance imaging. J Am Coll Cardiol 2009;54:255-62.

114. Laffon E, Galy-Lacour C, Laurent F, Ducassou D, Marthan R. MRI quantification of the role of the reflected pressure wave on coronary and ascending aortic blood flow. Physiol Meas 2003;24:681-92.

115. Efstathopoulos EP, Patatoukas G, Pantos I, Benekos O, Katritsis D, Kelekis NL. Measurement of systolic and diastolic arterial wall shear stress in the ascending aorta. Phys Med 2008;24:196-203.

116. Saremi F, Grizzard JD, Kim RJ. Optimizing cardiac MR imaging: practical remedies for artifacts. Radiographics 2008;28:1161-87.

117. Ferreira PF, Gatehouse PD, Mohiaddin RH, Firmin DN. Cardiovascular magnetic resonance artefacts. J Cardiovasc Magn Reson 2013;15:41.

118. Bansal RC, Chandrasekaran K, Ayala K, Smith DC. Frequency and explanation of false negative diagnosis of aortic dissection by aortography and transesophageal echocardiography. J Am Coll Cardiol 1995;25:1393-401.

119. Erbel R, Engberding R, Daniel W, Roelandt J, Visser C, Rennollet H. Echocardiography in diagnosis of aortic dissection. Lancet 1989;1:457-61.

120. Moore AG, Eagle KA, Bruckman D, Moon BS, Malouf JF, Fattori R, et al. Choice of computed tomography, transesophageal echocardiography, magnetic resonance imaging, and aortography in acute aortic dissection:

International Registry of Acute Aortic Dissection (IRAD). Am J Cardiol 2002;89:1235-8.

121. Nienaber CA, Eagle KA. Aortic dissection: new frontiers in diagnosis and management: Part I: from etiology to diagnostic strategies. Circulation 2003;108:628-35.

122. Shiga T, Wajima Z, Apfel CC, Inoue T, Ohe Y. Diagnostic accuracy of transesophageal echocardiography, helical computed tomography, and magnetic resonance imaging for suspected thoracic aortic dissection: systematic review and meta-analysis. Arch Intern Med 2006;166: 1350-6.

123. Svensson LG, Labib SB, Eisenhauer AC, Butterly JR. Intimal tear without hematoma: an important variant of aortic dissection that can elude current imaging techniques. Circulation 1999;99:1331-6.

124. von Kodolitsch Y, Csosz SK, Koschyk DH, Schalwat I, Loose R, Karck M, et al. Intramural hematoma of the aorta: predictors of progression to dissection and rupture. Circulation 2003;107:1158-63.

125. Weintraub AR, Erbel R, Gorge G, Schwartz SL, Ge J, Gerber T, et al. Intravascular ultrasound imaging in acute aortic dissection. J Am Coll Cardiol 1994;24:495-503.

126. Yamada E, Matsumura M, Kyo S, Omoto R. Usefulness of a prototype intravascular ultrasound imaging in evaluation of aortic dissection and comparison with angiographic study, transesophageal echocardiography, computed tomography, and magnetic resonance imaging. Am J Cardiol 1995;75:161-5.

127. Nienaber CA, Kische S, Skriabina V, Ince H. Noninvasive imaging approaches to evaluate the patient with known or suspected aortic disease. Circ Cardiovasc Imaging 2009;2:499-506.

128. Vilacosta I, Roman JA. Acute aortic syndrome. Heart 2001;85:365-8.

129. Hagan PG, Nienaber CA, Isselbacher EM, Bruckman D, Karavite DJ, Russman PL, et al. The International Registry of Acute Aortic Dissection (IRAD): new insights into an old disease. JAMA 2000;283:897-903.

130. Lansman SL, Saunders PC, Malekan R, Spielvogel D. Acute aortic syndrome. J Thorac Cardiovasc Surg 2010;140:S92-7. discussion S142-S146.

131. Macura KJ, Corl FM, Fishman EK, Bluemke DA. Pathogenesis in acute aortic syndromes: aortic dissection, intramural hematoma, and penetrating atherosclerotic aortic ulcer. AJR Am J Roentgenol 2003;181: 309-16.

132. Ramanath VS, Oh JK, Sundt TM 3rd, Eagle KA. Acute aortic syndromes and thoracic aortic aneurysm. Mayo Clin Proc 2009;84:465-81.

133. Vilacosta I, Aragoncillo P, Canadas V, San Roman JA, Ferreiros J, Rodriguez E. Acute aortic syndrome: a new look at an old conundrum. Heart 2009;95:1130-9.

134. Higgins CB. Modern imaging of the acute aortic syndrome. Am J Med 2004;116:134.

135. Murashita T, Kunihara T, Shiiya N, Aoki H, Myojin K, Yasuda K. Is preservation of the aortic valve different between acute and chronic type A aortic dissections? Eur J Cardiothorac Surg 2001;20:967-72.

136. Pego-Fernandes PM, Stolf NA, Moreira LF, Pereira Barreto AC, Bittencourt D, Jatene AD. Management of aortic insufficiency in chronic aortic dissection. Ann Thorac Surg 1991;51:438-42.

137. Shimono T, Kato N, Yasuda F, Suzuki T, Yuasa U, Onoda K, et al. Transluminal stent-graft placements for the treatments of acute onset and chronic aortic dissections. Circulation 2002;106:I241-7.

138. Weber TF, Ganten MK, Bockler D, Geisbusch P, Kopp-Schneider A, Kauczor HU, et al. Assessment of thoracic aortic conformational changes by four-dimensional computed tomography angiography in patients with chronic aortic dissection type b. Eur Radiol 2009;19:245-53.

139. DeBakey ME, Henly WS. Surgical treatment of angina pectoris. Circulation 1961;23:111-20.

140. Debakey ME, Henley WS, Cooley DA, Morris GC Jr., Crawford ES, Beall AC Jr. SURGICAL MANAGEMENT OF DISSECTING ANEURYSMS OF THE AORTA. J Thorac Cardiovasc Surg 1965;49: 130-49.

141. DeBakey ME, Beall ACJ, Cooley DA, Crawford ES, Morris GCJ, Garrett HE, et al. Dissecting aneurysms of the aorta. Surg Clin North Am 1966;46:1045-55.

142. Hirst AE Jr., Johns VJ Jr., Kime SW Jr. Dissecting aneurysm of the aorta: a review of 505 cases. Medicine (Baltimore) 1958;37:217-79.

143. Levinson DC, Edmaedes DT, Griffith GC. Dissecting aneurysm of the aorta; its clinical, electrocardiographic and laboratory features; a report of 58 autopsied cases. Circulation 1950;1:360-87.

144. Borst HG, Heinemann MK, Stone CD. Surgical Treatment of Aortic Dissection. New York: Churchill Livingstone; 1996.

145. Cecconi M, Chirillo F, Costantini C, Iacobone G, Lopez E, Zanoli R, et al. The role of transthoracic echocardiography in the diagnosis and management of acute type A aortic syndrome. Am Heart J 2012;163:112-8.

146. Evangelista A, Avegliano G, Aguilar R, Cuellar H, Igual A, Gonzalez-Alujas T, et al. Impact of contrast-enhanced echocardiography on the diagnostic algorithm of acute aortic dissection. Eur Heart J 2010;31: 472-9.

147. Adachi H, Omoto R, Kyo S, Matsumura M, Kimura S, Takamoto S, et al. Emergency surgical intervention of acute aortic dissection with the rapid diagnosis by transesophageal echocardiography. Circulation 1991;84: III14-9.

148. Ballal RS, Nanda NC, Gatewood R, D'Arcy B, Samdarshi TE, Holman WL, et al. Usefulness of transesophageal echocardiography in assessment of aortic dissection. Circulation 1991;84:1903-14.

149. Goldstein SA. Echocardiographic evaluation of aortic dissection. Cardiac Ultrasound Today 2001;7:167-80.

150. Hashimoto S, Kumada T, Osakada G, Kubo S, Tokunaga S, Tamaki S, et al. Assessment of transesophageal Doppler echography in dissecting aortic aneurysm. J Am Coll Cardiol 1989;14:1253-62.

151. Evangelista A, Aguilar R, Cuellar H, Thomas M, Laynez A, Rodriguez-Palomares J, et al. Usefulness of real-time three-dimensional transoesophageal echocardiography in the assessment of chronic aortic dissection. Eur J Echocardiogr 2011;12:272-7.

152. Erbel R, Oelert H, Meyer J, Puth M, Mohr-Katoly S, Hausmann D, et al. Effect of medical and surgical therapy on aortic dissection evaluated by transesophageal echocardiography. Implications for prognosis and therapy. The European Cooperative Study Group on Echocardiography. Circulation 1993;87:1604-15.

153. Keane MG, Wiegers SE, Yang E, Ferrari VA, St John Sutton MG, Bavaria JE. Structural determinants of aortic regurgitation in type A dissection and the role of valvular resuspension as determined by intraoperative transesophageal echocardiography. Am J Cardiol 2000;85:604-10.

154. Evangelista A, Dominguez R, Sebastia C, Salas A, Permanyer-Miralda G, Avegliano G, et al. Long-term follow-up of aortic intramural hematoma: predictors of outcome. Circulation 2003;108:583-9.

155. Evangelista A, Dominguez R, Sebastia C, Salas A, Permanyer-Miralda G, Avegliano G, et al. Prognostic value of clinical and morphologic findings in short-term evolution of aortic intramural haematoma. Therapeutic implications. Eur Heart J 2004;25:81-7.

156. Appelbe AF, Walker PG, Yeoh JK, Bonitatibus A, Yoganathan AP, Martin RP. Clinical significance and origin of artifacts in transesophageal echocardiography of the thoracic aorta. J Am Coll Cardiol 1993;21: 754-60.

157. Evangelista A, Garcia-del-Castillo H, Gonzalez-Alujas T, Dominguez-Oronoz R, Salas A, Permanyer-Miralda G, et al. Diagnosis of ascending aortic dissection by transesophageal echocardiography: utility of M-mode in recognizing artifacts. J Am Coll Cardiol 1996;27:102-7.

158. Losi MA, Betocchi S, Briguori C, Manganelli F, Ciampi Q, Pace L, et al. Determinants of aortic artifacts during transesophageal echocardiography of the ascending aorta. Am Heart J 1999;137:967-72.

159. Vignon P, Spencer KT, Rambaud G, Preux PM, Krauss D, Balasia B, et al. Differential transesophageal echocardiographic diagnosis between linear artifacts and intraluminal flap of aortic dissection or disruption. Chest 2001;119:1778-90.

160. Harris KM, Strauss CE, Eagle KA, Hirsch AT, Isselbacher EM, Tsai TT, et al. Correlates of delayed recognition and treatment of acute type A aortic dissection: the International Registry of Acute Aortic Dissection (IRAD). Circulation 2011;124:1911-8.

161. Sommer T, Fehske W, Holzknecht N, Smekal AV, Keller E, Lutterbey G, et al. Aortic dissection: a comparative study of diagnosis with spiral CT,

multiplanar transesophageal echocardiography, and MR imaging. Radiology 1996;199:347-52.

162. Yoshida S, Akiba H, Tamakawa M, Yama N, Hareyama M, Morishita K, et al. Thoracic involvement of type A aortic dissection and intramural hematoma: diagnostic accuracy–comparison of emergency helical CT and surgical findings. Radiology 2003;228:430-5.

163. Burns MA, Molina PL, Gutierrez FR, Sagel SS. Motion artifact simulating aortic dissection on CT. AJR Am J Roentgenol 1991;157:465-7.

164. Duvernoy O, Coulden R, Ytterberg C. Aortic motion: a potential pitfall in CT imaging of dissection in the ascending aorta. J Comput Assist Tomogr 1995;19:569-72.

165. Qanadli SD, El Hajjam M, Mesurolle B, Lavisse L, Jourdan O, Randoux B, et al. Motion artifacts of the aorta simulating aortic dissection on spiral CT. J Comput Assist Tomogr 1999;23:1-6.

166. Zeman RK, Berman PM, Silverman PM, Davros WJ, Cooper C, Kladakis AO, et al. Diagnosis of aortic dissection: value of helical CT with multiplanar reformation and three-dimensional rendering. AJR Am J Roentgenol 1995;164:1375-80.

167. Abbara S, Kalva S, Cury RC, Isselbacher EM. Thoracic aortic disease: spectrum of multidetector computed tomography imaging findings. J Cardiovasc Comput Tomogr 2007;1:40-54.

168. Shapiro MD, Dodd JD, Kalva S, Wittram C, Hsu J, Nasir K, et al. A comprehensive electrocardiogram-gated 64-slice multidetector computed tomography imaging protocol to visualize the coronary arteries, thoracic aorta, and pulmonary vasculature in a single breath hold. J Comput Assist Tomogr 2009;33:225-32.

169. Cheong B, Flamm SD. Use of electrocardiographic gating in computed tomography angiography of the ascending thoracic aorta. J Am Coll Cardiol 2007;49:1751; author reply 1751-2.

170. Chung JH, Ghoshhajra BB, Rojas CA, Dave BR, Abbara S. CT angiography of the thoracic aorta. Radiol Clin North Am 2010;48:249-64, vii.

171. DeSanctis RW, Doroghazi RM, Austen WG, Buckley MJ. Aortic dissection. N Engl J Med 1987;317:1060-7.

172. Goetti R, Baumuller S, Feuchtner G, Stolzmann P, Karlo C, Alkadhi H, et al. High-pitch dual-source CT angiography of the thoracic and abdominal aorta: is simultaneous coronary artery assessment possible? AJR Am J Roentgenol 2010;194:938-44.

173. Moon MC, Greenberg RK, Morales JP, Martin Z, Lu Q, Dowdall JF, et al. Computed tomography-based anatomic characterization of proximal aortic dissection with consideration for endovascular candidacy. J Vasc Surg 2011;53:942-9.

174. Yoshikai M, Ikeda K, Itoh M, Noguchi R. Detection of coronary artery disease in acute aortic dissection: the efficacy of 64-row multidetector computed tomography. J Card Surg 2008;23:277-9.

175. Das KM, Abdou SM, El-Menyar A, Khulaifi AA, Nabti AL. Coronary artery dissection with rupture of aortic valve commissure following type A aortic dissection: the role of 64-slice MDCT. J Card Surg 2008;23:548-50.

176. Beeres M, Schell B, Mastragelopoulos A, Herrmann E, Kerl JM, Gruber-Rouh T, et al. High-pitch dual-source CT angiography of the whole aorta without ECG synchronisation: initial experience. Eur Radiol 2012;22:129-37.

177. Karlo C, Leschka S, Goetti RP, Feuchtner G, Desbiolles L, Stolzmann P, et al. High-pitch dual-source CT angiography of the aortic valve-aortic root complex without ECG-synchronization. Eur Radiol 2011;21:205-12.

178. Wuest W, Anders K, Schuhbaeck A, May MS, Gauss S, Marwan M, et al. Dual source multidetector CT-angiography before Transcatheter Aortic Valve Implantation (TAVI) using a high-pitch spiral acquisition mode. Eur Radiol 2012;22:51-8.

179. Fujioka C, Horiguchi J, Kiguchi M, Yamamoto H, Kitagawa T, Ito K. Survey of aorta and coronary arteries with prospective ECG-triggered 100-kV 64-MDCT angiography. AJR Am J Roentgenol 2009;193:227-33.

180. Ayaram D, Bellolio MF, Murad MH, Laack TA, Sadosty AT, Erwin PJ, et al. Triple rule-out computed tomographic angiography for chest pain: a diagnostic systematic review and meta-analysis. Acad Emerg Med 2013;20:861-71.

181. Poon M, Rubin GD, Achenbach S, Attebery TW, Berman DS, Brady TJ, et al. Consensus update on the appropriate usage of cardiac computed tomographic angiography. J Invasive Cardiol 2007;19:484-90.

182. Cigarroa JE, Isselbacher EM, DeSanctis RW, Eagle KA. Diagnostic imaging in the evaluation of suspected aortic dissection. Old standards and new directions. N Engl J Med 1993;328:35-43.

183. Nienaber CA, Spielmann RP, von Kodolitsch Y, Siglow V, Piepho A, Jaup T, et al. Diagnosis of thoracic aortic dissection. Magnetic resonance imaging versus transesophageal echocardiography. Circulation 1992;85:434-47.

184. von Kodolitsch Y, Simic O, Nienaber CA. Aneurysms of the ascending aorta: diagnostic features and prognosis in patients with Marfan's syndrome versus hypertension. Clin Cardiol 1998;21:817-24.

185. Chang JM, Friese K, Caputo GR, Kondo C, Higgins CB. MR measurement of blood flow in the true and false channel in chronic aortic dissection. J Comput Assist Tomogr 1991;15:418-23.

186. Nijm GM, Swiryn S, Larson AC, Sahakian AV. Characterization of the magnetohydrodynamic effect as a signal from the surface electrocardiogram during cardiac magnetic resonance imaging. IEEE; 2006.

187. Williams DM, Joshi A, Dake MD, Deeb GM, Miller DC, Abrams GD. Aortic cobwebs: an anatomic marker identifying the false lumen in aortic dissection–imaging and pathologic correlation. Radiology 1994;190:167-74.

188. Fattori R, Nienaber CA. MRI of acute and chronic aortic pathology: pre-operative and postoperative evaluation. J Magn Reson Imaging 1999;10:741-50.

189. Pitcher A, Cassar TE, Leeson P, Francis JM, Blair E, Wordsworth PB, et al. Aortic dissection: visualisation of aortic blood flow and quantification of wall shear stress using time-resolved, 3D phase-contrast MRI. J Cardiovasc Magn Reson 2011;13:1-2.

190. Krinsky G, Rofsky N, Flyer M, Giangola G, Maya M, DeCoroto D, et al. Gadolinium-enhanced three-dimensional MR angiography of acquired arch vessel disease. AJR Am J Roentgenol 1996;167:981-7.

191. Zhu H, Buck DG, Zhang Z, Zhang H, Wang P, Stenger VA, et al. High temporal and spatial resolution 4D MRA using spiral data sampling and sliding window reconstruction. Magn Reson Med 2004;52:14-8.

192. Clough R, Hussain T, Uribe S, Taylor P, Rezavi R, Schaeffter T, et al. An MRI examination for evaluation of aortic dissection using a blood pool agent. J Cardiovasc Magn Reson 2010;12:O63.

193. Movsowitz HD, Levine RA, Hilgenberg AD, Isselbacher EM. Transesophageal echocardiographic description of the mechanisms of aortic regurgitation in acute type A aortic dissection: implications for aortic valve repair. J Am Coll Cardiol 2000;36:884-90.

194. La Canna G, Maisano F, De Michele L, Grimaldi A, Grassi F, Capritti E, et al. Determinants of the degree of functional aortic regurgitation in patients with anatomically normal aortic valve and ascending thoracic aorta aneurysm. Transoesophageal Doppler echocardiography study. Heart 2009;95:130-6.

195. Armstrong WF, Bach DS, Carey L, Chen T, Donovan C, Falcone RA, et al. Spectrum of acute dissection of the ascending aorta: a transesophageal echocardiographic study. J Am Soc Echocardiogr 1996;9:646-56.

196. Whitley W, Tanaka KA, Chen EP, Glas KE. Acute aortic dissection with intimal layer prolapse into the left ventricle. Anesth Analg 2007;104:774-6.

197. Park KH, Lim C, Choi JH, Chung E, Choi SI, Chun EJ, et al. Midterm change of descending aortic false lumen after repair of acute type I dissection. Ann Thorac Surg 2009;87:103-8.

198. Tsai TT, Evangelista A, Nienaber CA, Myrmel T, Meinhardt G, Cooper JV, et al. Partial thrombosis of the false lumen in patients with acute type B aortic dissection. N Engl J Med 2007;357:349-59.

199. Rousseau H, Chabbert V, Maracher MA, El Aassar O, Auriol J, Massabuau P, et al. The importance of imaging assessment before endovascular repair of thoracic aorta. Eur J Vasc Endovasc Surg 2009;38:408-21.

200. Bartel T, Eggebrecht H, Muller S, Gutersohn A, Bonatti J, Pachinger O, et al. Comparison of diagnostic and therapeutic value of transesophageal

echocardiography, intravascular ultrasonic imaging, and intraluminal phased-array imaging in aortic dissection with tear in the descending thoracic aorta (type B). Am J Cardiol 2007;99:270-4.

201. Swaminathan M, Lineberger CK, McCann RL, Mathew JP. The importance of intraoperative transesophageal echocardiography in endovascular repair of thoracic aortic aneurysms. Anesth Analg 2003;97:1566-72.

202. Chavan A, Hausmann D, Dresler C, Rosenthal H, Jaeger K, Haverich A, et al. Intravascular ultrasound-guided percutaneous fenestration of the intimal flap in the dissected aorta. Circulation 1997;96:2124-7.

203. Lee DY, Williams DM, Abrams GD. The dissected aorta: part II. Differentiation of the true from the false lumen with intravascular US. Radiology 1997;203:32-6.

204. Wain RA, Marin ML, Ohki T, Sanchez LA, Lyon RT, Rozenblit A, et al. Endoleaks after endovascular graft treatment of aortic aneurysms: classification, risk factors, and outcome. J Vasc Surg 1998;27:69-78; discussion 78-80.

205. Koschyk DH, Meinertz T, Hofmann T, Kodolitsch YV, Dieckmann C, Wolf W, et al. Value of intravascular ultrasound for endovascular stent-graft placement in aortic dissection and aneurysm. J Card Surg 2003;18:471-7.

206. Orihashi K, Matsuura Y, Sueda T, Watari M, Okada K, Sugawara Y, et al. Echocardiography-assisted surgery in transaortic endovascular stent grafting: role of transesophageal echocardiography. J Thorac Cardiovasc Surg 2000;120:672-8.

207. Bossone E, Evangelista A, Isselbacher E, Trimarchi S, Hutchison S, Gilon D, et al. Prognostic role of transesophageal echocardiography in acute type A aortic dissection. Am Heart J 2007;153:1013-20.

208. Fattouch K, Sampognaro R, Navarra E, Caruso M, Pisano C, Coppola G, et al. Long-term results after repair of type a acute aortic dissection according to false lumen patency. Ann Thorac Surg 2009;88:1244-50.

209. Song JM, Kim SD, Kim JH, Kim MJ, Kang DH, Seo JB, et al. Long-term predictors of descending aorta aneurysmal change in patients with aortic dissection. J Am Coll Cardiol 2007;50:799-804.

210. Hata N, Tanaka K, Imaizumi T, Ohara T, Ohba T, Shinada T, et al. Clinical significance of pleural effusion in acute aortic dissection. Chest 2002;121:825-30.

211. Evangelista A, Salas A, Ribera A, Ferreira-Gonzalez I, Cuellar H, Pineda V, et al. Long-term outcome of aortic dissection with patent false lumen: predictive role of entry tear size and location. Circulation 2012;125:3133-41.

212. Krukenberg E. Beitrage zur frage des aneurysma dissecans. Beitr Pathol Anat Allg Pathol 1920;67:329-51.

213. Murray JG, Manisali M, Flamm SD, VanDyke CW, Lieber ML, Lytle BW, et al. Intramural hematoma of the thoracic aorta: MR image findings and their prognostic implications. Radiology 1997;204:349-55.

214. Banning AP. Aortic intramural hematoma. N Engl J Med 1997;337:1476-7.

215. Chao CP, Walker TG, Kalva SP. Natural history and CT appearances of aortic intramural hematoma. Radiographics 2009;29:791-804.

216. O'Gara PT, DeSanctis RW. Acute aortic dissection and its variants. Toward a common diagnostic and therapeutic approach. Circulation 1995;92:1376-8.

217. Park KH, Lim C, Choi JH, Sung K, Kim K, Lee YT, et al. Prevalence of aortic intimal defect in surgically treated acute type A intramural hematoma. Ann Thorac Surg 2008;86:1494-500.

218. Evangelista A, Mukherjee D, Mehta RH, O'Gara PT, Fattori R, Cooper JV, et al. Acute intramural hematoma of the aorta: a mystery in evolution. Circulation 2005;111:1063-70.

219. Ionescu AA, Vinereanu D, Wood A, Fraser AG. Periaortic fat pad mimicking an intramural hematoma of the thoracic aorta: lessons for transesophageal echocardiography. J Am Soc Echocardiogr 1998;11:487-90.

220. Sueyoshi E, Matsuoka Y, Sakamoto I, Uetani M, Hayashi K, Narimatsu M. Fate of intramural hematoma of the aorta: CT evaluation. J Comput Assist Tomogr 1997;21:931-8.

221. Kitai T, Kaji S, Yamamuro A, Tani T, Kinoshita M, Ehara N, et al. Detection of intimal defect by 64-row multidetector computed tomography in patients with acute aortic intramural hematoma. Circulation 2011;124:S174-8.

222. Wu MT, Wang YC, Huang YL, Chang RS, Li SC, Yang P, et al. Intramural blood pools accompanying aortic intramural hematoma: CT appearance and natural course. Radiology 2011;258:705-13.

223. Braverman AC. Penetrating atherosclerotic ulcers of the aorta. Curr Opin Cardiol 1994;9:591-7.

224. Cho KR, Stanson AW, Potter DD, Cherry KJ, Schaff HV. Sundt TMr. Penetrating atherosclerotic ulcer of the descending thoracic aorta and arch. J Thorac Cardiovasc Surg 2004;127:1393-9; discussion 1399-1401.

225. Cooke JP, Kazmier FJ, Orszulak TA. The penetrating aortic ulcer: pathologic manifestations, diagnosis, and management. Mayo Clin Proc 1988;63:718-25.

226. Hayashi H, Matsuoka Y, Sakamoto I, Sueyoshi E, Okimoto T, Hayashi K, et al. Penetrating atherosclerotic ulcer of the aorta: imaging features and disease concept. Radiographics 2000;20:995-1005.

227. Vilacosta I, San Roman JA, Aragoncillo P, Ferreiros J, Mendez R, Graupner C, et al. Penetrating atherosclerotic aortic ulcer: documentation by transesophageal echocardiography. J Am Coll Cardiol 1998;32:83-9.

228. Quint LE, Williams DM, Francis IR, Monaghan HM, Sonnad SS, Patel S, et al. Ulcerlike lesions of the aorta: imaging features and natural history. Radiology 2001;218:719-23.

229. Vilacosta I, San Roman JA, Ferreiros J, Aragoncillo P, Mendez R, Castillo JA, et al. Natural history and serial morphology of aortic intramural hematoma: a novel variant of aortic dissection. Am Heart J 1997;134:495-507.

230. Tristano AG, Tairouz Y. Painless right hemorrhagic pleural effusions as presentation sign of aortic dissecting aneurysm. Am J Med 2005;118:794-5.

231. Stanson AW, Kazmier FJ, Hollier LH, Edwards WD, Pairolero PC, Sheedy PF, et al. Penetrating atherosclerotic ulcers of the thoracic aorta: natural history and clinicopathologic correlations. Ann Vasc Surg 1986;1:15-23.

232. Coady MA, Rizzo JA, Hammond GL, Pierce JG, Kopf GS, Elefteriades JA. Penetrating ulcer of the thoracic aorta: what is it? How do we recognize it? How do we manage it? J Vasc Surg 1998;27:1006-16; discussion 1015–6.

233. Harris JA, Bis KG, Glover JL, Bendick PJ, Shetty A, Brown OW. Penetrating atherosclerotic ulcers of the aorta. J Vasc Surg 1994;19:90-8; discussion 98–9.

234. Kazerooni EA, Bree RL, Williams DM. Penetrating atherosclerotic ulcers of the descending thoracic aorta: evaluation with CT and distinction from aortic dissection. Radiology 1992;183:759-65.

235. Troxler M, Mavor AI, Homer-Vanniasinkam S. Penetrating atherosclerotic ulcers of the aorta. Br J Surg 2001;88:1169-77.

236. Yucel EK, Steinberg FL, Egglin TK, Geller SC, Waltman AC, Athanasoulis CA. Penetrating aortic ulcers: diagnosis with MR imaging. Radiology 1990;177:779-81.

237. Welch TJ, Stanson AW, Sheedy PF 2nd, Johnson CM, McKusick MA. Radiologic evaluation of penetrating aortic atherosclerotic ulcer. Radiographics 1990;10:675-85.

238. Bischoff MS, Geisbusch P, Peters AS, Hyhlik-Durr A, Bockler D. Penetrating aortic ulcer: defining risks and therapeutic strategies. Herz 2011;36:498-504.

239. Litmanovich D, Bankier AA, Cantin L, Raptopoulos V, Boiselle PM. CT and MRI in diseases of the aorta. AJR Am J Roentgenol 2009;193:928-40.

240. Salvolini L, Renda P, Fiore D, Scaglione M, Piccoli G, Giovagnoni A. Acute aortic syndromes: Role of multi-detector row CT. Eur J Radiol 2008;65:350-8.

241. Ledbetter S, Stuk JL, Kaufman JA. Helical (spiral) CT in the evaluation of emergent thoracic aortic syndromes. Traumatic aortic rupture, aortic aneurysm, aortic dissection, intramural hematoma, and penetrating atherosclerotic ulcer. Radiol Clin North Am 1999;37:575-89.

242. Levy JR, Heiken JP, Gutierrez FR. Imaging of penetrating atherosclerotic ulcers of the aorta. AJR Am J Roentgenol 1999;173:151-4.

243. Isselbacher EM. Thoracic and abdominal aortic aneurysms. Circulation 2005;111:816-28.

244. Johnston KW, Rutherford RB, Tilson MD, Shah DM, Hollier L, Stanley JC. Suggested standards for reporting on arterial aneurysms. Subcommittee on Reporting Standards for Arterial Aneurysms, Ad Hoc Committee on Reporting Standards, Society for Vascular Surgery and North American Chapter, International Society for Cardiovascular Surgery. J Vasc Surg 1991;13:452-8.

245. Coady MA, Rizzo JA, Hammond GL, Kopf GS, Elefteriades JA. Surgical intervention criteria for thoracic aortic aneurysms: a study of growth rates and complications. Ann Thorac Surg 1999;67:1922-6; discussion 1953-8.

246. La Canna G, Ficarra E, Tsagalau E, Nardi M, Morandini A, Chieffo A, et al. Progression rate of ascending aortic dilation in patients with normally functioning bicuspid and tricuspid aortic valves. Am J Cardiol 2006;98:249-53.

247. Michelena HI, Desjardins VA, Avierinos JF, Russo A, Nkomo VT, Sundt TM, et al. Natural history of asymptomatic patients with normally functioning or minimally dysfunctional bicuspid aortic valve in the community. Circulation 2008;117:2776-84.

248. Tzemos N, Therrien J, Yip J, Thanassoulis G, Tremblay S, Jamorski MT, et al. Outcomes in adults with bicuspid aortic valves. JAMA 2008;300:1317-25.

249. Davies RR, Goldstein LJ, Coady MA, Tittle SL, Rizzo JA, Kopf GS, et al. Yearly rupture or dissection rates for thoracic aortic aneurysms: simple prediction based on size. Ann Thorac Surg 2002;73:17-27; discussion 27-8.

250. Palomo AR, Schrager BR, Chahine RA. Anomalous origin of the right coronary artery from the ascending aorta high above the left posterior sinus of Valsalva of a bicuspid aortic valve. Am Heart J 1985;109:902-4.

251. Underwood MJ, El Khoury G, Deronck D, Glineur D, Dion R. The aortic root: structure, function, and surgical reconstruction. Heart 2000;83:376-80.

252. Svensson LG, Adams DH, Bonow RO, Kouchoukos NT, Miller DC, O'Gara PT, et al. Aortic valve and ascending aorta guidelines for management and quality measures. Ann Thorac Surg 2013;95:S1-66.

253. Loeys BL, Dietz HC, Braverman AC, Callewaert BL, De Backer J, Devereux RB, et al. The revised Ghent nosology for the Marfan syndrome. J Med Genet 2010;47:476-85.

254. Ammash NM, Sundt TM, Connolly HM. Marfan syndrome-diagnosis and management. Curr Probl Cardiol 2008;33:7-39.

255. Gautier M, Detaint D, Fermanian C, Aegerter P, Delorme G, Arnoult F, et al. Nomograms for aortic root diameters in children using two-dimensional echocardiography. Am J Cardiol 2010;105:888-94.

256. Hjerrild BE, Mortensen KH, Sorensen KE, Pedersen EM, Andersen NH, Lundorf E, et al. Thoracic aortopathy in Turner syndrome and the influence of bicuspid aortic valves and blood pressure: a CMR study. J Cardiovasc Magn Reson 2010;12:12.

257. Ho VB, Bakalov VK, Cooley M, Van PL, Hood MN, Burklow TR, et al. Major vascular anomalies in Turner syndrome: prevalence and magnetic resonance angiographic features. Circulation 2004;110:1694-700.

258. Matura LA, Ho VB, Rosing DR, Bondy CA. Aortic dilatation and dissection in Turner syndrome. Circulation 2007;116:1663-70.

259. Loeys BL, Chen J, Neptune ER, Judge DP, Podowski M, Holm T, et al. A syndrome of altered cardiovascular, craniofacial, neurocognitive and skeletal development caused by mutations in TGFBR1 or TGFBR2. Nat Genet 2005;37:275-81.

260. Loeys BL, Schwarze U, Holm T, Callewaert BL, Thomas GH, Pannu H, et al. Aneurysm syndromes caused by mutations in the TGF-beta receptor. N Engl J Med 2006;355:788-98.

261. Johnson PT, Chen JK, Loeys BL, Dietz HC, Fishman EK. Loeys-Dietz syndrome: MDCT angiography findings. AJR Am J Roentgenol 2007;189:W29-35.

262. Albornoz G, Coady MA, Roberts M, Davies RR, Tranquilli M, Rizzo JA, et al. Familial thoracic aortic aneurysms and dissections—incidence, modes of inheritance, and phenotypic patterns. Ann Thorac Surg 2006;82:1400-5.

263. Regalado E, Medrek S, Tran-Fadulu V, Guo DC, Pannu H, Golabbakhsh H, et al. Autosomal dominant inheritance of a predisposition to thoracic aortic aneurysms and dissections and intracranial saccular aneurysms. Am J Med Genet A 2011;155A:2125-30.

264. Pepin M, Schwarze U, Superti-Furga A, Byers PH. Clinical and genetic features of Ehlers-Danlos syndrome type IV, the vascular type. N Engl J Med 2000;342:673-80.

265. Fazel SS, Mallidi HR, Lee RS, Sheehan MP, Liang D, Fleischman D, et al. The aortopathy of bicuspid aortic valve disease has distinctive patterns and usually involves the transverse aortic arch. J Thorac Cardiovasc Surg 2008;135:901-7. 907.e1-2.

266. Holmes KW, Lehmann CU, Dalal D, Nasir K, Dietz HC, Ravekes WJ, et al. Progressive dilation of the ascending aorta in children with isolated bicuspid aortic valve. Am J Cardiol 2007;99:978-83.

267. Kari FA, Fazel SS, Mitchell RS, Fischbein MP, Miller DC. Bicuspid aortic valve configuration and aortopathy pattern might represent different pathophysiologic substrates. J Thorac Cardiovasc Surg 2012;144:516-7.

268. Michelena HI, Khanna AD, Mahoney D, Margaryan E, Topilsky Y, Suri RM, et al. Incidence of aortic complications in patients with bicuspid aortic valves. JAMA 2011;306:1104-12.

269. Schaefer BM, Lewin MB, Stout KK, Gill E, Prueitt A, Byers PH, et al. The bicuspid aortic valve: an integrated phenotypic classification of leaflet morphology and aortic root shape. Heart 2008;94:1634-8.

270. Siu SC, Silversides CK. Bicuspid aortic valve disease. J Am Coll Cardiol 2010;55:2789-800.

271. Schievink WI, Raissi SS, Maya MM, Velebir A. Screening for intracranial aneurysms in patients with bicuspid aortic valve. Neurology 2010;74:1430-3.

272. Ferencik M, Pape LA. Changes in size of ascending aorta and aortic valve function with time in patients with congenitally bicuspid aortic valves. Am J Cardiol 2003;92:43-6.

273. Plaisance BR, Winkler MA, Attili AK, Sorrell VL. Congenital bicuspid aortic valve first presenting as an aortic aneurysm. Am J Med 2012;125:e5-7.

274. Doty DB. Anomalous origin of the left circumflex coronary artery associated with bicuspid aortic valve. J Thorac Cardiovasc Surg 2001;122:842-3.

275. Higgins CB, Wexler L. Reversal of dominance of the coronary arterial system in isolated aortic stenosis and bicuspid aortic valve. Circulation 1975;52:292-6.

276. Hutchins GM, Nazarian IH, Bulkley BH. Association of left dominant coronary arterial system with congenital bicuspid aortic valve. Am J Cardiol 1978;42:57-9.

277. Roberts WC. The congenitally bicuspid aortic valve. A study of 85 autopsy cases. Am J Cardiol 1970;26:72-83.

278. Xenikakis T, Malliotakis P, Barbetakis N, Manousakis E, Hassoulas J. Congenital malformations of the aortic root: bicuspid aortic valve in combination with unruptured aneurysm of the left sinus of Valsalva and aberrant left coronary artery. Hellenic J Cardiol 2008;49:288-91.

279. Biner S, Rafique AM, Ray I, Cuk O, Siegel RJ, Tolstrup K. Aortopathy is prevalent in relatives of bicuspid aortic valve patients. J Am Coll Cardiol 2009;53:2288-95.

280. Cook CC, Gleason TG. Great vessel and cardiac trauma. Surg Clin North Am 2009;89:797-820, viii.

281. Lopera JE, Restrepo CS, Gonzales A, Trimmer CK, Arko F. Aortoiliac vascular injuries after misplacement of fixation screws. J Trauma 2010;69:870-5.

282. Burack JH, Kandil E, Sawas A, O'Neill PA, Sclafani SJ, Lowery RC, et al. Triage and outcome of patients with mediastinal penetrating trauma. Ann Thorac Surg 2007;83:377-82; discussion 382.

283. Dosios TJ, Salemis N, Angouras D, Nonas E. Blunt and penetrating trauma of the thoracic aorta and aortic arch branches: an autopsy study. J Trauma 2000;49:696-703.

284. Parmley LF, Mattingly TW, Manion WC, Jahnke EJJ. Nonpenetrating traumatic injury of the aorta. Circulation 1958;17:1086-101.

285. Mirvis SE. Thoracic vascular injury. Radiol Clin North Am 2006;44: 181-97, vii.

286. Patel NH, Stephens KE Jr., Mirvis SE, Shanmuganathan K, Mann FA. Imaging of acute thoracic aortic injury due to blunt trauma: a review. Radiology 1998;209:335-48.

287. Steenburg SD, Ravenel JG. Multi-detector computed tomography findings of atypical blunt traumatic aortic injuries: a pictorial review. Emerg Radiol 2007;14:143-50.

288. Pierangeli A, Turinetto B, Galli R, Caldarera L, Fattori R, Gavelli G. Delayed treatment of isthmic aortic rupture. Cardiovasc Surg 2000;8: 280-3.

289. Wintermark M, Wicky S, Schnyder P. Imaging of acute traumatic injuries of the thoracic aorta. Eur Radiol 2002;12:431-42.

290. Nicolaou G. Endovascular treatment of blunt traumatic thoracic aortic injury. Semin Cardiothorac Vasc Anesth 2009;13:106-12.

291. Nzewi O, Slight RD, Zamvar V. Management of blunt thoracic aortic injury. Eur J Vasc Endovasc Surg 2006;31:18-27.

292. Demetriades D, Gomez H, Velmahos GC, Asensio JA, Murray J, Cornwell EEr, et al. Routine helical computed tomographic evaluation of the mediastinum in high-risk blunt trauma patients. Arch Surg 1998;133:1084-8.

293. Malhotra AK, Fabian TC, Croce MA, Weiman DS, Gavant ML, Pate JW. Minimal aortic injury: a lesion associated with advancing diagnostic techniques. J Trauma 2001;51:1042-8.

294. Hsiang YN, Fragoso M, Lundkist A, Weis M. The natural history of intimal flaps caused by angioscopy. Ann Vasc Surg 1992;6:38-44.

295. Neville RF, Padberg FT Jr., DeFouw D, Hernandez J, Duran W. Hobson RWn. The arterial wall response to intimal injury in an experimental model. Ann Vasc Surg 1992;6:50-4.

296. Fisher RG, Sanchez-Torres M, Whigham CJ, Thomas JW. "Lumps" and "bumps" that mimic acute aortic and brachiocephalic vessel injury. Radiographics 1997;17:825-34.

297. Kodali S, Jamieson WR, Leia-Stephens M, Miyagishima RT, Janusz MT, Tyers GF. Traumatic rupture of the thoracic aorta. A 20-year review: 1969-1989. Circulation 1991;84:III40-6.

298. Mirvis SE, Pais SO, Shanmuganathan K. Atypical results of thoracic aortography performed to exclude aortic injury. Emergency Radiology 1994;1:24-31.

299. Mirvis SE, Shanmuganathan K, Buell J, Rodriguez A. Use of spiral computed tomography for the assessment of blunt trauma patients with potential aortic injury. J Trauma 1998;45:922-30.

300. Demetriades D, Velmahos GC, Scalea TM, Jurkovich GJ, Karmy-Jones R, Teixeira PG, et al. Diagnosis and treatment of blunt thoracic aortic injuries: changing perspectives. J Trauma 2008;64:1415-8; discussion 1418-9.

301. Dyer DS, Moore EE, Ilke DN, McIntyre RC, Bernstein SM, Durham JD, et al. Thoracic aortic injury: how predictive is mechanism and is chest computed tomography a reliable screening tool? A prospective study of 1,561 patients. J Trauma 2000;48:673-82; discussion 682-3.

302. Melton SM, Kerby JD, McGiffin D, McGwin G, Smith JK, Oser RF, et al. The evolution of chest computed tomography for the definitive diagnosis of blunt aortic injury: a single-center experience. J Trauma 2004; 56:243-50.

303. Mirvis SE, Shanmuganathan K. Diagnosis of blunt traumatic aortic injury 2007: still a nemesis. Eur J Radiol 2007;64:27-40.

304. Steenburg SD, Ravenel JG. Acute traumatic thoracic aortic injuries: experience with 64-MDCT. AJR Am J Roentgenol 2008;191: 1564-9.

305. Mirvis SE, Shanmuganathan K, Miller BH, White CS, Turney SZ. Traumatic aortic injury: diagnosis with contrast-enhanced thoracic CT– five-year experience at a major trauma center. Radiology 1996;200: 413-22.

306. Kalender WA, Seissler W, Klotz E, Vock P. Spiral volumetric CT with single-breath-hold technique, continuous transport, and continuous scanner rotation. Radiology 1990;176:181-3.

307. Huber-Wagner S, Lefering R, Qvick LM, Korner M, Kay MV, Pfeifer KJ, et al. Effect of whole-body CT during trauma resuscitation on survival: a retrospective, multicentre study. Lancet 2009;373:1455-61.

308. Fox SH, Tanenbaum LN, Ackelsberg S, He HD, Hsieh J, Hu H. Future directions in CT technology. Neuroimaging Clin N Am 1998;8: 497-513.

309. Klingenbeck-Regn K, Schaller S, Flohr T, Ohnesorge B, Kopp AF, Baum U. Subsecond multi-slice computed tomography: basics and applications. Eur J Radiol 1999;31:110-24.

310. Gunn ML. Imaging of aortic and branch vessel trauma. Radiol Clin North Am 2012;50:85-103.

311. Nguyen D, Platon A, Shanmuganathan K, Mirvis SE, Becker CD, Poletti PA. Evaluation of a single-pass continuous whole-body 16-MDCT protocol for patients with polytrauma. AJR Am J Roentgenol 2009;192:3-10.

312. Chirillo F, Totis O, Cavarzerani A, Bruni A, Farnia A, Sarpellon M, et al. Usefulness of transthoracic and transoesophageal echocardiography in recognition and management of cardiovascular injuries after blunt chest trauma. Heart 1996;75:301-6.

313. Goarin JP, Catoire P, Jacquens Y, Saada M, Riou B, Bonnet F, et al. Use of transesophageal echocardiography for diagnosis of traumatic aortic injury. Chest 1997;112:71-80.

314. Goarin JP, Cluzel P, Gosgnach M, Lamine K, Coriat P, Riou B. Evaluation of transesophageal echocardiography for diagnosis of traumatic aortic injury. Anesthesiology 2000;93:1373-7.

315. Mollod M, Felner JM. Transesophageal echocardiography in the evaluation of cardiothoracic trauma. Am Heart J 1996;132:841-9.

316. Smith MD, Cassidy JM, Souther S, Morris EJ, Sapin PM, Johnson SB, et al. Transesophageal echocardiography in the diagnosis of traumatic rupture of the aorta. N Engl J Med 1995;332:356-62.

317. Vignon P, Gueret P, Vedrinne JM, Lagrange P, Cornu E, Abrieu O, et al. Role of transesophageal echocardiography in the diagnosis and management of traumatic aortic disruption. Circulation 1995;92:2959-68.

318. Vignon P, Lang RM. Use of Transesophageal Echocardiography for the Assessment of Traumatic Aortic Injuries. Echocardiography 1999;16: 207-19.

319. Vignon P, Boncoeur MP, Francois B, Rambaud G, Maubon A, Gastinne H. Comparison of multiplane transesophageal echocardiography and contrast-enhanced helical CT in the diagnosis of blunt traumatic cardiovascular injuries. Anesthesiology 2001;94:615-22; discussion 5A.

320. Cinnella G, Dambrosio M, Brienza N, Tullo L, Fiore T. Transesophageal echocardiography for diagnosis of traumatic aortic injury: an appraisal of the evidence. J Trauma 2004;57:1246-55.

321. Downing SW, Sperling JS, Mirvis SE, Cardarelli MG, Gilbert TB, Scalea TM, et al. Experience with spiral computed tomography as the sole diagnostic method for traumatic aortic rupture. Ann Thorac Surg 2001;72:495-501; discussion 501-2.

322. Saletta S, Lederman E, Fein S, Singh A, Kuehler DH, Fortune JB. Transesophageal echocardiography for the initial evaluation of the widened mediastinum in trauma patients. J Trauma 1995;39:137-41; discussion 141-2.

323. Azizzadeh A, Valdes J, Miller CC 3rd, Nguyen LL, Estrera AL, Charlton-Ouw K, et al. The utility of intravascular ultrasound compared to angiography in the diagnosis of blunt traumatic aortic injury. J Vasc Surg 2011; 53:608-14.

324. Fattori R, Celletti F, Bertaccini P, Galli R, Pacini D, Pierangeli A, et al. Delayed surgery of traumatic aortic rupture. Role of magnetic resonance imaging. Circulation 1996;94:2865-70.

325. Gavelli G, Canini R, Bertaccini P, Battista G, Bna C, Fattori R. Traumatic injuries: imaging of thoracic injuries. Eur Radiol 2002;12:1273-94.

326. Peterson BG, Matsumura JS, Morasch MD, West MA, Eskandari MK. Percutaneous endovascular repair of blunt thoracic aortic transection. J Trauma 2005;59:1062-5.

327. Rousseau H, Dambrin C, Marcheix B, Richeux L, Mazerolles M, Cron C, et al. Acute traumatic aortic rupture: a comparison of surgical and stent-graft repair. J Thorac Cardiovasc Surg 2005;129:1050-5.

328. Connolly HM, Huston J 3rd, Brown RD Jr., Warnes CA, Ammash NM, Tajik AJ. Intracranial aneurysms in patients with coarctation of the aorta: a prospective magnetic resonance angiographic study of 100 patients. Mayo Clin Proc 2003;78:1491-9.

329. Warnes CA, Williams RG, Bashore TM, Child JS, Connolly HM, Dearani JA, et al. ACC/AHA 2008 guidelines for the management of adults with congenital heart disease: a report of the American College of Cardiology/American Heart Association Task Force on Practice Guidelines (Writing Committee to Develop Guidelines on the Management of Adults With Congenital Heart Disease). Developed in Collaboration With the American Society of Echocardiography, Heart Rhythm Society, International Society for Adult Congenital Heart Disease, Society for Cardiovascular Angiography and Interventions, and Society of Thoracic Surgeons. J Am Coll Cardiol 2008;52:e143-263.

330. Montgomery DH, Ververis JJ, McGorisk G, Frohwein S, Martin RP, Taylor WR. Natural history of severe atheromatous disease of the thoracic aorta: a transesophageal echocardiographic study. J Am Coll Cardiol 1996;27:95-101.

331. Amarenco P, Duyckaerts C, Tzourio C, Henin D, Bousser MG, Hauw JJ. The prevalence of ulcerated plaques in the aortic arch in patients with stroke. N Engl J Med 1992;326:221-5.

332. Dee W, Geibel A, Kasper W, Konstantinides S, Just H. Mobile thrombi in atherosclerotic lesions of the thoracic aorta: the diagnostic impact of transesophageal echocardiography. Am Heart J 1993;126:707-10.

333. Kronzon I, Tunick PA. Atheromatous disease of the thoracic aorta: pathologic and clinical implications. Ann Intern Med 1997;126:629-37.

334. Moldveen-Geronimus M, Merriam JCJ. Cholesterol embolization. From pathological curiosity to clinical entity. Circulation 1967;35:946-53.

335. Tunick PA, Perez JL, Kronzon I. Protruding atheromas in the thoracic aorta and systemic embolization. Ann Intern Med 1991; 115:423-7.

336. Tobler HG, Edwards JE. Frequency and location of atherosclerotic plaques in the ascending aorta. J Thorac Cardiovasc Surg 1988;96:304-6.

337. Solberg LA, Strong JP. Risk factors and atherosclerotic lesions. A review of autopsy studies. Arteriosclerosis 1983;3:187-98.

338. Gu X, He Y, Li Z, Kontos MC, Paulsen WH, Arrowood JA, et al. Relation between the incidence, location, and extent of thoracic aortic atherosclerosis detected by transesophageal echocardiography and the extent of coronary artery disease by angiography. Am J Cardiol 2011;107:175-8.

339. Khoury Z, Gottlieb S, Stern S, Keren A. Frequency and distribution of atherosclerotic plaques in the thoracic aorta as determined by transesophageal echocardiography in patients with coronary artery disease. Am J Cardiol 1997;79:23-7.

340. Amarenco P, Cohen A, Baudrimont M, Bousser MG. Transesophageal echocardiographic detection of aortic arch disease in patients with cerebral infarction. Stroke 1992;23:1005-9.

341. Hofmann T, Kasper W, Meinertz T, Geibel A, Just H. Echocardiographic evaluation of patients with clinically suspected arterial emboli. Lancet 1990;336:1421-4.

342. Horowitz DR, Tuhrim S, Budd J, Goldman ME. Aortic plaque in patients with brain ischemia: diagnosis by transesophageal echocardiography. Neurology 1992;42:1602-4.

343. Jones EF, Kalman JM, Calafiore P, Tonkin AM, Donnan GA. Proximal aortic atheroma. An independent risk factor for cerebral ischemia. Stroke 1995;26:218-24.

344. Karalis DG, Chandrasekaran K, Victor MF, Ross JJJ, Mintz GS. Recognition and embolic potential of intraaortic atherosclerotic debris. J Am Coll Cardiol 1991;17:73-8.

345. Nihoyannopoulos P, Joshi J, Athanasopoulos G, Oakley CM. Detection of atherosclerotic lesions in the aorta by transesophageal echocardiography. Am J Cardiol 1993;71:1208-12.

346. Rubin DC, Plotnick GD, Hawke MW. Intraaortic debris as a potential source of embolic stroke. Am J Cardiol 1992;69:819-20.

347. Toyoda K, Yasaka M, Nagata S, Yamaguchi T. Aortogenic embolic stroke: a transesophageal echocardiographic approach. Stroke 1992;23: 1056-61.

348. Fazio GP, Redberg RF, Winslow T, Schiller NB. Transesophageal echocardiographically detected atherosclerotic aortic plaque is a marker for coronary artery disease. J Am Coll Cardiol 1993;21:144-50.

349. Witteman JC, Kannel WB, Wolf PA, Grobbee DE, Hofman A, D'Agostino RB, et al. Aortic calcified plaques and cardiovascular disease (the Framingham Study). Am J Cardiol 1990;66:1060-4.

350. Pignoli P, Tremoli E, Poli A, Oreste P, Paoletti R. Intimal plus medial thickness of the arterial wall: a direct measurement with ultrasound imaging. Circulation 1986;74:1399-406.

351. Atherosclerotic disease of the aortic arch as a risk factor for recurrent ischemic stroke. The French Study of Aortic Plaques in Stroke Group. N Engl J Med 1996;334:1216-21.

352. Agmon Y, Khandheria BK, Meissner I, Schwartz GL, Petterson TM, O'Fallon WM, et al. Independent association of high blood pressure and aortic atherosclerosis: A population-based study. Circulation 2000;102:2087-93.

353. Amarenco P, Cohen A, Tzourio C, Bertrand B, Hommel M, Besson G, et al. Atherosclerotic disease of the aortic arch and the risk of ischemic stroke. N Engl J Med 1994;331:1474-9.

354. Barazangi N, Wintermark M, Lease K, Rao R, Smith W, Josephson SA. Comparison of computed tomography angiography and transesophageal echocardiography for evaluating aortic arch disease. J Stroke Cerebrovasc Dis 2011;20:436-42.

355. Barbut D, Lo YW, Hartman GS, Yao FS, Trifiletti RR, Hager DN, et al. Aortic atheroma is related to outcome but not numbers of emboli during coronary bypass. Ann Thorac Surg 1997;64:454-9.

356. Di Tullio MR, Sacco RL, Savoia MT, Sciacca RR, Homma S. Aortic atheroma morphology and the risk of ischemic stroke in a multiethnic population. Am Heart J 2000;139:329-36.

357. Ferrari E, Vidal R, Chevallier T, Baudouy M. Atherosclerosis of the thoracic aorta and aortic debris as a marker of poor prognosis: benefit of oral anticoagulants. J Am Coll Cardiol 1999;33:1317-22.

358. Hartman GS, Peterson J, Konstadt SN, Hahn R, Szatrowski TP, Charlson ME, et al. High reproducibility in the interpretation of intraoperative transesophageal echocardiographic evaluation of aortic atheromatous disease. Anesth Analg 1996;82:539-43.

359. Katz ES, Tunick PA, Rusinek H, Ribakove G, Spencer FC, Kronzon I. Protruding aortic atheromas predict stroke in elderly patients undergoing cardiopulmonary bypass: experience with intraoperative transesophageal echocardiography. J Am Coll Cardiol 1992;20:70-7.

360. Kurra V, Lieber ML, Sola S, Kalahasti V, Hammer D, Gimple S, et al. Extent of thoracic aortic atheroma burden and long-term mortality after cardiothoracic surgery: a computed tomography study. JACC Cardiovasc Imaging 2010;3:1020-9.

361. Sharma U, Tak T. Aortic atheromas: current knowledge and controversies: a brief review of the literature. Echocardiography 2011;28:1157-63.

362. Thenappan T, Ali Raza J, Movahed A. Aortic atheromas: current concepts and controversies-a review of the literature. Echocardiography 2008;25:198-207.

363. Tunick PA, Kronzon I. Atheromas of the thoracic aorta: clinical and therapeutic update. J Am Coll Cardiol 2000;35:545-54.

364. Cohen A, Tzourio C, Bertrand B, Chauvel C, Bousser MG, Amarenco P. Aortic plaque morphology and vascular events: a follow-up study in patients with ischemic stroke. FAPS Investigators. French Study of Aortic Plaques in Stroke. Circulation 1997;96:3838-41.

365. Negishi K, Tsuchiya H, Nakajima M, Goto K, Kurosawa K, Fukuda N, et al. The seabed-like appearance of atherosclerotic plaques: three-dimensional transesophageal echocardiographic images of the aortic arch causing cholesterol crystal emboli. J Am Soc Echocardiogr 2010;23:1222.e1-4.

366. Piazzese C, Tsang W, Sotaquira M, Kronzon I, Lang RM, Caiani EG. Semiautomated detection and quantification of aortic plaques from three-dimensional transesophageal echocardiography. J Am Soc Echocardiogr 2014;27:758-66.

367. Blauth CI, Cosgrove DM, Webb BW, Ratliff NB, Boylan M, Piedmonte MR, et al. Atheroembolism from the ascending aorta. An

emerging problem in cardiac surgery. J Thorac Cardiovasc Surg 1992; 103:1104; discussion 1111-2.

368. Davila-Roman VG, Barzilai B, Wareing TH, Murphy SF, Schechtman KB, Kouchoukos NT. Atherosclerosis of the ascending aorta. Prevalence and role as an independent predictor of cerebrovascular events in cardiac patients. Stroke 1994;25:2010-6.

369. Ribakove GH, Katz ES, Galloway AC, Grossi EA, Esposito RA, Baumann FG, et al. Surgical implications of transesophageal echocardiography to grade the atheromatous aortic arch. Ann Thorac Surg 1992;53:758-61; discussion 762-3.

370. Wareing TH, Davila-Roman VG, Barzilai B, Murphy SF, Kouchoukos NT. Management of the severely atherosclerotic ascending aorta during cardiac operations. A strategy for detection and treatment. J Thorac Cardiovasc Surg 1992;103:453-62.

371. Wareing TH, Davila-Roman VG, Daily BB, Murphy SF, Schechtman KB, Barzilai B, et al. Strategy for the reduction of stroke incidence in cardiac surgical patients. Ann Thorac Surg 1993;55: 1400-7; discussion 1407-8.

372. Bar-Yosef S, Anders M, Mackensen GB, Ti LK, Mathew JP, Phillips-Bute B, et al. Aortic atheroma burden and cognitive dysfunction after coronary artery bypass graft surgery. Ann Thorac Surg 2004;78: 1556-62.

373. Goto T, Baba T, Matsuyama K, Honma K, Ura M, Koshiji T. Aortic atherosclerosis and postoperative neurological dysfunction in elderly coronary surgical patients. Ann Thorac Surg 2003;75:1912-8.

374. Bolotin G, Domany Y, de Perini L, Frolkis I, Lev-Ran O, Nesher N, et al. Use of intraoperative epiaortic ultrasonography to delineate aortic atheroma. Chest 2005;127:60-5.

375. Royse C, Royse A, Blake D, Grigg L. Screening the thoracic aorta for atheroma: a comparison of manual palpation, transesophageal and epiaortic ultrasonography. Ann Thorac Cardiovasc Surg 1998;4:347-50.

376. Sylivris S, Calafiore P, Matalanis G, Rosalion A, Yuen HP, Buxton BF, et al. The intraoperative assessment of ascending aortic atheroma: epiaortic imaging is superior to both transesophageal echocardiography and direct palpation. J Cardiothorac Vasc Anesth 1997;11:704-7.

377. Suvarna S, Smith A, Stygall J, Kolvecar S, Walesby R, Harrison M, et al. An intraoperative assessment of the ascending aorta: a comparison of digital palpation, transesophageal echocardiography, and epiaortic ultrasonography. J Cardiothorac Vasc Anesth 2007;21:805-9.

378. Bergman P, van der Linden J, Forsberg K, Ohman M. Preoperative computed tomography or intraoperative epiaortic ultrasound for the diagnosis of atherosclerosis of the ascending aorta? Heart Surg Forum 2004;7:E245-9; discussion E249.

379. Glas KE, Swaminathan M, Reeves ST, Shanewise JS, Rubenson D, Smith PK, et al. Guidelines for the performance of a comprehensive intraoperative epiaortic ultrasonographic examination: recommendations of the American Society of Echocardiography and the Society of Cardiovascular Anesthesiologists; endorsed by the Society of Thoracic Surgeons. J Am Soc Echocardiogr 2007;20:1227-35.

380. van der Linden J, Hadjinikolaou L, Bergman P, Lindblom D. Postoperative stroke in cardiac surgery is related to the location and extent of atherosclerotic disease in the ascending aorta. J Am Coll Cardiol 2001; 38:131-5.

381. Aarts NJ, Schurink GW, Schultze Kool LJ, Bode PJ, van Baalen JM, Hermans J, et al. Abdominal aortic aneurysm measurements for endovascular repair: intra- and interobserver variability of CT measurements. Eur J Vasc Endovasc Surg 1999;18:475-80.

382. Tenenbaum A, Garniek A, Shemesh J, Fisman EZ, Stroh CI, Itzchak Y, et al. Dual-helical CT for detecting aortic atheromas as a source of stroke: comparison with transesophageal echocardiography. Radiology 1998; 208:153-8.

383. Ibanez B, Badimon JJ, Garcia MJ. Diagnosis of atherosclerosis by imaging. Am J Med 2009;122:S15-25.

384. Kamdar AR, Meadows TA, Roselli EE, Gorodeski EZ, Curtin RJ, Sabik JF, et al. Multidetector computed tomographic angiography in planning of reoperative cardiothoracic surgery. Ann Thorac Surg 2008;85:1239-45.

385. Fayad ZA, Fuster V, Fallon JT, Jayasundera T, Worthley SG, Helft G, et al. Noninvasive in vivo human coronary artery lumen and wall imaging using black-blood magnetic resonance imaging. Circulation 2000;102: 506-10.

386. Fayad ZA, Nahar T, Fallon JT, Goldman M, Aguinaldo JG, Badimon JJ, et al. In vivo magnetic resonance evaluation of atherosclerotic plaques in the human thoracic aorta: a comparison with transesophageal echocardiography. Circulation 2000;101:2503-9.

387. Kronzon I, Tunick PA. Aortic atherosclerotic disease and stroke. Circulation 2006;114:63-75.

388. Saam T, Hatsukami TS, Takaya N, Chu B, Underhill H, Kerwin WS, et al. The vulnerable, or high-risk, atherosclerotic plaque: noninvasive MR imaging for characterization and assessment. Radiology 2007;244:64-77.

389. Osler W. The Gulstonian Lectures, on Malignant Endocarditis. Br Med J 1885;1:467-70.

390. Gomes MN, Choyke PL, Wallace RB. Infected aortic aneurysms. A changing entity. Ann Surg 1992;215:435-42.

391. Johansen K, Devin J. Mycotic aortic aneurysms. A reappraisal. Arch Surg 1983;118:583-8.

392. Clough RE, Black SA, Lyons OT, Zayed HA, Bell RE, Carrell T, et al. Is endovascular repair of mycotic aortic aneurysms a durable treatment option? Eur J Vasc Endovasc Surg 2009;37:407-12.

393. Moneta GL, Taylor LM Jr., Yeager RA, Edwards JM, Nicoloff AD, McConnell DB, et al. Surgical treatment of infected aortic aneurysm. Am J Surg 1998;175:396-9.

394. Gornik HL, Creager MA. Aortitis. Circulation 2008;117:3039-51.

395. Revest M, Decaux O, Cazalets C, Verohye JP, Jego P, Grosbois B. Thoracic infectious aortitis: microbiology, pathophysiology and treatment. Rev Med Interne 2007;28:108-15.

396. Cooke PA, Ehrenfeld WK. Successful management of mycotic aortic aneurysm: report of a case. Surgery 1974;75:132-6.

397. Scher LA, Brener BJ, Goldenkranz RJ, Alpert J, Brief DK, Parsonnet V, et al. Infected aneurysms of the abdominal aorta. Arch Surg 1980;115: 975-8.

398. Malouf JF, Chandrasekaran K, Orszulak TA. Mycotic aneurysms of the thoracic aorta: a diagnostic challenge. Am J Med 2003;115:489-96.

399. Narang AT, Rathlev NK. Non-aneurysmal infectious aortitis: a case report. J Emerg Med 2007;32:359-63.

400. Choi SJ, Lee JS, Cheong MH, Byun SS, Hyun IY. F-18 FDG PET/CT in the management of infected abdominal aortic aneurysm due to Salmonella. Clin Nucl Med 2008;33:492-5.

401. Lupi-Herrera E, Sanchez-Torres G, Marcushamer J, Mispireta J, Horwitz S, Vela JE. Takayasu's arteritis. Clinical study of 107 cases. Am Heart J 1977; 93:94-103.

402. Ishikawa K. Diagnostic approach and proposed criteria for the clinical diagnosis of Takayasu's arteriopathy. J Am Coll Cardiol 1988;12:964-72.

403. Bezerra Lira-Filho E, Campos O, Lazaro Andrade J, Henrique Fischer C, Godoy Nunes C, Cavalcanti Lins A, et al. Thoracic aorta evaluation in patients with Takayasu's arteritis by transesophageal echocardiography. J Am Soc Echocardiogr 2006;19:829-34.

404. Schmidt WA, Nerenheim A, Seipelt E, Poehls C, Gromnica-Ihle E. Diagnosis of early Takayasu arteritis with sonography. Rheumatology (Oxford) 2002;41:496-502.

405. Yamada I, Shibuya H, Matsubara O, Umehara I, Makino T, Numano F, et al. Pulmonary artery disease in Takayasu's arteritis: angiographic findings. AJR Am J Roentgenol 1992;159:263-9.

406. Kissin EY, Merkel PA. Diagnostic imaging in Takayasu arteritis. Curr Opin Rheumatol 2004;16:31-7.

407. Meave A, Soto ME, Reyes PA, Cruz P, Talayero JA, Sierra C, et al. Prepulseless Takayasu's arteritis evaluated with 18F-FDG positron emission tomography and gadolinium-enhanced magnetic resonance angiography. Tex Heart Inst J 2007;34:466-9.

408. Marie I, Proux A, Duhaut P, Primard E, Lahaxe L, Girszyn N, et al. Long-term follow-up of aortic involvement in giant cell arteritis: a series of 48 patients. Medicine (Baltimore) 2009;88:182-92.

409. Salvarani C, Cantini F, Boiardi L, Hunder GG. Polymyalgia rheumatica and giant-cell arteritis. N Engl J Med 2002;347:261-71.

410. Nuenninghoff DM, Hunder GG, Christianson TJ, McClelland RL, Matteson EL. Incidence and predictors of large-artery complication (aortic aneurysm, aortic dissection, and/or large-artery stenosis) in patients with giant cell arteritis: a population-based study over 50 years. Arthritis Rheum 2003;48:3522-31.

411. Zehr KJ, Mathur A, Orszulak TA, Mullany CJ, Schaff HV. Surgical treatment of ascending aortic aneurysms in patients with giant cell aortitis. Ann Thorac Surg 2005;79:1512-7.

412. Stanson AW. Imaging findings in extracranial (giant cell) temporal arteritis. Clin Exp Rheumatol 2000;18:S43-8.

413. Blockmans D, Bley T, Schmidt W. Imaging for large-vessel vasculitis. Curr Opin Rheumatol 2009;21:19-28.

414. Furst W, Banerjee A. Release of glutaraldehyde from an albumin-glutaraldehyde tissue adhesive causes significant in vitro and in vivo toxicity. Ann Thorac Surg 2005;79:1522-8; discussion 1529.

415. Mesana TG, Caus T, Gaubert J, Collart F, Ayari R, Bartoli J, et al. Late complications after prosthetic replacement of the ascending aorta: what did we learn from routine magnetic resonance imaging follow-up? Eur J Cardiothorac Surg 2000;18:313-20.

416. Halstead JC, Meier M, Etz C, Spielvogel D, Bodian C, Wurm M, et al. The fate of the distal aorta after repair of acute type A aortic dissection. J Thorac Cardiovasc Surg 2007;133:127-35.

417. Orton DF, LeVeen RF, Saigh JA, Culp WC, Fidler JL, Lynch TJ, et al. Aortic prosthetic graft infections: radiologic manifestations and implications for management. Radiographics 2000;20:977-93.

418. Altiok E, Koos R, Schroder J, Brehmer K, Hamada S, Becker M, et al. Comparison of two-dimensional and three-dimensional imaging techniques for measurement of aortic annulus diameters before transcatheter aortic valve implantation. Heart 2011;97:1578-84.

419. Isselbacher EM. Diseases of the Aorta. In: Braunwald E, editor. Heart Disease: a Textbook of Cardiovascular Medicine. Philadelphia: WB Saunders; 2001.

420. Mohr-Kahaly S, Erbel R, Kearney P, Puth M, Meyer J. Aortic intramural hemorrhage visualized by transesophageal echocardiography: findings and prognostic implications. J Am Coll Cardiol 1994;23: 658-64.

421. Nienaber CA, von Kodolitsch Y, Petersen B, Loose R, Helmchen U, Haverich A, Spielmann RP. Intramural hemorrhage of the thoracic aorta. Diagnostic and therapeutic implications. Circulation 1995;92: 1465-72.

422. Keren A, Kim CB, Hu BS, Eyngorina I, Billingham ME, Mitchell RS, et al. Accuracy of biplane and multiplane transesophageal echocardiography in diagnosis of typical acute aortic dissection and intramural hematoma. J Am Coll Cardiol 1996;28:627-36.

423. Harris KM, Braverman AC, Gutierrez FR, Barzilai B, Davila-Roman VG. Transesophageal echocardiographic and clinical features of aortic intramural hematoma. J Thorac Cardiovasc Surg 1997;114: 619-26.

424. Nishigami K, Tsuchiya T, Shono H, Horibata Y, Honda T. Disappearance of aortic intramural hematoma and its significance to the prognosis. Circulation 2000;102:III243-7.

425. Ganaha F, Miller DC, Sugimoto K, Do YS, Minamiguchi H, Saito H, et al. Prognosis of aortic intramural hematoma with and without penetrating atherosclerotic ulcer: a clinical and radiological analysis. Circulation 2002;106:342-8.

426. Attia R, Young C, Fallouh HB, Scarci M. In patients with acute aortic intramural haematoma is open surgical repair superior to conservative management? Interact Cardiovasc Thorac Surg 2009;9:868-71.